Thesis for the degree of Doctor of Philosophy in
Thermo- and Fluid Dynamics

Aerodynamics of vehicle platooning

JOHANNES TÖRNELL

Department of Mechanics and Maritime Sciences
CHALMERS UNIVERSITY OF TECHNOLOGY
Göteborg, Sweden 2023

Aerodynamics of vehicle platooning
JOHANNES TÖRNELL
ISBN 978-91-7905-801-2

Doktorsavhandlingar vid Chalmers tekniska högskola
Ny serie nr. 5267
ISSN 0346-718X

Chalmers University of Technology
SE–412 96 Göteborg
Sweden
Telephone: +46 (0)31–772 1000

Cover:
Iso-surfaces of the instantaneous q-criterion colored by velocity for two platoons, one with two trucks and one with a truck leading a car.

Chalmers Digitaltryck
Göteborg, Sweden 2023

"Learn from yesterday, live for today, hope for tomorrow. The important thing is not to stop questioning." -Albert Einstein

Aerodynamics of vehicle platooning

Johannes Törnell
Department of Mechanics and Maritime Sciences
Chalmers University of Technology

Abstract

Many factors are pushing automotive manufacturers to increase the efficiency of their fleets; some of these are legislative (requiring reduced greenhouse gas emissions) as well as ensuring sufficient range and power consumption in electric vehicles. An important part of improving the energy efficiency of road vehicles is reducing their aerodynamic drag. Much effort has gone into improving the aerodynamics of trucks, cars, and buses. There are, however, limits on the attainable aerodynamic performance due to several different factors.

This thesis focuses on a relatively unutilized way of reducing the aerodynamic drag of vehicles, that is, vehicles driving in close proximity, or platooning. Although such a solution has long been envisioned as a way of reducing drag, it is only now becoming possible with advancements in vehicle automation and communication. Platooning is, however, regularly, and successfully used in many sports.

Although there have been many studies on the topic, the focus has mostly been on the differences in drag. This thesis attempts to improve the understanding of the observed changes in drag for a cab over engine style tractor-trailer, a passenger car, and a coach bus. The work herein was performed using both CFD simulations and wind tunnel experiments. The aerodynamics of platoons were investigated for separation distances between 0.5m and 30m, 0m and 0.5m lateral offsets, and 0°, 5°, and 10° yaw angles, to emulate wind conditions. The effects for different vehicle types are generally similar, although with varying magnitudes depending on the combination.

The results showed that the aerodynamic phenomena of the leading vehicle are, in most cases, fairly straightforward, with a base pressure increase due to the pressure field emanating from the trailing vehicle's stagnation area. This causes a reduction in drag with a decreased distance and a reduction of the relative savings under yaw conditions. The effects on the trailing vehicle are more complex as they are dominated by changes to the flow field. Many of the changes are generated by the leading vehicle slowing the flow before the trailing vehicle, as well as slight changes to the flow angularity. This typically causes the relative pressure on the front to trend toward zero and the pressure in the tractor-trailer gap to increase. At yaw, similar effects remain, but the trailing vehicle also experiences a decrease in the effective yaw angle, similar to that of a lower yaw angle. The effects on the leading and trailing vehicles generally combine to reduce the drag of the entire platoon as the separation distance decreases. Yawed flow tends to reduce the relative savings for the platoon as a whole, while a lateral offset can recover some of it.

Keywords: aerodynamics, drag, wake, side wind, platooning, close proximity, lateral offset, inter-vehicle distance, yaw, cab over engine, truck

Acknowledgments

The work presented here would not have been possible were it not for the multitude of people who have lent me their support throughout. First, I would like to thank my main supervisor Prof. Simone Sebben for all her support and feedback throughout the project, and for pushing me to do better. I would also like to thank all of my current and past industrial supervisors, all of whom have shown a great interest in the project and provided valuable insight into different areas. Dr. Per Elofsson for all his invaluable knowledge on truck aerodynamics and for supporting me in the experimental campaigns, and for the great discussions on platooning, both research oriented and commercially. Dr. David Söderblom for all of his support in the early parts of the project, for helping me learn about the aerodynamics of trucks and for all the discussions on how to develop the numerical method. Alexander Broniewicz for all the help from the side of Volvo Cars and for helping me bring the right people together to enable the experimental campaign to move forward. Vojtech Sedlak for all of his help in navigating the channels at Volvo Cars, and for the many great discussions and support in the experimental campaigns. Further, I would like to extend my thanks to all of the people at both Volvo Cars and at Scania for their help in preparing for and executing my slightly unorthodox wind tunnel experiments.

I would also like to thank the Swedish Energy Agency, Scania, and Volvo Cars for their funding of this project, without which none of this would have been possible. Next, I would like to thank the Swedish National Infrastructure for Supercomputing (SNIC), Chalmers Center for Computational Science (C3SE), and the National Supercomputer Centre (NSC) for their support with computing resources, which has enabled much of this work.

To all my colleagues and friends at VEAS, past and present, thank you for all the support and for making it the great place of work that it is. Thank you for all the great discussions, on- and off-topic, and for all the fun activities. A special thank you to Sonja for always having back and best interests in mind.

To my family, thank you for all your support, believing in me, and inspiring me to keep moving forwards. To all of my friends outside of Chalmers, thank you for all the great times, for keeping me in check and for helping me forget about work when i have needed it. Finally, to my love Christina, you have always been there to support me when i needed it, both in good and bad times, given me countless laughs and distracted me from work when i've needed to be. For this I amd eternally grateful to you.

Nomenclature

A	Area	$[m^2]$
C_{D}	Drag coefficient	[-]
$C_{\mathrm{D}}A$	Drag area	$[m^2]$
$C_{\mathrm{D\ counts}}$	Drag coefficient in counts, $1C_{\mathrm{D\ count}} = 0.001\ C_{\mathrm{D}}$	[-]
C_{P}	Pressure coefficient	[-]
C_{r}	Rolling resistance coefficient	[-]
m	Mass	[kg]
u_{i}	Velocity component i	[m/s]
f	Frequency	[Hz]
Re	Reynolds Number	[-]
Σ	Standard Deviation	[-]
Σ_{i}	Standard deviation of drag with i averaged samples	[-]
n	number of samples	[-]
k	number of samples available	[-]
i	number of samples used for averaging	[-]
ΔF_{avg}	uncertainty of force measurement	[N]
k_{res}	resolved turbulent kinetic energy	[J]
k_{mod}	modeled turbulent kinetic energy	[J]
$u'_{\mathrm{i\ X1}}$	Velocity component i fluctuation for point X1	[m/s]
$u'_{\mathrm{i\ X2}}$	Velocity component i fluctuation for point X2	[m/s]
$u_{\mathrm{i\ RMS\ X1}}$	Root mean square of the velocity component i fluctuation for point X1	[m/s]

Abbreviations

CFD	Computational Fluid Dynamics
CFL	Courant– Friedrichs– Lewy
CO_2	Carbon Dioxide
COE	Cab-over Engine
EU	European Union
GHG	Greenhouse Gas
IDDES	Improved Delayed Detached Eddy Simulation
IVD	Inter-Vehicle Distance
LES	Large Eddy Simulation
OEM	Original Equipment Manufacturer
RANS	Reynolds-Averaged Navier– Stokes
SUV	Sports Utility Vehicle
SST	Shear-Stress Transport
TVR	Turbulent Viscosity Ratio
URANS	Unsteady Reynolds-Averaged Navier– Stokes

Thesis

This thesis consists of an extended summary of the four included papers, listed below.

I. Törnell, J., Sebben, S., and Söderblom, D., *Influence of inter-vehicle distance on the aerodynamics of a two-truck platoon* in: International Journal of Automotive Technology, Vol. 22, No. 3, pp. 747-760 (2021), DOI 10.1007/s12239-021-0068-5

II. Törnell, J., Sebben, S., and Elofsson, P., *Experimental investigation of a two-truck platoon considering inter-vehicle distance, lateral offset and yaw* in: Journal of Wind Engineering and Industrial Aerodynamics, Volume 213, 2021, 104596, ISSN 0167-6105, https://doi.org/10.1016/j.jweia.2021.104596.

III. Törnell, J., Sebben, S., and Elofsson, P., *Influence of Yaw and Lateral Offset on the Aerodynamics of a Two-Truck Platoon* in: SAE Int. J. Commer. Veh. 16(2):2023, https://doi.org/10.4271/02-16-02-0010.

IV. Törnell, J., Sebben, S., and Elofsson, P., *The effects of separation distance and yaw on the drag of a truck and SUV platoon* to be submitted to Journal of Wind Engineering and Industrial Aerodynamics.

Division of work

I. All setup, simulation work, and formal analysis for Paper I was done by Törnell. Törnell wrote the first manuscript which was discussed, reviewed, and revised by all authors.

II. The instrumentation of the models was carried out by Törnell. The original plan for the experiments was done by Törnell and then discussed and revised by all authors. The experiments were performed by Törnell and Elofsson. The formal analysis of the results was done by Törnell. Törnell wrote the first manuscript, which was discussed, reviewed, and revised by all authors.

III. Setup of simulations and formal analysis was done by Törnell. Simulations were run by Törnell and at Scania. Experimental results are from Paper II. Törnell wrote the first manuscript which was discussed, reviewed, and revised by all authors.

IV. The instrumentation of the models was carried out by Törnell. The original plan for the experiments was done by Törnell and then discussed and revised by all authors. The experiments were performed by Törnell. The formal analysis of the results was done by Törnell. Setup of simulations and formal analysis was done by Törnell. Simulations were run by Törnell and at Scania. Törnell wrote the first manuscript, which was discussed, reviewed, and revised by all authors.

Other relevant publications

I. J. Törnell, J, Sebben, S., Elofsson, P. *Experimental Study of the Drag Behavior of Cab Over Engine Trucks in Close Proximity* in: Fourth international conference in numerical and experimental aerodynamics of road vehicles and trains (Aerovehicles4), Berlin, Germany, August 24-26, 2020 (pp. 196-199)

Table of Contents

Part I

Extended summary

Chapter 1

Introduction

As the society we live in moves toward a more connected and delivery-based way of life, seen by the rise of online purchasing of goods, the use of road transport has intensified. Today, roughly 28% of the greenhouse gas (GHG) emissions from transport in Europe come from light- and heavy-duty trucking [1]. Although this number is significantly smaller than that for passenger cars (roughly 45%), truck manufacturers and operating truck companies are pressured to reduce their carbon footprint. This is due to strict governmental regulations, people's awareness of the harmful effects of GHG emissions on the global climate, and the fact that for the operating truck businesses, fuel consumption represents roughly one-third of the total cost of ownership. A transition to electrification in both the private and commercial transport sectors has been initiated. Notably, the electrification of long-distance trucking is more problematic than that of passenger cars, as the energy consumption of long-distance trucking is much larger per vehicle and, therefore, will take longer. These societal changes in combination with the harmful effects of CO2 and the need for electrification of vehicles forces manufacturers to improve the efficiency of their fleet.

One way to lower greenhouse gas emissions and decrease the energy usage of vehicles is to reduce their aerodynamic resistance. There are several ways to accomplish better aerodynamics, and all Original Equipment Manufacturers (OEM) work continuously toward delivering products with lower drag values. There is, however, a limit on how low drag values can be achieved for individual vehicles using established aerodynamic solutions, and companies are finding it more difficult to achieve further improvements. As an alternative to reduce the fleet average energy consumption, concepts such as platooning (two or more vehicles driving in close proximity) are being considered. Although platooning has long been envisioned as a way to reduce aerodynamic resistance in road transport, it is only recently that the concept has become more realistic as sensor and vehicle automation technology progresses, allowing vehicles to travel safely in close proximity. Platooning has been shown to have a significant benefit for trucks, as many trucks travel on similar routes and on long haul.

Despite the large body of literature available on the aerodynamic gains and the flow around simplified vehicle bodies traveling in a convoy, there is a knowledge gap regarding this type of flow around more complex geometries. Therefore, this thesis aims to complement and increase the understanding of the aerodynamic behavior of realistic vehicle shapes in close proximity. The focus of the underlying work of

this thesis is on the development of experimental and numerical procedures for measuring, calculating and analyzing the flow phenomena in platooning of mixed sets of three different vehicle types, a cab over engine (COE) style tractor-trailer, a bus, and an SUV.

1.1 Objectives

This thesis is the result of a Ph.D. project at Chalmers University of Technology in collaboration with Scania CV and Volvo Car Corporation. The main objective of this project is to better understand the behavior of vehicles traveling in a platoon and how to maximize their performance. The project can be split into the following sub-objectives:

- Map and understand the behavior of aerodynamic resistance of different vehicles at varying inter-vehicle distances, lateral offsets, and yaw angles;
- Understand the flow physics and phenomena that create the changes mapped in the first objective;
- Understand how these phenomena can be used or negated to improve performance in different scenarios;
- Test these hypotheses numerically and experimentally to investigate their effect on performance.

The investigations in this project will be carried out using both numerical and experimental tools to enable both a thorough understanding of the system and to validate and expand the results.

1.2 Limitations

- Numerical and experimental resources are limited in this project. This means that not all possible platooning combinations will be investigated;
- Lack of capability to measure flow accurately for small models in the wind tunnel meant that CFD is used to complement the analysis;
- Only one design of each vehicle type (truck, bus, SUV) will be used, as creating more physical models is outside the project's budget;

1.3 Outline

The first chapter provided a short summary of the reasoning and objectives behind this work. In chapter 2, a review of the relevant literature and the gap that the present study intends to fill is discussed. After that, a section on the methods used, both numerical and experimental, is presented. Whereafter, the results from the four studies performed are presented. The thesis ends with conclusions, some suggestions for future work, and the appended papers.

Chapter 2

Background

2.1 Environmental aspects

As global warming and pollution issues become more evident and prevalent, legislations are drafted and passed to combat further degradation of the environment. Roughly 12% of global greenhouse gas emissions are emitted by road transport, of which 40% is freight [2]. From available research, it has been documented that the potential reduction in fuel consumption from platooning can be up to 15% [3–7], which would yield a total reduction of 360 million tons of CO_2 per year or 0.7% of the annual global emissions. The effects for cars is likely more limited as the driving conditions are generally less beneficial for platooning, however, they are still up to 10% in some cases of highway traffic[8]. Although realistic reductions are expected to be somewhat less, there is still and expected gain making platooning an alternative of interest. Furthermore, new European legislation has been adopted, forcing truck manufacturers to reduce their average fleet CO_2 emissions by 15% by 2025 and 30% by 2030, further pressuring OEMs to find new solutions. EU legislations forcing car manufacturers to reduce their fleet emissions are also in place.

2.2 Aerodynamics of trucks

As discussed in the introduction, there is a considerable drive to reduce the fuel consumption of road vehicles with multiple contributing factors, especially for trucks. The focus of this thesis lies in understanding the aerodynamic forces acting on vehicles driving in close proximity using both experimental and numerical simulations. The aerodynamic forces become the dominant force to overcome at roughly 80 km/h, although this is highly dependent on vehicle weight, making them important to reduce for highway transit (Figure 2.1).

There are various methods to reduce the aerodynamic drag of a truck and here only a few will be described. Some typical solutions are not feasible to implement, at least in the EU, where the maximum length of the complete vehicle is restricted (for example boat tail and front end extensions). Other possibilities are available such as optimizing the shape of the cab and underbody as well as air-deflectors on the cab. This air deflector has to be set correctly as the aerodynamic drag is sensitive

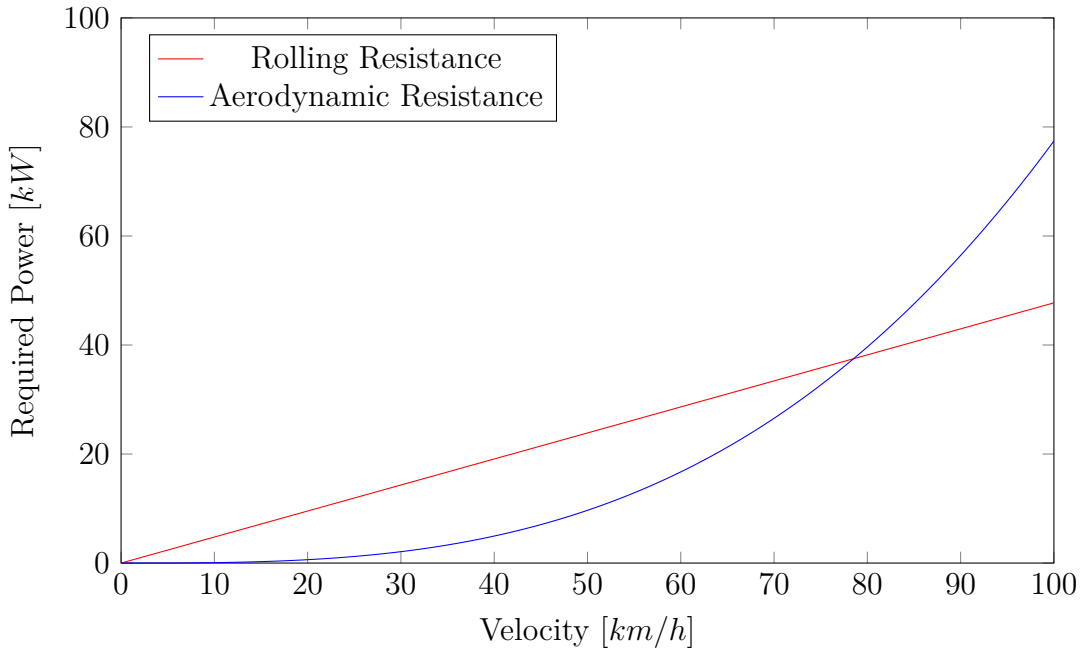

Figure 2.1: *Power required to overcome rolling and aerodynamic resistances. Cd=0.6, A=10m^2, Cr=0.005, m=35000kg*

to the angle of the deflector, as shown by Cooper [9]. Other modifications can be made to the trailer, such as adding skirts to the underbody. There are, however, issues with these that limits their adaptation on the road. Another commonly used feature to reduce the drag of a truck is front edge rounding, which is quite sensitive with respect to Reynolds number and yaw, according to Cooper [10]. Many of these have been studied and consistently show that they will reduce aerodynamic drag efficiently [9, 11–14]. All of these features or additions have limitations, and as vehicles become increasingly aerodynamic and the existing features become more refined, new methods have to be found and adopted.

The large size of trucks gives rise to difficulties in experimental investigations, which means that aerodynamic analysis of trucks using scale models is commonplace. This downsizing of the model presents several issues that have to be addressed, such as their Reynolds behavior, which can be affected by yaw [15]. Studies have recommended that Reynolds numbers in excess of 3 million based on the square root of the frontal area should be used [16]. Leuschen suggests that if a Reynolds number equivalent to less than 40% of full scale is used, several speed sweeps should be performed to ensure Reynolds independence of the results [15]. Moving ground simulation also has the potential to affect the results where the influence of air deflectors can be sensitive to the use of a moving ground system [17]. Comparisons have been made between scale models and full-scale trucks have demonstrated good correlation for smaller yaw angles. The discrepancy at large yaw angles is partially thought to be due to blockage effects that are difficult to compensate for [18].

Another way of investigating the aerodynamics of trucks is through numerical simulations, which have been shown to yield good results by Martini et al. [19], especially when unsteady approaches are used, Sengupta et al. [20]. Steady state methods have proven to be unsuitable for investigating platooning[21].

2.3 Aerodynamics of cars

Drag reduction methods for cars differ from those of trucks as there is larger freedom to modify the shape of the vehicle. As aerodynamics of passenger cars is a very large topic and intrinsically tied with the design language of the brand, it will not be further discussed here. The interested reader is directed to Hucho [22].

2.4 Platooning

Vehicles driving in close proximity, or platooning, has long been envisioned as a means to reduce the fuel consumption of road vehicles. McAuliffe et al. and Mihelic et al. have shown that the efficiency of a double trailer configuration is more efficient than two trucks in close proximity [23, 24]. This, however, does not negate the possible benefits. As double trailers might not yield sufficient cargo capacity, can be prevented by legislation in some countries or for practical reasons such as less flexibility. The formation of platoons has been investigated in several studies and demonstrated that small adjustments to departure schedules have the potential to increase the number of platoons on the road [25, 26]. Although many obstacles for real-world platooning remain, such as vehicle communication, legislation, planning, and safety, further research is needed to understand the potential benefits and drawbacks. Moreover, the benefits of driving in close proximity are not limited to the aerodynamic improvements but stretch further into optimal control and potentially several automated vehicles led by a single truck with a driver.

2.5 Effects of platooning

As the concept of platooning is not new, there is a significant body of literature on the subject. This, however, is focused on either very simple bodies or North American style trucks. This section is split up into four parts: three based on the different ways of analyzing the performance of vehicles in close proximity and one section on studies in other areas that are applicable to platooning.

2.5.1 Fuel consumption testing/On road testing

The main benefits of using fuel consumption testing on a test track to analyze platooning are that the real change in fuel consumption can be observed and the it is the closest possible way of testing to a real-world case. However, this method has several drawbacks, such as limited data on the actual aerodynamics and difficulty in separating out the change in aerodynamic drag. Further, it is also challenging to compensate for all environmental factors such as temperature, wind, and atmospheric pressure. As will be discussed in this thesis, the influence of yaw conditions can be significant on the performance seen in a platooning scenario.

There have been numerous such studies using North American style trucks and cab over engine (COE) style trucks. Several investigations on the effects of inter-vehicle distance showed savings of up to 8% for the leading truck and 20% for the trailing truck [3–7, 27, 28]. Arturo et al. [3] also included passenger vehicles where the maximum saving for a trailing car was 16%. However, some effects can reduce the efficiency of platooning, such as engine fans being utilized to cool the engine [29], lateral offset [30] (although, this increases cooling flow[31] and can reduce the need for the cooling fan), curved roads [30], and cut-ins from surrounding traffic [32]. This reduction in efficiency can potentially mitigated by different solutions. The magnitude of the penalty varies between the different studies.

Several changes can be made to increase further the efficiency of vehicles driving in close proximity, such as improving the aerodynamics of the trailer. The effects from surrounding traffic which both have been reported to be mostly additive by Bonnet et al. [5] and McAuliffe et al. [33]. In the case of using different variations of trailers, it can be important to position the vehicles correctly, as different trailers will yield different savings depending on their position, as shown by McAuliffe et al. [32].

The drag trends for the leading and trailing trucks differ greatly, although the internal vehicles of a four truck platoon see the largest and similar fuel-consumption reduction[34]. It has been shown that the leading truck only sees a benefit of driving in front of another vehicle for relatively short inter-vehicle distances, whereas the trailing truck experiences a significant benefit even at longer distances [23, 35, 36] and exhibits a local minima of savings at shorter distances [5, 23, 37, 38]. Studies utilizing the measurement of drag force on a test track have investigated the effects of lateral offset and yaw and established that a platoon, in general, has less yaw sensitivity than an isolated vehicle. The studies also confirmed that a lateral offset increases drag if an equal probability of wind direction is assumed and that the drag levels of an in-line platoon and one with a lateral offset in the leeward direction are similar. Moreover, they also demonstrated that surrounding traffic has a significant impact on the performance of vehicles in a platoon [39].

2.5.2 Wind tunnel experiments

To avoid some of the downsides of fuel consumption testing, it is also possible to investigate these phenomena in a wind tunnel. This has the benefit of a stable test environment and more accurate measurements of aerodynamic forces. However, it has similar drawbacks to those of fuel consumption testing, where it is often difficult, slow, or expensive to measure the flow around the vehicles. Further, it is often complicated to create a realistic scenario due to the need for fairly small-scale models as well as difficulties in using a rolling road condition. As these limitations can be challenging to overcome regarding available wind tunnels and costs, many currently published studies have utilized small-scale models with stationary ground planes. Nevertheless, all these studies have given a good insight into the general behavior of platoons. Wind tunnel tests show similar trends to the fuel economy tests done on road in terms of a local minima in the aerodynamic drag reduction [40–46], reduced cooling [40], effects from surrounding traffic [47] and some negative impact from the lateral offset with no side wind [43].

The aerodynamic shape of vehicles driven in close proximity is of great importance and generally favors less aerodynamic vehicles. That is, platooning is particularly favorable for leading vehicles with a non-aerodynamic base and trailing vehicles with a non-aerodynamic front [42, 45–54]. The effects have also been shown to be the strongest toward the nearest neighbors in the platoon, where changes in IVD to the vehicle immediately in front or behind have the overwhelmingly largest impact [55, 56].

As the conditions are more controllable in a wind tunnel, effects of yaw can be properly analyzed. Yaw conditions reduce the efficiency of platooning, although the effect is small at short IVDs [57]. McAuliffe et al. [40] have shown that improvements can be made using lateral offset in yaw conditions.

Longer platoons have also been investigated experimentally demonstrating larger savings with more vehicles [41] as well as similar drag for the mid to late vehicles in a platoon [48, 54, 58], indicating that these drag figures could be extended to represent a significantly longer convoy. It has been noted that some of the effects of vehicles driving in close proximity show similar trends to the behavior of a tractor-trailer gap when changing the gap length [53]. The platooning effect of smaller vehicle types has been shown to be up to 7% for an SUV[47]. The effect of radii and boat tails have also shown to have differing effects in platooning, where a decreased front edge radii has shown to improve efficiency in platooning and the addition of boat-tails has shown both improved and decreased performance depending on conditions[59]. Finally, Telionis et al. attempted to identify the flow phenomena that affect vehicles in close proximity [44], and Tadakuma et al. [60] tried to develop a mathematical model to estimate the drag of vehicles driving in close proximity.

2.5.3 Numerical investigations

To further analyze the system and gain more insight into the flow, numerical simulations can be used. The downside to numerical simulations is the uncertainty of the accuracy toward the real world. Numerical simulations can be significantly more expensive when investigating a large number of vehicle combinations and flow conditions. Additionally, as demonstrated by Norby [21], and also observed by the author and others [16, 61], unsteady methods, such as hybrid RANS/LES models need to be used for accuracy, further increasing the costs of simulations

The drag reduction trends seen in numerical studies generally agree with those from experiments, such as small to no effect on the leading vehicle when the IVD is greater than 20m, Smith et al. [62], and fuel savings of up to 23% [63]. It has also been shown that the effects of lateral offset can be detrimental to the performance of platooning [61, 64, 65], with the trailing truck being more affected than the leading truck [61]. According to Vegendla et al. [63], driving side by side has a negative impact on aerodynamic drag. The negative effect on the trailing vehicle from yaw discussed in [62] has, as in experimental studies, been partially mitigated by the use of lateral offset [66]. Similar effects to those seen in wind tunnel studies, where longer platoons yielded larger savings and a plateau of drag toward the end, have also been seen in numerical studies [67, 68]. The effects of platooning with mixed traffic has also been investigated and drag reductions up to 80% for the trailing cars[69] Numerical studies have largely been used to understand the phenomena affecting vehicles in close proximity.

Bruneau et al. have shown that the effects on the leading vehicle are predominately pressure-based and stem from the stagnation pressure of the trailing truck [70]. The same study also showed that the effects on the trailing vehicle originate from changes to the flow due to the wake of the leading vehicle [70]. The flow phenomena affecting cars in close proximity have also been explained by Ebrahim et al. [71]. It has been shown in some studies that the drag for the trailing truck does not strictly decrease with distance [66, 71, 72]. A potential explanation for this was presented by Gheyssens et al. as the sensitive nature of frontal edge rounding [73]. Another reason for this behavior has been put forth by Ebrahim et al. is the aerodynamic optimization of lone vehicles being detrimental to their performance while driving in close proximity [71]. Some of the numerical studies have also attempted to analyze the real-world implications on cooling, which has shown significant reductions in cooling flow and some increases in coolant temperature [72, 74, 75]. Finally, Ebrahim et al. [76] showed numerically that shorter models can be used to generate similar wakes for the study of platooning in limited length wind tunnel test sections.

2.5.4 Other related studies

Many insights on the physics of vehicles driving in close proximity come from research on sports, particularly cycling and motorsports, train aerodynamics and basic research on very simplified bodies [77–79].

In competitive cycling riders tend to group together to reduce aerodynamic drag. Large reductions in drag were observed by Blocken et al. [80] in smaller groups of cyclists, with a tendency for the drag to become more or less constant for the latter riders if the number of riders is greater than six. They also studied much larger groups of cyclists and showed that a drag reduction of up to 95% is possible [81]; this is, however, not likely to apply to road vehicles.

Perhaps the largest area of research relevant to platooning is the study of cargo trains, where the positioning of containers can greatly impact the aerodynamic resistance. It has been shown that the gap between wagons is of great importance [82], that yaw conditions impact the slipstreaming effect negatively [83], and that a lower loading efficiency, equating to longer distances between containers, yields higher drag [84]. The wake structures between containers were studied by Maleki et al. [85],showing similarities to those found when two trucks are driving in close proximity. Li et al. [82] confirmed that the flow over a container is affected mainly by the upstream distance and Maleki et al. [86] established that both RANS and URANS are inappropriate methods for analyzing the flow of bodies in close proximity. As in trains, the tractor-trailer gap also exhibits similar behavior to a truck convoy at very close separation distances [87, 88].

A further area that requires sound understanding for investigation of platooning, especially in experimental studies, is the Reynolds behavior and the influence of moving ground simulation. The use of a moving ground simulation system can have an impact on the wake, especially for cars [89–94]. Other local changes to the flow [95, 96], and large effects on the absolute drag value obtained have also been observed with changes to the ground simulation used [97]. Furthermore, some studies confirm slight changes to the Reynolds behavior of vehicles when a moving ground simulation is added [98, 99].

Telionis et al. investigated the usage of alternative methods for investigating vehicles driving in close proximity using a towing tank [44]. That study concluded that the drag and side forces change significantly when a car overtakes a truck, and large side forces are generated for the car. Jacuzzi et al. also attempted to improve the aerodynamics of vehicles in close proximity, such as with race cars in drafting formation [100].

Finally, a comparison between simulation results and wind tunnel experiments present several issues. Ljungskog et al. investigated the influence of adding the wind tunnel to the simulations and found that the absolute drag values obtained improved, however, with no significant improvements to the prediction of deltas [101].

Chapter 3

Methodology

3.1 Definitions

To enable a clear discussion on platooning and its aerodynamic effects, some definitions are necessary. These relate to the positioning of the vehicles in the convoy, the distance between them, the lateral offset, and the angle of the incoming flow, as shown in Figure 3.1. This thesis considers platoons of two trucks, and mixed platoons where a truck is combined with a passenger vehicle or a bus. The first vehicle in the platoon is termed the leading vehicle, and the second is termed the trailing vehicle. The spacing between them is taken as the distance from the rear-most part of the leading vehicle to the front-most part of the trailing vehicle and is named the inter-vehicle distance (IVD). In this work, the IVD is mostly limited to 0.5m to 30m (expressed in full-scale equivalent distances). This distance range was deemed as a reasonable minimum and maximum value equal to or lower than what is encountered on roads today. Some CFD simulations were also performed with longer distances to understand the potential savings experienced at typical current distances.

To further characterize the positioning, particularly of the trailing vehicle, a lateral displacement (lateral offset) is defined as the horizontal distance between the longitudinal centerlines of the two vehicles. As seen in Figure 3.1, the offset is toward the right side in the direction of travel, which is also the leeward direction under yaw conditions. In this study, the values have been limited to the corresponding space available in a single highway lane in Europe, roughly 3.6m, restricting the lateral offset to 1m, with a typical vehicle width of 2.6m.

In order to provide additional insight into the real-world behavior of vehicles driving in close proximity, side-wind conditions were also considered. The yaw conditions investigated in this thesis were 0°, 5°, and 10° of yaw.

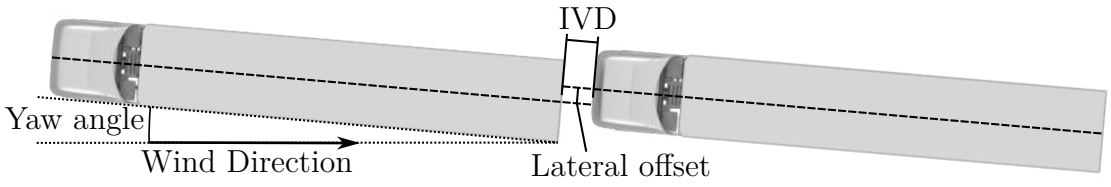

Figure 3.1: *Positioning in the platoon (leading or trailing), inter-vehicle distance (IVD), lateral offset, and yaw angle.*

3.2 Geometry

The geometries studied in this thesis were a slightly modified cab over engine (COE) style truck with a three-axle trailer, a defeatured sports utility vehicle (SUV), and a simplified bus. The simplifications were made to decrease complexity for manufacturing and to facilitate the CFD simulations. The modifications were not expected to impact the results significantly.

3.2.1 Cab over engine trucks

The numerical and physical models used were a simplified version of a COE original truck with dimensions 16.5m in length, 4m in height, and 2.6m in width. The physical model was a 1/6th scale model. The modifications made were a defeaturing of internal geometries, e.g., no cables in the engine bay and a smoothed engine, removal of small components, removal of split-lines and side-view mirrors, and a simplified cooling package. Rendered images of the model can be seen in Figure 3.2, showing the exterior, the engine bay, and the undercarriage. In the experiments, only one of the trucks was equipped with rotating wheels. This truck, referred to hereafter as the measurement model, was held fixed during the test campaigns. The second truck, named the dummy model (leading vehicle in Figure 3.18a), was moved around and was used to create a representative blockage for platooning. The tractor of this model was identical to that of the measurement model. The trailer undercarriage for this model was simplified, consisting of a rectangle with added half-circles to represent the wheels. It also had added side skirts in order to minimize the impact of the simplified underbody.

Both the numerical and experimental models had cooling packages that were representative of those on real trucks. In CFD, the cooling package consisted of three porous regions with appropriate resistances for the three different coolers. In the physical models, the cooling package was represented by a combined mesh and honeycomb set.

The scale models were instrumented with probes to measure surface pressures at critical locations. The pressure taps consisted of drilled holes instrumented with time-resolved pressure sensors on the measurement model, while the dummy model was fitted with average pressure sensors. Figure 3.2 shows the location of the pressure probes. Although it would have been of interest to measure the pressures on the front radii, no probes were installed to minimize the risk of induced detachment, as the radii region is sensitive to separation. The pressure taps were instead added behind the radii but used to infer pressure changes on them.

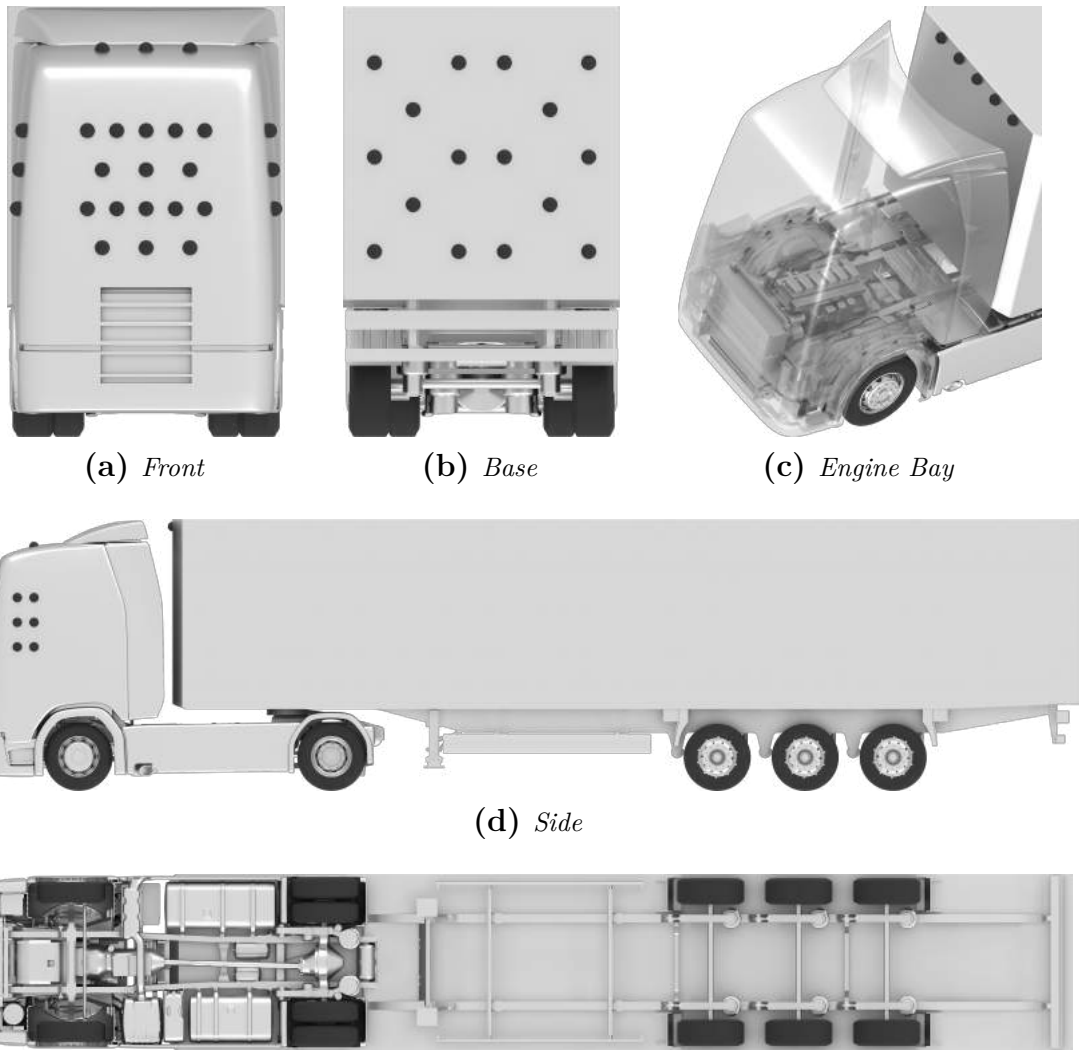

(a) *Front* **(b)** *Base* **(c)** *Engine Bay*

(d) *Side*

(e) *Bottom*

Figure 3.2: *The COE tractor-trailer model used in this study. The black dots indicate positions of pressure probes.*

3.2.2 Passenger vehicle

The second vehicle used in this thesis was a simplified sports utility vehicle (SUV). The simplifications made considered the direction of the design of modern electric cars, such as no side view mirrors, a flat floor, and a sealed grille. Additionally de-features were solid wheels, and the removal of the engine bay and split-lines. The model was built in 1/6th scale and consisted of an internal frame with milled blocks forming the outer shape and aluminum wheels with a thick rubber coating to enable the use of the moving ground system in the wind tunnel. The car was instrumented with 62 pressure ports, Figure 3.3, measuring averaged pressures. Some of the

pressure ports are near edges of curved surfaces and could thus potentially induce some separation, especially for the ports in front of the wheelhouse. This is not expected to be a significant issue as the main use of the car is to produce representative blockage and be used as a representative vehicle. From what had been seen previously, the low pressure areas on convex surfaces at the front of a vehicle has a large impact on the drag in platooning and is thus of great interest, thus necessitating pressure ports on these surfaces. The ports are holes that are drilled perpendicular to the surface and have tubes glued into them which are then cut flush with the surface.

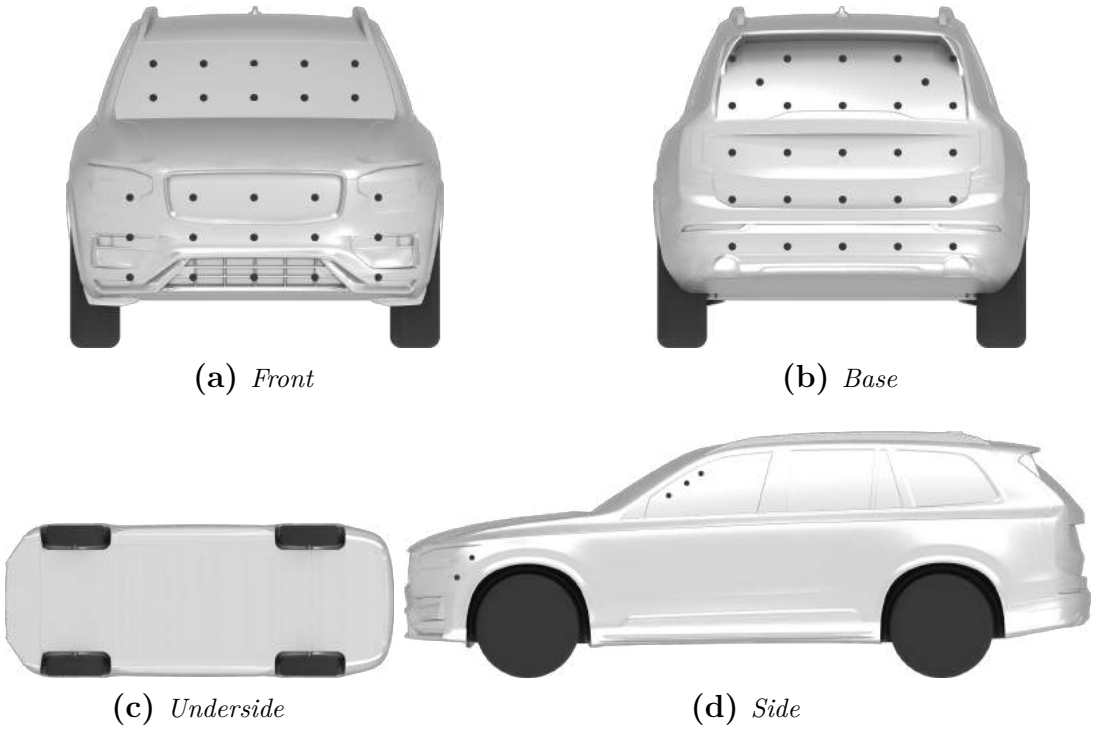

(a) *Front* **(b)** *Base*

(c) *Underside* **(d)** *Side*

Figure 3.3: *Simplified sports utility vehicle used. Black dots indicate positions of pressure taps in the physical model.*

3.2.3 Bus

The third geometry was a simplified coach bus with a flat floor, no sideview mirrors, and a closed engine bay and cooling. The physical model was also 1/6th scale, but without rotating wheels. It was only used for blockage effect, and no forces were measured on it. The vehicle was equipped with a pressure measurement system with 62 pressure points, Figure 3.4, with average pressure recorded.

(a) *Front* **(b)** *Side*

(c) *Front* **(d)** *Bottom*

Figure 3.4: *Simplified bus. Black dots indicate positions of pressure taps in the physical model.*

3.3 Numerical method

3.3.1 Domain and mesh

The simulations were carried out using STAR-CCM+ version 2019.1,2020.2 and 2022.2 with the $k-\omega$ SST IDDES model using a hexahedral-dominated unstructured grid with prism layers on the vehicle surface and ground. The implicit time-marching scheme was second-order accurate; a hybrid scheme using 85% central differencing and 15% second-order upwinding was used for the convection terms. For all platoon combinations, domain size was (281.0m-300.5m)×104m×40m, corresponding to 5 vehicle lengths upstream, 10 vehicle lengths downstream, 40 vehicle widths wide, and 10 vehicle heights tall (the vehicle dimensions being that of the COE truck), the variation of length of the domain was to keep the distance from the last vehicle to the outlet constant. This size was chosen to minimize the effects of domain boundaries and to allow for simulations with lateral offset and yaw.

When the truck was simulated, the surfaces were split into five refinement sections and five refinement volumes, as seen in Figure 3.5. These splits and levels were selected to capture the flow physics sufficiently while minimizing the number of elements used to save computational time. The cell sizes used and the meshes investigated are given in Table 3.1; the mesh size used in this thesis was the medium level. The evaluation of the three meshes and motivation for the choice of mesh can be found in Section 3.4. Although the discussion presented here refers to the study on the two-truck platoon, it is to be said that, based on the knowledge acquired, similar investigations were performed for the combined platoons (truck-car and

truck-bus). More details of these investigations can be found in paper IV.

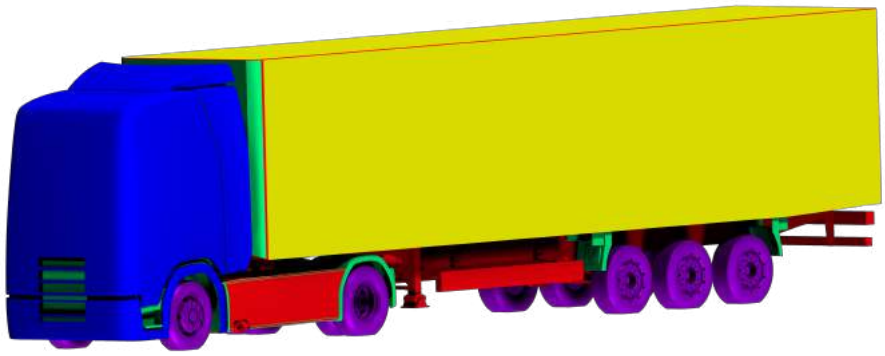

(a) *Levels of surface mesh size for the truck. The settings represented by each color can be found in Table 3.1*

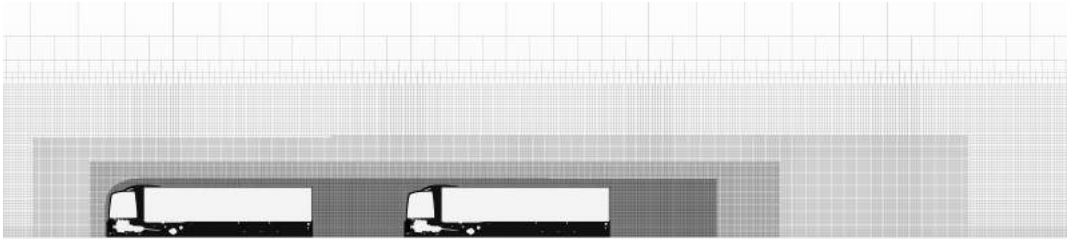

(b) *Section of the mesh at y=0 for a truck-truck simulation*

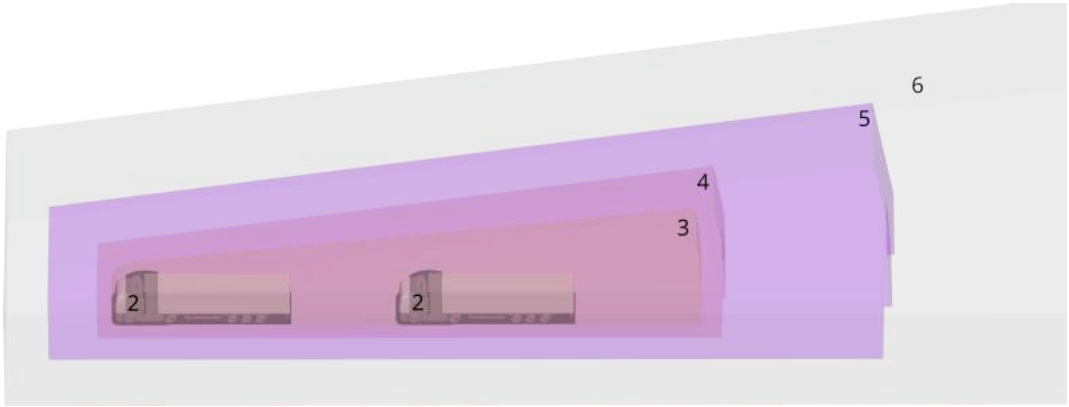

(c) *Levels of volume refinement under yaw conditions, the refinement boxes for the zero yaw cases are not swept toward the leeward side but are otherwise the same. The numbers refer to the levels that can be found in Table 3.1.*

Figure 3.5: *Mesh strategy.*

Mesh Resolution	Low	Medium	High
Base size	40mm	30mm	20mm
Level 1 (Blue/Red)	10mm	7.5mm	5mm
Level 2 (Green)	20mm	15mm	10mm
Level 3 (Yellow)	40mm	30mm	20mm
Level 4	80mm	60mm	40mm
Level 5	160mm	120mm	80mm
Level 6	320mm	240mm	160mm
Low y+ no. prism layers, cell size level 1 (Blue)	12	12	10
High y+ no. prism layers, cell size level 1 (Red)	3	3	2
High y+ no. prism layers, cell size level 2 (Green)	4	4	3
High y+ no. prism layers, cell size level 3 (Yellow)	6	6	4
Wheel mesh size	20mm	15mm	10mm
Wheel no. prism layers	10	10	8
Total cell count (platoon)	150M	240M	460M

Table 3.1: *Mesh study performed with the two-truck platoon. Surface and volume refinement levels, and number of prism layers for low, medium, and high mesh resolutions. Colors refer to surface refinement levels in Figure 3.5; the volume refinement boxes are numbered in the same figure.*

3.3.2 Convergence and solver settings

It is important to ensure sufficient convergence within each time step when using an implicit time discretization scheme. The simulations performed within this thesis used seven inner iterations per time step, allowing all residuals to drop well below 1e-3 within each time step. Flushing, clearing the domain of initial transients and establishing a developed flow, was done with more inner iterations as larger time steps take longer to converge. The domain was flushed for 22s before any averaging was initiated to ensure a fully developed flow field. This flushing consisted of 15s with a time step of 0.1s, followed by 5s at 0.01s, and finally 2s with the time step used during averaging, 0.8ms for the procedure used in this thesis. This final 2s equals roughly one flow passage of the entire platoon at the longest IVD, 20m. The flow field and forces were then averaged for 10s following the flushing portion to ensure reliable and reproducible results.

Some solver instabilities can occur when utilizing an automated mesher with thin prism layers on complex geometries. A velocity-dependent smoothing was therefore implemented to improve the simulation stability. This was done by applying gradient smoothing to cells with a velocity higher than 100m/s at the end of each time step. Further, to remain stable, some simulations required the removal of a few hundred cells during the initial part of the flushing period.

3.3.3 Boundary conditions

As the numerical investigations in this thesis mainly pertain to a highway environment, the boundary conditions were set to emulate the relative velocity between the vehicle and the road with a moving wall condition on the floor set to the same value as the inlet velocity, 25m/s. The outlet had a pressure outlet boundary condition, and the walls and ceiling were zero-gradient boundaries. For simulations with yaw, a velocity inlet was imposed on the left wall of the domain and a pressure outlet on the right side. So as to remain consistent with wind tunnel experiments when simulating cross-wind conditions, the wind velocity was the same as for zero yaw conditions, and only the direction of the incoming flow changed. The surfaces on the vehicle were set as no-slip boundaries, and the wheels were given the appropriate rotational speed. The cooling package was simulated as porous regions with the associated resistances, and the forces resulting from these regions were included in the calculation of the total drag coefficient times frontal area, $C_D A$.

3.3.4 Post processing methods

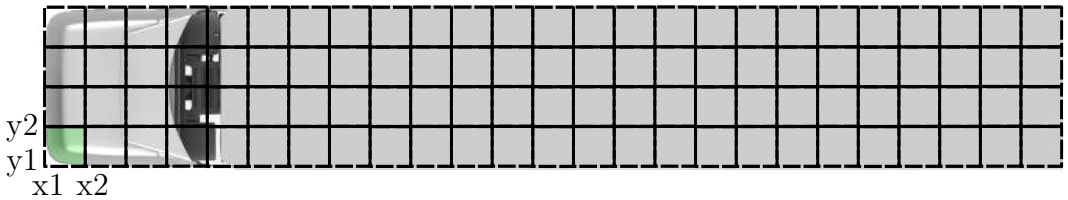

Figure 3.6: *Examplified binning for a bin B (in green) with the edges x1,x2,y1, and y2. Note that the actual bin size used is smaller.*

Distributed force plots, hereafter called X-ray plots, were used to ease the analysis of the numerical results and to identify areas that are sensitive to changing conditions. These were created by setting up a grid in the x-y and x-z planes. The faces of the vehicles surface were then sorted into different bins that correlate to this grid, after which their individual forces were calculated and summed for each of the bins, exemplified in Eq 3.1 and Figure 3.6 for a bin B in the x-y plane with edges x1,x2,y1, and y2 for the quantity F.

$$B = \sum_{x=x1}^{x2} \sum_{y=y1}^{y2} \sum_{z} F(x, y, z) \tag{3.1}$$

Once this data was acquired, it was then subtracted from the corresponding configuration to produce a plot with differences in drag contributions. This data is displayed using surface plots, giving a fast and easy way to visualize areas of further investigation. Examples of such plots will be presented and discussed in the results chapter.

To analyze the benefits of platooning for the individual leading or trailing vehicle, a quantity named platooning reduction, $\Delta C_{d,PR}A$, is defined according to Equation 3.2. In this equation, the drag area of the leading or trailing vehicle, $C_{d,Platoon}$, is subtracted by the corresponding values of an isolated truck, $C_{d,Isolated}$, at a chosen yaw angle configuration. To further evaluate the benefits under combined conditions of yaw and lateral offset, as well as comparing changes caused by yaw, Equation 3.3 is proposed. In this equation, the reduction of two selected configurations, C1 and C2, is subtracted to result in a delta reduction, $\Delta\Delta C_{d,PR,C1-C2}A$.

$$\Delta C_{d,PR}A = (C_{d,Platoon} - C_{d,Isolated})A \tag{3.2}$$

$$\Delta\Delta C_{d,PR}A = (C_{d,Platoon} - C_{d,Isolated})_{C1}A - (C_{d,Platoon} - C_{d,Isolated})_{C2}A \tag{3.3}$$

3.4 Accuracy of the simulation procedure

3.4.1 Mesh and time step resolution

As mentioned in Section 3.3.1, mesh studies were conducted for platoons with all vehicle combinations. Here, only the results for the two-truck platoon are presented. C_DA results for the three different mesh levels presented in Table 3.1 are shown in Figure 3.7, where the changes between meshes for the leading truck are small, while the meshes for the trailing truck are larger, especially for shorter distances. This could be due to an insufficiently resolved wake from the leading truck, causing changes in the oncoming flow for the truck behind. As the main interests in this thesis are drag delta trends and not absolute values, a 30mm base size mesh (medium resolution) was chosen since the deltas for this mesh are consistent with those of the highest resolution mesh. The computing resources required are roughly halved for this mesh compared to the finest, providing for the possibility of more simulations. The mesh studies performed with the car and bus confirmed this, enabling a straightforward comparison between the different configurations.

In order to find a proper time step length during the averaging period, a set of simulations were performed. For the initial simulations with two trucks, four time steps were tested with a separation distance, IVD, of 10m. These were 1.6ms, 0.8ms, 0.4ms, and 0.2ms. These results are presented in Figure 3.8 and show that decreasing the time step below 0.8ms does not yield any large changes in drag. Similar studies were performed for an isolated passenger vehicle and bus, although with 4ms, 0.8ms, and 0.2ms. As the goal is to understand the changes in drag, which are often large, a time step of 0.8ms was deemed to be sufficiently small to yield reliable results for all platoon combinations.

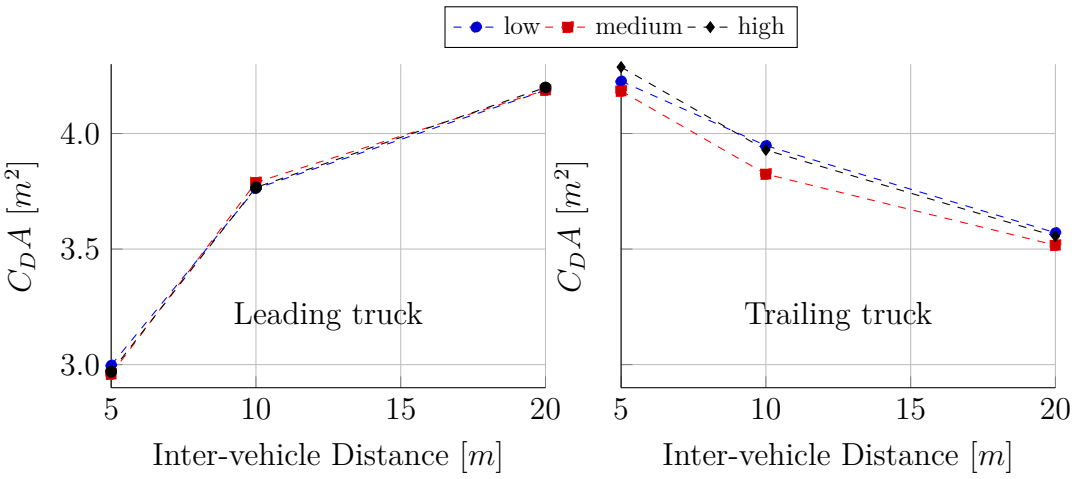

Figure 3.7: *C_DA v inter-vehicle distance for three different mesh resolutions according to Table 3.1.*

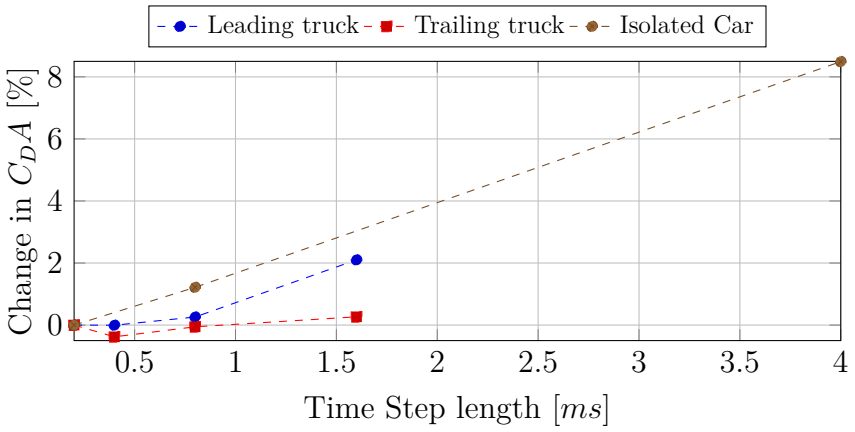

Figure 3.8: *C_DA v time step length during the averaging period.*

3.4.2 Averaging time

A sufficient averaging time is required to ensure reliable forces and flowfields; however, the minimum viable averaging time should be used as the computational time increases linearly with it. There are several ways to ensure that this is the case, and two of them have been considered in this thesis using the two-truck platoon. The first one is described in Eq. 3.4 and represents the standard deviation of a moving mean of C_DA.

$$\sigma_i = \sigma\left(\sum_{j=n}^{n+i} C_{D,j}\right), n = 1, 2, 3, \ldots, k-i, i = 1, 2, 3, \ldots, k \tag{3.4}$$

The results from this analysis are shown in Figure 3.9 and imply that an averaging time of 8s is sufficient for a low standard deviation for the leading truck. This is

true for the trailing truck as well, although the standard deviation is somewhat higher. This method of analysis is not very useful close to an averaging time of 10s, as the number of samples decreases when the averaging time becomes longer. However, some data can be inferred from the lower end of the graph by extrapolating the trends. This extrapolation would yield an uncertainty that is well below 5 C_DA counts (0.005 C_DA) (roughly 0.12% of the total drag) with an averaging time of 10s. This is significantly smaller than the expected changes seen in a platooning scenario and is thus deemed acceptable.

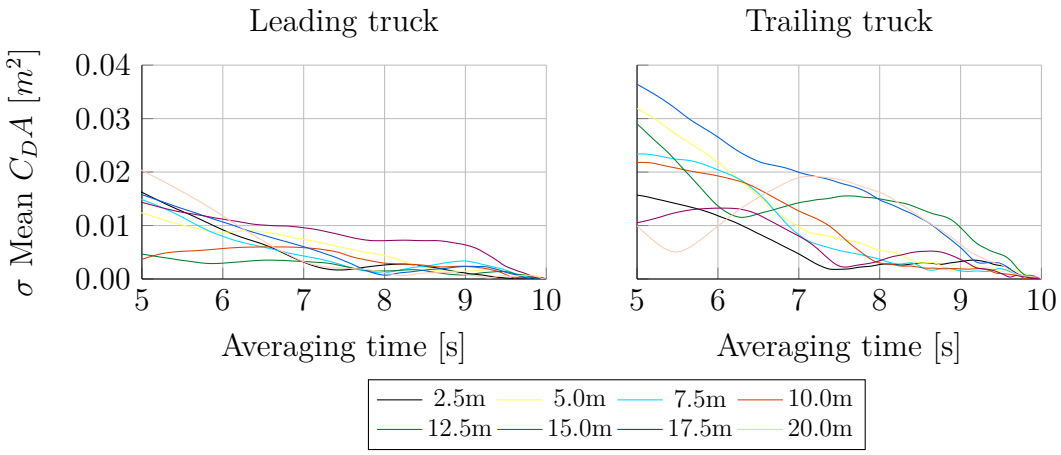

Figure 3.9: *Uncertainty of final C_DA as a function of averaging time.*

Additionally, the second approach used Eq. 3.4 to estimate the uncertainty of the mean value if the force fluctuations were normally distributed and random (see Figure 3.10a).

$$\Delta F_{avg} = \frac{\sigma}{\sqrt{n}} \tag{3.5}$$

The estimated uncertainty for both trucks as a function of IVD is shown in Figure 3.10b, where the averaging time used was 10s. The drag fluctuations are significantly larger for the trailing truck, thus yielding greater uncertainty. Further, the uncertainty is slightly higher for lower IVDs, except for the 2.5m case. This is likely due to a larger influence of the leading truck's wake as the distance decreases. The stabilized effect seen at 0.5m is believed to be due to a change in flow structures leading to smaller fluctuations. Although this gives an estimation of uncertainty, it is likely an optimistic estimation. A further study on the averaging time for a mixed platoon with a car or bus was not performed, as both vehicles are smaller, which should result in a lower needed averaging time.

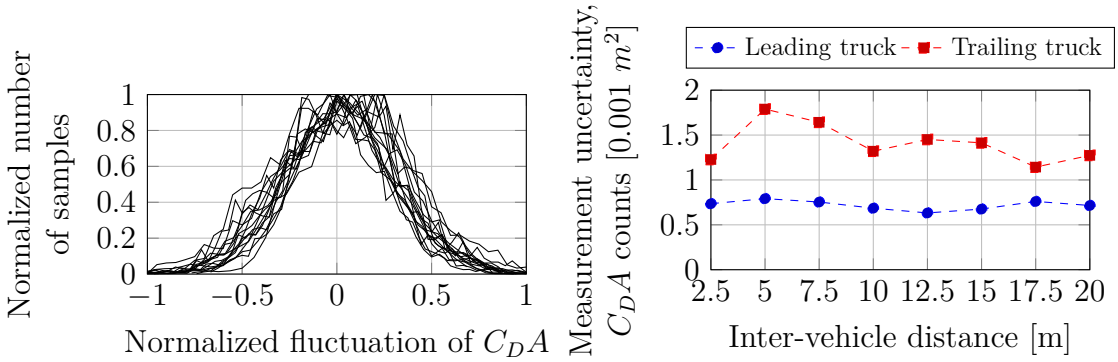

(a) *Normalized C_DA fluctuations v number of times they occur, showing a normal distribution of force fluctuations around the mean drag value. The fluctuations are normalized with the absolute value of the largest or smallest value, depending on which is greater.*

(b) *Uncertainty of C_DA value measured in 1/1000 C_DA.*

Figure 3.10: *Standard deviation of mean C_DA versus time of averaging.*

3.4.3 Flow field analysis

Model derived values

To investigate the reliability of the simulation method, the turbulent viscosity ratio (TVR), the IDDES blending factor, and the Courant–Friedrichs–Lewy (CFL) criteria were analyzed, Figure 3.11. As seen in Figure 3.11a, there are no significant jumps in the TVR, and the values are reasonably low in most areas except close to the truck surfaces and ground. These higher TVR values are expected near surfaces as these areas are handled by URANS in the IDDES model used. This is visible in Figure 3.11b, where the model switches quickly to LES mode outside areas close to the truck surface. Furthermore, the areas close to the surface (boundary layer) are shielded by the IDDES model and remain in URANS mode. Finally, the CFL number is around 1 or lower in most areas, except where large accelerations in the flow occur, see Figure 3.11c. Ekman et al. [102] have shown that for scale-resolving simulations using an implicit time marching scheme, a CFL number of up to 20 is acceptable, even if a high degree of accuracy is required. The values presented here are well within this requirement.

Resolved turbulent kinetic energy ratio

$$k_{\%res} = 100 * \frac{k_{res}}{k_{res} + k_{mod}}, \quad k_{res} = \frac{1}{2}(u_i' u_i'). \tag{3.6}$$

(a) *Turbulent viscosity ratio*

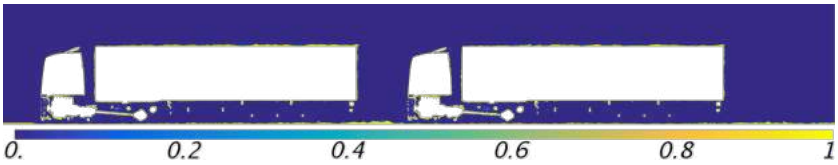

(b) *IDDES blending function indicating which mode is used: 0 being LES and 1 URANS*

(c) *CFL number, instantaneous values*

Figure 3.11: *Cut planes at y=0 showing TVR, IDDES blending factor, and CFL for a 2.5m inter-vehicle distance.*

To ensure that the mesh is sufficiently refined for the simulation, the percentage of resolved turbulent kinetic energy is computed in Eq. 3.6. Pope [103] suggests that this metric should be above 80% for a well-resolved LES; this is shown to be true outside the boundary layers in Figure 3.12.

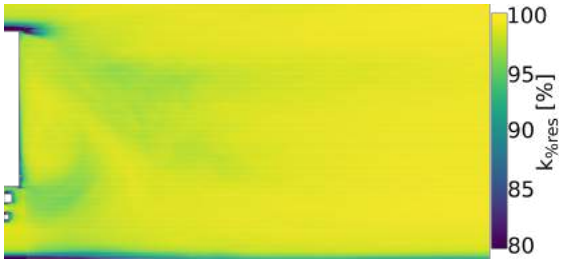

Figure 3.12: *Percentage of total kinetic energy that is resolved for the wake at y=0.*

Two-point correlation

To further assess the validity of the mesh, a two-point correlation investigation was performed for a plane along the symmetry line of the wake of an isolated truck. This type of analysis has previously been used in [104, 105] and provides a better measurement of mesh resolution of an LES-type simulation than the energy spectra

or the resolved turbulent kinetic ratio [103] presented in the previous section. The normalized two-point correlation is defined in Eq. 3.7 and calculated for all points in the plane.

$$C_{u_i u_i}(x_1, x_2) = \frac{\overline{{u_i}'_{x_1} {u_i}'_{x_2}}}{u^2_{i_{rms}x1}} \tag{3.7}$$

Figure 3.13 shows the number of cells having a normalized correlation of 0.1 or greater. The graphs were split up into correlation in the x and z direction for the different velocity components. The value of 0.1 was chosen to indicate that there was no longer any correlation between the two points, as it would not be feasible to assess the correlation for each point manually. According to Davidsson [106], a minimum of 8 cells is recommended to be correlated for a coarse LES. This is shown to be true for most cells in the wake except for the span-wise velocity in the z-direction, Figure 3.13d, where the correlation in the top shear layer of the wake is poor. These deficiencies are attributed to the small scale of the span-wise structures present in the shear layer not being sufficiently captured by the mesh. There are further small areas of insufficient correlation around the rear underrun protection underneath the trailer as well as near the surface of the trailer. These are not expected to significantly impact the results of the simulations as these areas are not a primary point of interest.

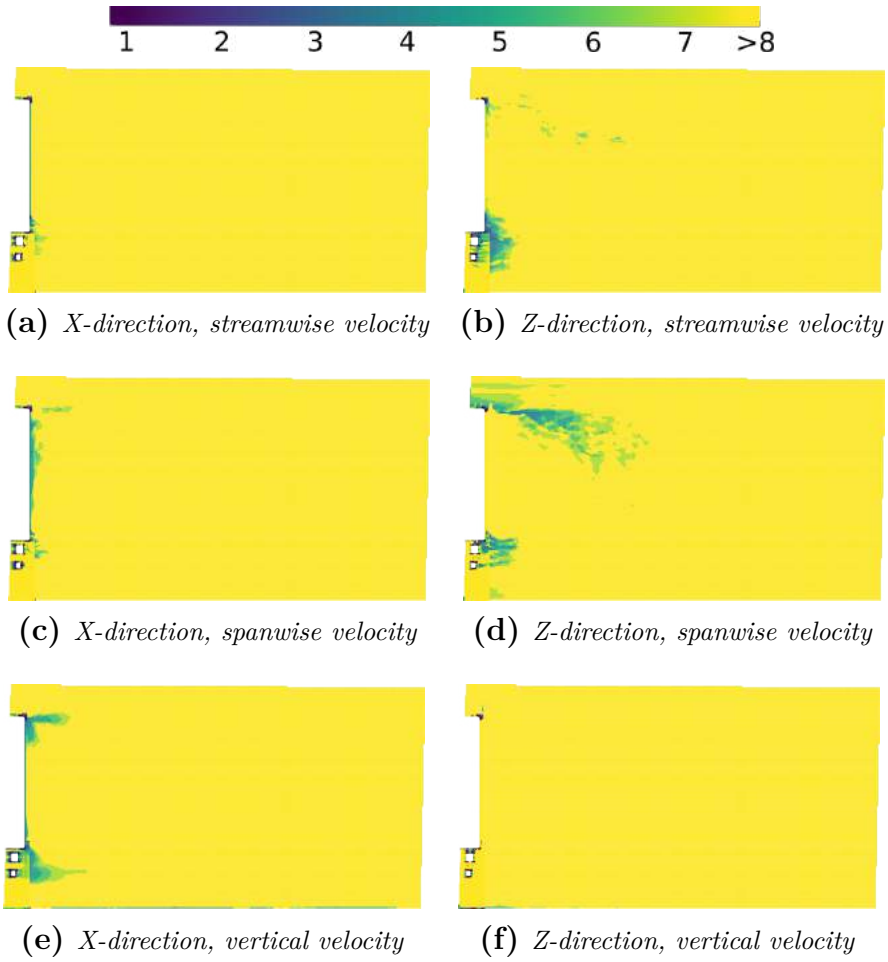

(a) *X-direction, streamwise velocity* **(b)** *Z-direction, streamwise velocity*

(c) *X-direction, spanwise velocity* **(d)** *Z-direction, spanwise velocity*

(e) *X-direction, vertical velocity* **(f)** *Z-direction, vertical velocity*

Figure 3.13: *Two-point correlation: Number of cells until the correlation drops below 0.1 for the wake at y=0.*

3.4.4 Comparison with wind tunnel data

This section consists of a comparison of the CFD and experimental data to further ensure the reliability of the numerical results. The normalization is made toward the corresponding values for an isolated vehicle, and the focus is on capturing the right trends rather than absolute values.

Figure 3.14 presents the normalized $C_D A$ values for both the numerical and experimental methods and shows that the general trends agreed well with each other. Some differences in the deltas between configurations can be seen, where the numerical method generally yielded a larger decrease for the leading vehicle and a smaller decrease for the trailing vehicle. The experimental results showed smaller savings for the leading vehicle and larger savings for the trailing vehicle.

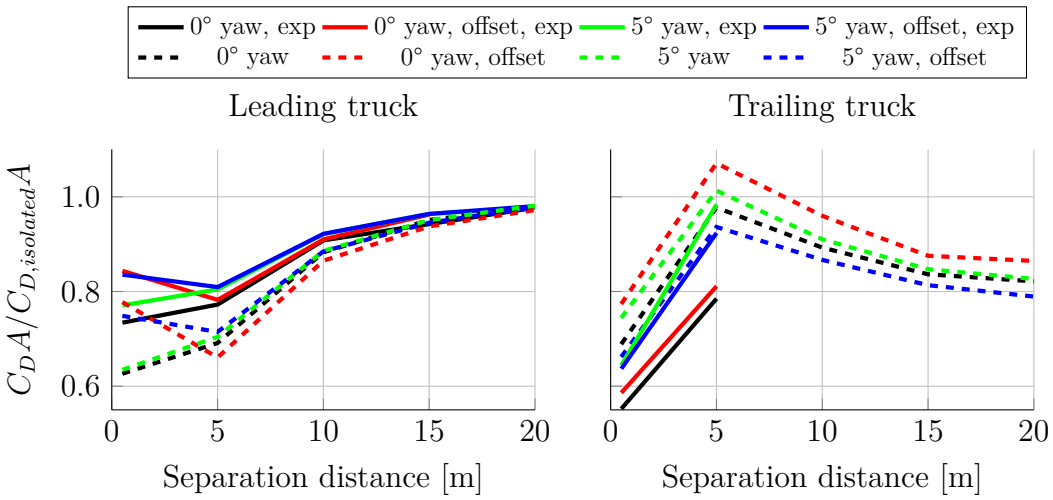

Figure 3.14: *Normalized C_DA versus separation distance for the leading and trailing trucks with and without lateral offset (0.5m) and yaw.*

Surface coefficient of pressure, averaged over all probes on one surface, were also compared for the different scenarios. Figure 3.15 shows good agreement of base pressure between the two methods. The same is valid for the front surfaces of the trailing truck, Figure 3.16a, although with an over-estimation in CFD of the stagnation pressure for all distances and for the tractor trailer gap at short distances.

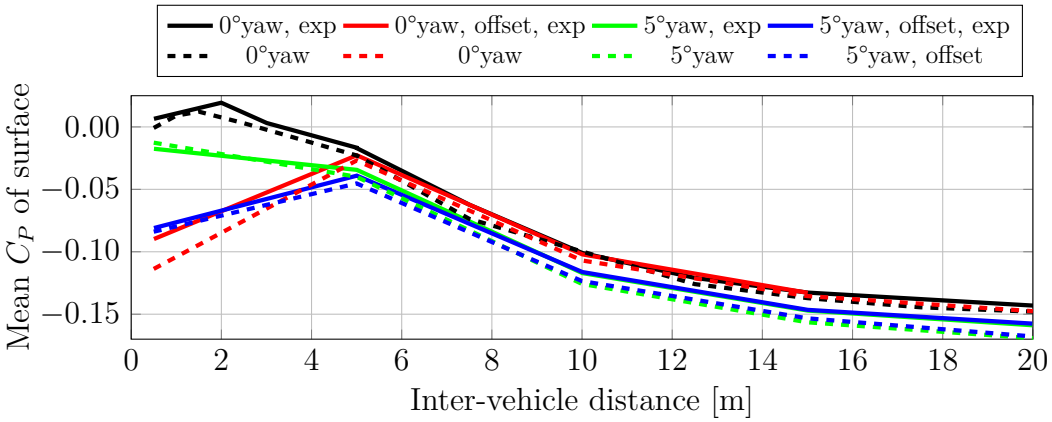

Figure 3.15: *Average C_P on the base of the leading vehicle versus IVD, experimental data in solid and CFD is dashed. Measurement model.*

Some of the discrepancies between the two methods can be attributed to the models not being identical, with the dummy model having side skirts and a different undercarriage. Additionally, the mounting solution likely had an impact on the results, something which was not replicated in CFD.

With the results from this comparison as well as the analysis of the mesh and time step resolutions, the numerical procedure was deemed sufficiently accurate to

explore the aerodynamic interactions between two vehicles.

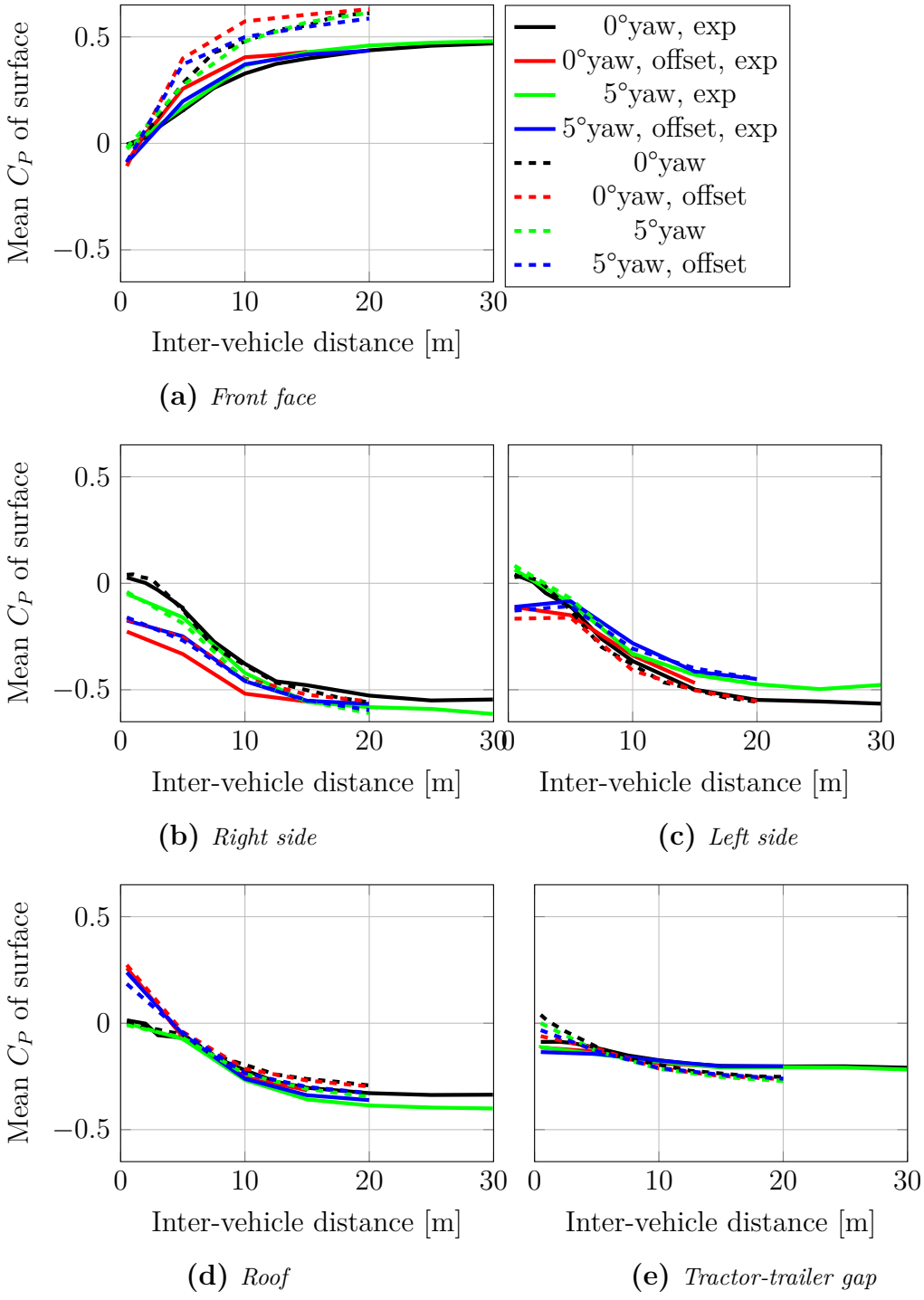

(a) *Front face*

(b) *Right side*

(c) *Left side*

(d) *Roof*

(e) *Tractor-trailer gap*

Figure 3.16: *Average C_P on the different surfaces on the front of the trailing truck versus IVD, experimental data (dummy model) in solid and CFD is dashed.*

3.5 Experimental method

3.5.1 Wind tunnel

The experimental portion of this thesis was carried out in the Volvo Cars Aerodynamic wind tunnel. This tunnel is a slotted wall wind tunnel with a cross-sectional area of $27.1m^2$ and a slot open ratio of 30%. The tunnel is equipped with a ground simulation and boundary layer control system consisting of a suction scoop, distributed suction, and tangential blowers behind each of the five belts. The distributed suction system consists of a perforated floor with two portions; the part in front of the turntable has an open area ratio of 8.9%, and the portion on the turntable has an open area ratio of 4.5%. The five-belt system consists of four wheel-drive units and a center belt which is 5.3m long and 1m wide—roughly twice as long and wide as the truck model used. Forces are measured through an underfloor balance. The uncertainty of Cd measurements within a test is 0.5%Cd for a single isolated model. The drag values are corrected for both blockage and horizontal bouyancy, the correction is, however, small and only varies with 1% of the drag value, and thus does not influence the results significantly. The correction is only based on the isolated vehicle and not further corrected for the second vehicles presence. Two pressure measurement systems were used in this work (a PSI ESP-64HD pressure scanner for the dummy model and car, and FIRST SENSOR SensorTechnics HCLA0025DB were used with three Dewesoft Sirius HD-STGS modules for the truck when it was used as the measurement model) and both yield an uncertainty of roughly $0.003C_P$.

An outline of the wind tunnel test section is shown in Figure 3.17. The light green area in this figure represents the space that was occupied by the models, the red-filled area represents the area covered by the measurement model, and the outlined red rectangles represent two examples of positions for the dummy model. The maximum IVD investigated was 30m (full-scale equivalent), the maximum yaw angle was 5°, and the maximum lateral offset was 1m. A single yaw angle was chosen given fairly strict limitations of the time available in the wind tunnel and 5° is usually a good approximation for the wind-averaged drag for a COE truck, commonly used in the industry for development. For further information on the wind tunnel, its ground simulation system, and flow quality, see [104, 107].

3.5.2 Experimental setup

So as to enable experimental investigations of platooning in the Volvo Cars wind tunnel, scale models had to be used. This meant that a custom mounting solution and experienced personnel were required for safe operation on the moving belt. As the model itself and the belt were unable to support the full weight of the model, it had to be suspended from the ceiling.

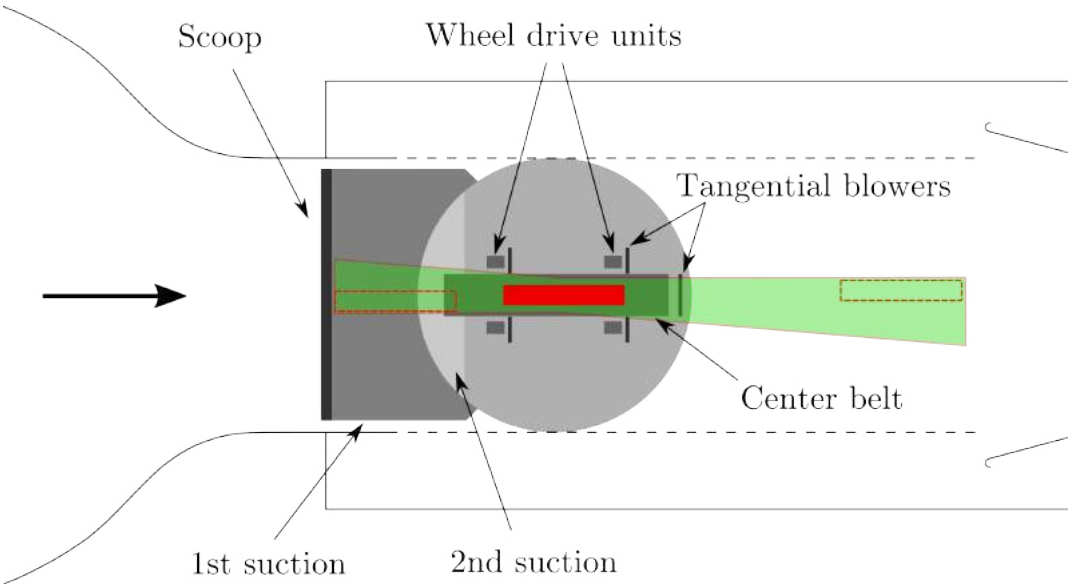

Figure 3.17: *Layout of the ground simulation system and the available space in the test section for varying IVD, lateral offset, and yaw.*

This was done by mounting a steel beam to the ceiling of the wind tunnel from which two 6mm steel cables were attached and then ran through the model's roof to the model's internal beams (see Figure 3.18a). This suspension of the model has the benefit of enabling the use of the wind tunnel's existing balance as the cables hang vertically and will thus not absorb the forces experienced by the model, assuming small movements of the vehicle. The stability of the model was ensured by pre-tensioning the cables. However, as the model is not constrained in the ground plane with these wires, it also had to be attached by 6mm steel cables to the existing restraint posts of the wind tunnel. These posts are usually fastened to the vehicle being tested in the wind tunnel and are connected to the balance below the floor. This is how forces were measured in this experiment. These cables will have an impact on the drag measured on the vehicle; however, this has been disregarded, as the main interests in this study were the differences between configurations and not the absolute values. The force on a set of isolated cables represents roughly 15% of the total drag of the truck. Without this force measured with the dummy model in many different positions, it is difficult to compute the difference in drag generated from the cables for different IVDs. This effect is not optimal and will influence the wind tunnel results, especially for the car, but no other feasible way of mounting the models was available, and thus the forces, including the cables, will be reported here.

In one of the experimental campaigns, the drag produced by the cables was also investigated, Figure 3.19, and showed that it does add a portion that changes the magnitudes of the trends. In order to quantify this drag, the cables were mounted in a similar fashion to what they would be mounted with a vehicle being present.

(a) *Leading truck is the dummy model, and the trailing truck is the measurement model.*

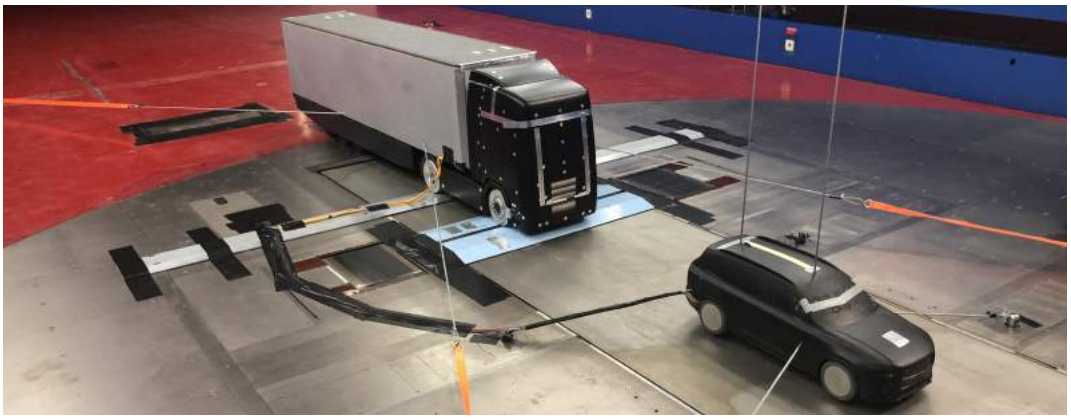

(b) *Car mounted for force measurement and dummy truck behind elevated off belt on the metal beams*

(c) *Dummy bus model in front of measurement model.*

Figure 3.18: *Mounting solution and models used for the different experimental campaigns.*

The force measured will be overestimated as more of the cables are exposed when connected to each other instead of a vehicle, Figure 3.18b. This is not considered in this thesis due to the complication of estimating changes in drag on the cables due to the wake of a vehicle in front.

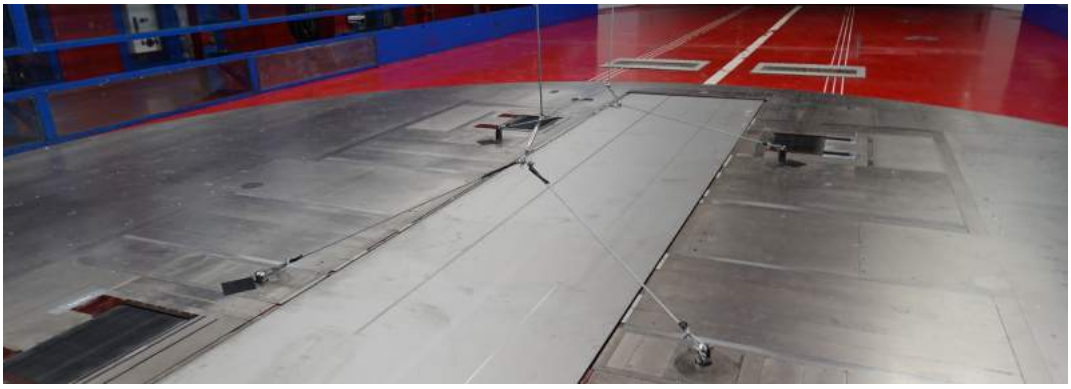

Figure 3.19: *Setup for measuring drag on cables.*

In the first experimental campaign with two trucks, investigating the effects between two trucks, the center belt drives the wheels of the truck, and the belt is not attached to the balance, the rolling resistance had to be removed from the total drag. This was done by setting the center belt to the correct speed with the wind off and taring the balance before the wind is turned on for each force measurement. These rolling resistance values should remain correct even if the model moves slightly due to aerodynamic forces, as the wheels are free-floating in the vertical direction. Unfortunately, after this first campaign, which included all truck-truck platooning scenarios, some damage was observed to the belt bearings, which meant that the rest of the experiments had to be run with some clearance between the wheels and center belt; this clearance was around 5mm. As in all subsequent tests, SUV-truck and bus-truck platoons, the wheels of the measurement models did not rotate; this taring was no longer necessary.

The dummy model was resting on the floor and held up by itself, and restrained in the ground plane by 6mm cables to existing holes in the floor. When the dummy model was placed over the center belt, it had to be held away from the belt to avoid damage to both the belt and the model. This was done by inserting a 20mm thick beveled beam underneath the wheels of the dummy model, and for the case of forces being measured on the car, two beams, one for the rear axle and one for the front on the tractor, Figure 3.18b. This elevation could potentially have an influence on the results; this is, however, disregarded as there was no other solution available at the time of the test.

All wheel-drive units were run at the corresponding wind speed to minimize the drag generated by them, as they are directly attached to the balance. Furthermore, two different modes were used for the boundary layer control system. When the dummy model was behind the measurement mode, the suction scoop and

distributed suction system were turned on; when it was in front of the measurement model, the suction was turned off as the dummy model stood on the system itself. Tangential blowing was not used to ease future comparisons with numerical simulations.

Chapter 4

Results

This chapter consists of a summary of the results of this thesis, split into four sections. Changes in drag are discussed in the first section, identifying configurations of interest to study further. The following section presents distributed and accumulated forces on the vehicles, CdA versus x (along the length of the vehicle), and X-ray plots, marking the areas for flow field analysis. The section after describes the different flow phenomena observed in platooning, and finally, a short section on where, in terms of IVD and conditions, the different effects are most dominant.

All forces are normalized toward the forces experienced by an isolated vehicle, and the distances presented are full-scale equivalent. Most of the analysis is directed to the platoon of two trucks as more experimental and numerical data fo this combination is available, and many of the effects are similar to the other combinations. Additionally, no direct comparison will be made between the numerical and experimental results. If this is of interest the reader is encouraged to review the included papers.

4.1 Drag forces experienced by vehicles in a platoon

The results presented in this section have been normalized towards the same isolated vehicle under the same yaw conditions. This normalization will make the relative drag reduction under yaw conditions seem smaller, as the drag his higher under yawed conditions. Normalization enables direct comparison between wind-tunnel and experimental data, as the values between these methods differ due to the cables used, as well as between different vehicle types. The absolute C_DA deltas for the configurations shown in this chapter can be found in Appendix A. Although three different geometries were used in this study, some common trends of the drag behavior were evident when these were placed as the leading or trailing model. A general observation was that a small vehicle (passenger car) will not have an especially significant influence on a large vehicle (truck or bus), with the opposite being true for a large vehicle leading a smaller vehicle.

4.1.1 Leading vehicle

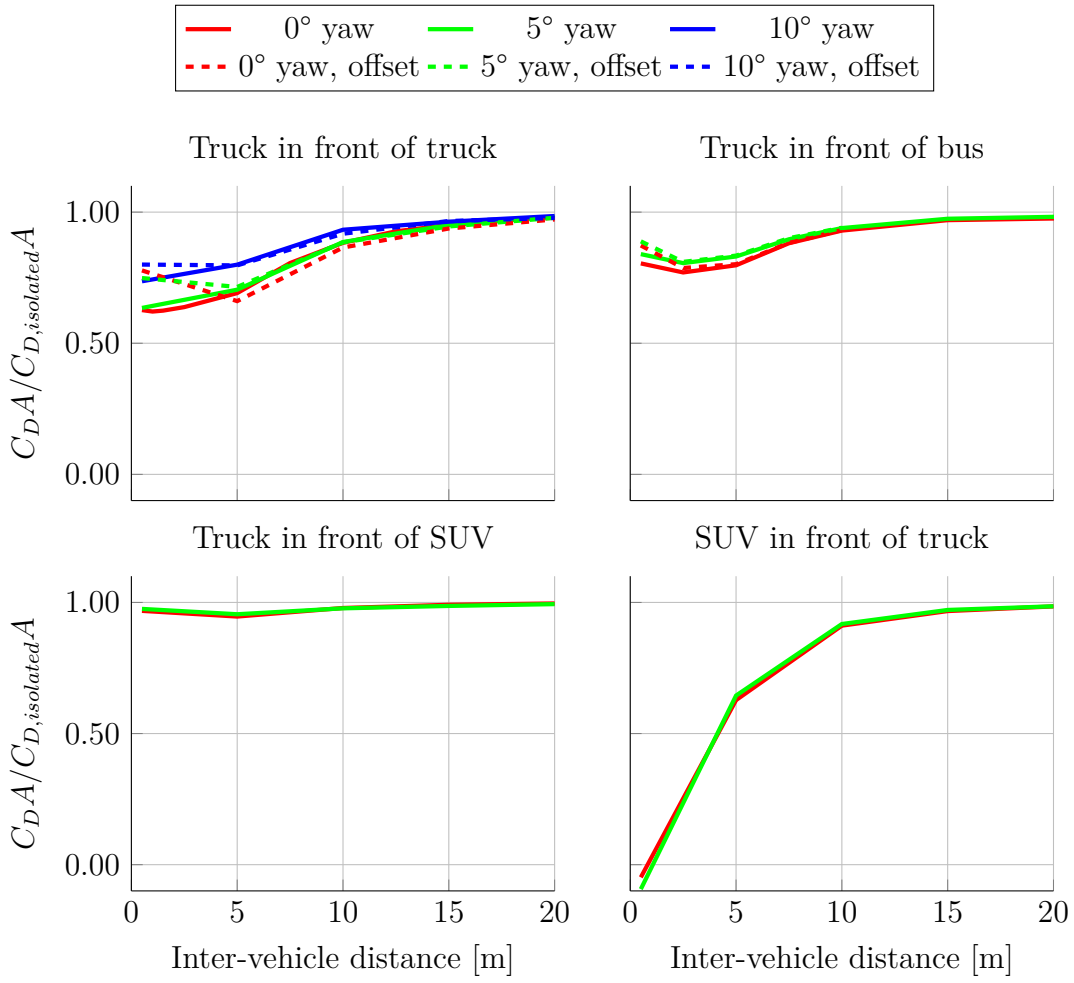

Figure 4.1: *Normalized C_DA versus separation distance for the leading vehicle with and without lateral offset (0.5m) and yaw. Results from CFD computations, except for truck in front of bus results which are experimental.*

In this section, the drag force experienced by the leading vehicle is discussed. As mentioned in the methodology section, force measurements in the wind tunnel were only performed for the truck and passenger car, as these were the models placed on the center belt. For the present, there are no CFD simulations of the bus as the leading vehicle, so the plots in Figure 4.1 refer solely to the truck and the SUV.

In general, the results show that, for the range of conditions considered, the drag is reduced as the distance separating the two vehicles decreases, except for some configurations in which the truck experiences some drag increase at distances lower than 5m (these will be explained in further detail in Section 4.3). Moreover, as expected, the drag reductions for the truck in front of the car (Figure 4.1) are

quite small. For the case of the SUV as the leading vehicle, drag goes even negative at the shortest distance, 0.5m. Other observations from the figures are that the proportional drag change of the leading vehicle is quite insensitive to changes in yaw angle from 0°to 5°. For a 10-yaw angle (only studied with the truck–truck combination), there is a reduction of efficiency for all distances investigated. This means that the benefit of an increased base pressure caused by the vehicle behind is not enough to overcome the negative effect of a large yaw angle. When a lateral offset is applied, an increment in drag is noted at IVDs shorter than 5m, otherwise the leading truck is practically unresponsive to this condition and its drag behaves as without the offset. The differences in absolute magnitude between the truck and bus as the second vehicle (Figure 4.1b) should not be compared too closely, as the drag reduction measured in the experimental campaigns tended to be lower for the leading vehicle and larger for the trailing vehicle compared to the CFD simulations.

4.1.2 Trailing vehicle

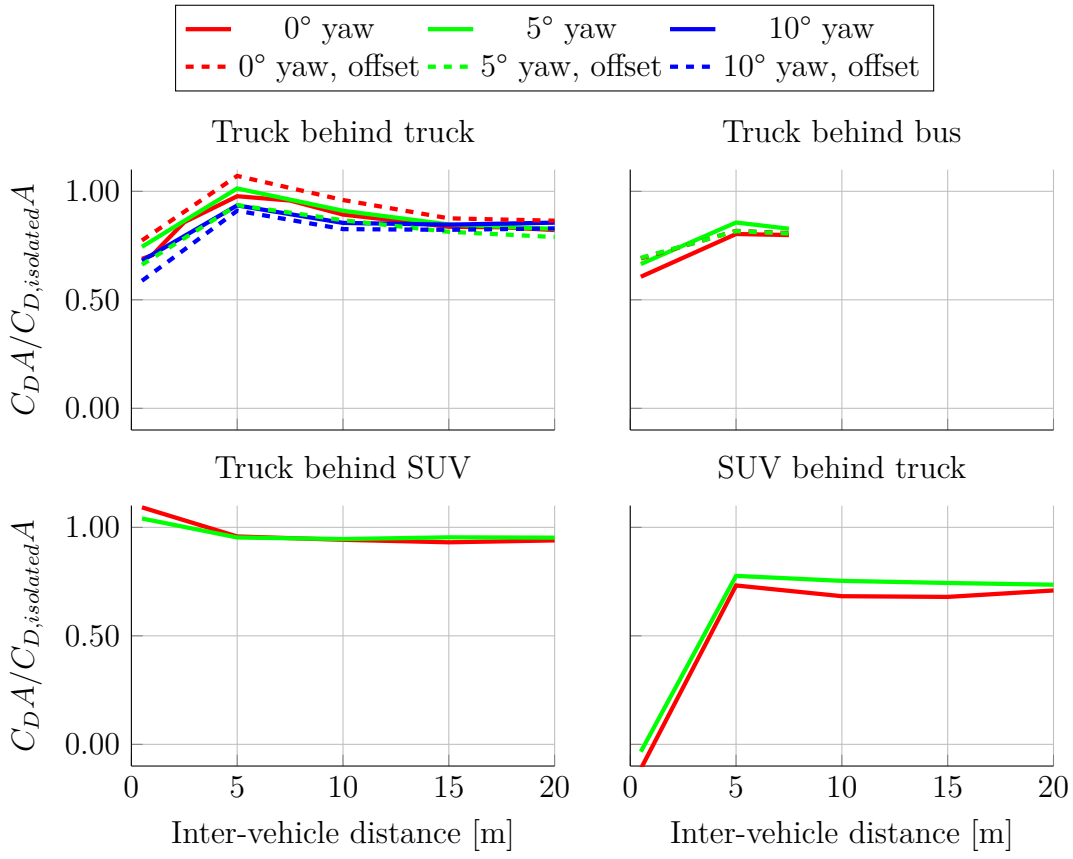

Figure 4.2: *Normalized C_DA versus separation distance for the trailing vehicle with and without lateral offset (0.5m) and yaw. Results from CFD computations, except for truck behind a bus results which are experimental.*

The trailing vehicle, particularly the truck, sees a more complex change of normalized drag when varying separation distance, lateral offset, and yaw, Figure 4.2. One of the general trends is that the drag tends to increase with a reduced distance, from 20m to around 5m. This behavior has also been observed in other studies using trucks [23, 29, 33, 40]. Furthermore, it can be seen that for a distance below around 5m, the drag decreases rapidly, even down to negative values for a car behind a truck. The changes seen for a truck driving behind a car, Figure 4.2, are distinct from the other platoon combinations, with an increase in drag toward the lowest IVD.

A noteworthy point on the truck in combination with both a bus and truck is that there is a decrease in efficiency when the vehicles are not aligned at zero yaw and that small yaw angles tend to degrade the performance. Additionally, the trailing truck in a truck–truck combination, Figure 4.2, shows a proportional drag change improvement at high yaw angles such as 10°, particularly with an offset.

The reasons for this will be explored in Section 4.3.

4.2 Drag force distribution and accumulation

Due to the complex nature of both flow and pressure changes, as well as the many different parameter combinations in platooning and model configurations, a method for fast identification of local changes in drag is necessary. For this, X-ray plots and accumulated drag along the vehicle, using both $\Delta C_{D,PR}A$ and $\Delta\Delta C_{D,PR}A$, are used to identify which areas of the vehicles see changes in drag. This information will then be used in the next section to find the aerodynamic phenomena responsible for these changes.

4.2.1 Leading vehicle

The effects on the leading truck, on a truck–truck combination, are fairly straight forward, and as expected from the shape of the drag reduction curves seen in the previous section. For a platoon at 0° yaw at several separation distances, Figure 4.3a, most of the change in drag stems from the base of the leading vehicle, with a small contribution from the undercarriage of the trailer for the truck. Small yaw angles do not affect the leading vehicle much (not shown here); however, a moderate loss of performance is seen at short distances and 10° yaw. This loss of performance mainly stems from changes in the undercarriage of the trailer (toward the end), Figure 4.3b.

The truck also sees a small increase in drag from the upper half of the trailer base when leading a car at 0.5m IVD, Figure 4.4a, red on the upper half and blue on the lower half. If the car is instead ahead of the truck, at very short distances it sees a small increase in drag from the sides of the base and front, and a large decrease at the base, Figure 4.4b.

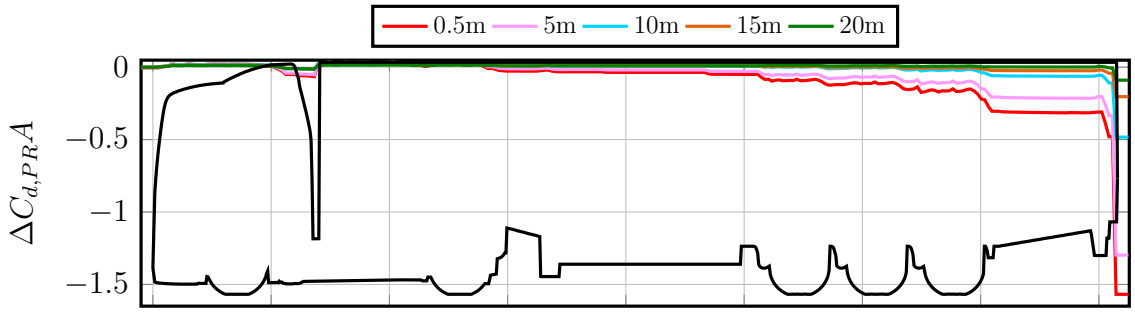

(a) *$\Delta C_{d,PR}A$ for 0°yaw. Values calculated according to Eq. 3.2*

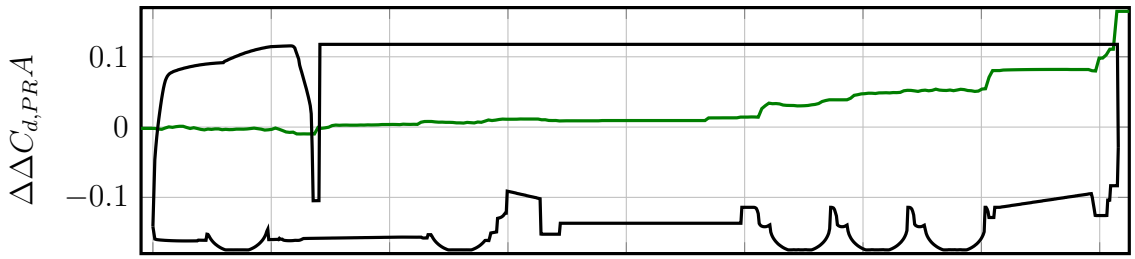

(b) *$\Delta\Delta C_{d,PR}A$ with a 5m IVD. Values calculated according to Eq. 3.3 with C1=10°yaw and C2=0°yaw*

Figure 4.3: *Delta drag accumulation along the leading vehicle in a platoon of two trucks and no lateral offset. Numerical results.*

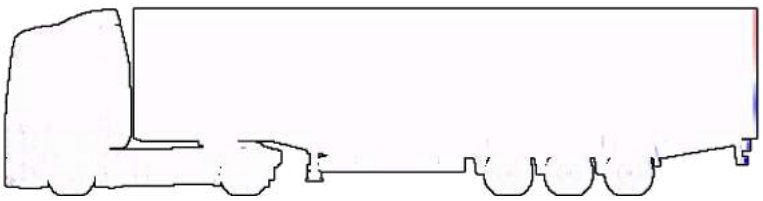

(a) *Leading Truck with a car as the trailing vehicle.*

(b) *Leading Car with a truck as the trailing vehicle.*

Figure 4.4: *X-ray plots of $\Delta C_{d,PR}A$ with zero yaw, zero lateral offset, and 0.5m IVD. Values calculated according to Eq. 3.2 Red indicates an increase in drag; blue indicates a decrease. The colors at the base of the car are saturated and only indicate an area of qualitative increase or decrease. Numerical results.*

4.2.2 Trailing vehicle

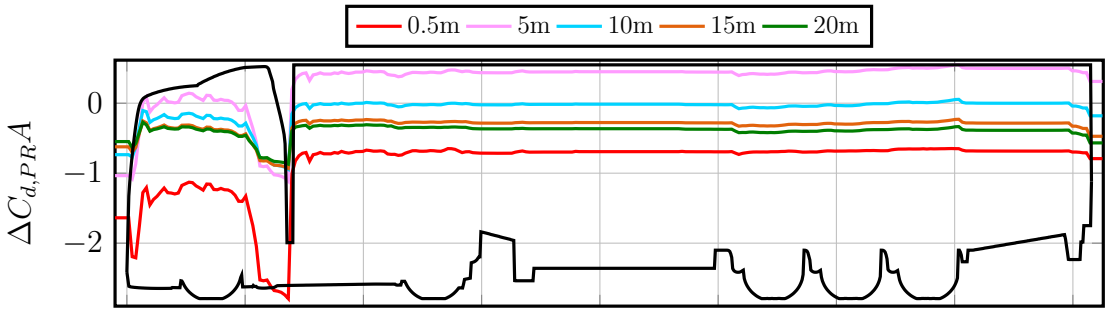

(a) *$\Delta C_{d,PR}A$ for 0°yaw. Values calculated according to Eq 3.2*

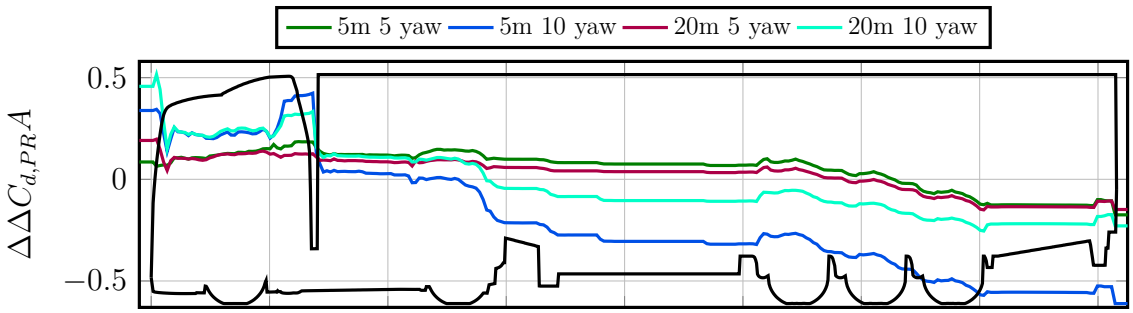

(b) *$\Delta\Delta C_{d,PR}A$, zero lateral offset, C1=as stated in legend, C2= 5m or 20m and 0°yaw. Values calculated according to Eq 3.3*

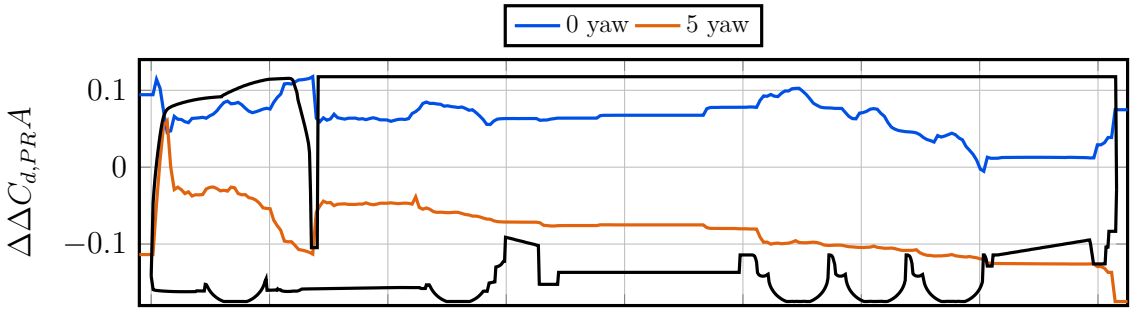

(c) *$\Delta\Delta C_{d,PR}A$, 10m IVD, C1=as stated in legend with 0.5m lateral offset, C2=as stated in legend without lateral offset. Values calculated according to Eq 3.3*

Figure 4.5: *Delta drag distribution along the trailing vehicle in a platoon of two trucks. Numerical results*

As presented earlier, the effects of platooning on the trailing vehicle are more complex, as observed by the drag behavior with decreased separation distance, Figure 4.2. This indicates that there are different flow effects present and that these vary in strength with distance.

From Figure 4.5a, it can be seen that a majority of drag reduction for the

(a) *5m IVD, 5°yaw*

(b) *5m IVD, 10°yaw*

(c) *20m IVD, 5°yaw*

(d) *20m IVD, 10°yaw*

Figure 4.6: *X-ray plots for the trailing vehicle created using Eq. 3.3 with zero lateral offset, C1=as stated in legend,C2=0°yaw. Red indicates an increase in drag; blue indicates a decrease. The colors at the front are saturated and only indicate an area of qualitative increase or decrease. Numerical results.*

trailing vehicle in a truck–truck combination at zero yaw comes from the front half of the vehicle. For the case of zero yaw, three main areas contribute to large changes in drag, namely the front face, front corners, and the tractor-trailer gap. In general, the areas that reduce drag on the front of an isolated vehicle (low-pressure areas, such as front corners or convex surfaces) tend to see an increase in drag with a decreased IVD when the vehicle is in a platoon as the trailing vehicle, and vice versa for the areas that create drag for an isolated vehicle (stagnation areas and the tractor-trailer gap).

An increasing yaw angle does not yield a consistent change in drag for the trailing vehicle, as was seen in the previous section. Thus, there are likely several effects that cause added or decreased drag; these can be seen in Figure 4.5b, where variations in drag along the trailing vehicle are studied at 5 and 20m separation distances with 5°and 10°yaw and compared to an equivalent 0°yaw case. These are even more evident in the X-ray plots of Figure 4.6. The areas that see the most change under yaw are the front, where a larger yaw angle and larger IVD creates a higher drag contribution. The trailer undercarriage experiences a decrease in drag; this reduction grows with a decreased separation distance and increased yaw

angle. The changes on the front of the vehicle due to yaw typically consist of an increase in drag on the leeward corner of the vehicle as well as the front face. The windward side sees a decrease in drag and so does the leeward corner at 20m IVD and 10° yaw. It can also be noted that the drag over the tractor-trailer gap decreases with larger yaw angles, compared to the effect seen at 0° yaw.

(a) *0°yaw*

(b) *5°yaw*

Figure 4.7: *X-ray plots for the trailing vehicle created using Eq. 3.3, C1=as stated in legend with lateral offset,C2=as stated in legend without lateral offset. Red indicates an increase in drag; blue indicates a decrease. The colors at the front are saturated and only indicate an area of qualitative increase or decrease. Numerical results.*

A lateral offset is investigated in Figure 4.5c to see how sensitive platooning is for alignment of the vehicles. The figure shows that lateral offset has different effects depending on if the vehicles are in yaw conditions or not. Lateral offset causes an increase in drag on the front of the trailing vehicle and a decrease over the front radii for a zero-yaw case, yielding an increase in drag post the immediate front portion of the truck; see Figure 4.7 for better visualization of the phenomena. For the 5°yaw case, the inverse is true, with a further reduction being present over the trailer undercarriage, gap, and base of the truck. This is confirmed in Figure 4.7b, and the exposed front half of the trailing vehicle experiences added drag, where the area of lower drag extends further to the right side of the vehicle in yaw conditions. From this information, it can be concluded that the area of focus for an extended flow field analysis of the trailing truck should be the aerodynamics of the tractor and the undercarriage of the trailer.

A truck trailing a car at an IVD of 0.5m sees a decrease in drag on the lower half of the front face and only small changes on the radii, while the upper half of the front face sees a substantial increase in drag, Figure 4.8a. The effects on the car are, generally, similar to those of the truck, except for an additional decrease in drag from the base of the vehicle, Figure 4.8b.

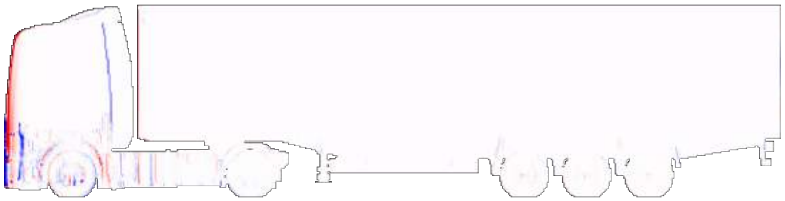

(a) *Truck in front of car*

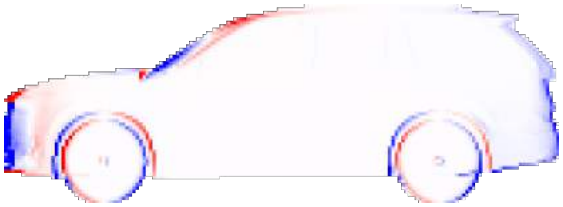

(b) *Car in front of truck*

Figure 4.8: *X-ray plots of $\Delta C_{d,PR}A$ with zero yaw, zero lateral offset, and 0.5m IVD. Values calculated according to Eq. 3.2 Red indicates an increase in drag; blue indicates a decrease. The colors at the front of the car are saturated and only indicate an area of qualitative increase or decrease. Numerical results.*

4.3 Aerodynamic phenomena

To understand further the changes in drag seen in previous sections and how to improve the drag reduction from platooning, a closer look into the flow behavior is presented in this section. Most of the discussions will concentrate on the truck–truck platoon combination, as these results provide a good overview of the aerodynamic phenomena in general. A few cases involving other vehicle combinations will also be presented, especially if they show a particular phenomenon only present for that combination.

4.3.1 Leading vehicle

The improvements seen for the leading vehicle under zero yaw conditions mainly stem from the increase in base pressure due to the stagnation pressure of the trailing vehicle, Figure 4.9. The rate of change of the base pressure with respect to IVD is, however, reduced as the stagnation pressure of the trailing vehicle becomes lower at shorter IVDs. Figure 4.9 also shows the increase in pressure on the base, where the pressure contours remain similar for 20 and 10m. For distances below 5m, a different pressure and flow field is observed between the two trucks. This is potentially caused by the trailing vehicle entering the recirculation region of the wake and changing its structure, entraining the two counter-rotating vortices of the recirculating wake and compressing them. This is well observed in Figure 4.10 for the 2.5m and 0.5m cases.

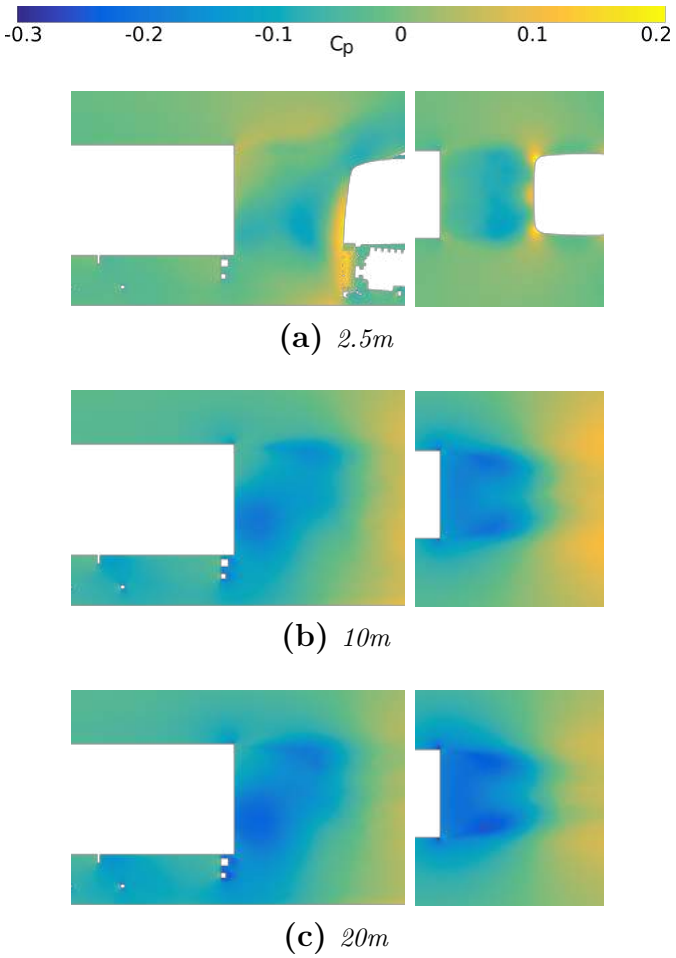

(a) *2.5m*

(b) *10m*

(c) *20m*

Figure 4.9: *Coefficient of pressure for three separation distances, Leading truck, Y=0 plane (left column), and Z=2.5m plane (right column). Numerical results*

Low sensitivity to lateral offset is seen for the leading vehicle as the pressure increase emanating from the trailing vehicle expands in a radial fashion forwards, meaning that the pressure increase is fairly stable in the lateral direction but changes rapidly in the longitudinal direction, Figure 4.11. Futhermore, lateral offset also causes an increase in stagnation pressure on the trailing vehicle, thus improving the benefit observed for the leading vehicle.

As plotted in Figure 4.1, the drag reduction due to platooning is less effective at 10° yaw. The reason for the additional drag generated by the underbody under large yaw angles can be seen in Figure 4.12 for an isolated vehicle and the leading vehicle in a platoon of two trucks. Compared to the isolated vehicle, a larger asymmetry in the wake, as well as changes in the flow underneath the trailer, can be seen in the platoon. More lateral flow as well as larger low-velocity areas can be seen in the figure. These changes are similar to those occurring when the yaw angle is increased, and will hereafter be called an increase in effective yaw angle. The increase in effective yaw angle is caused by the blockage of the trailing vehicle

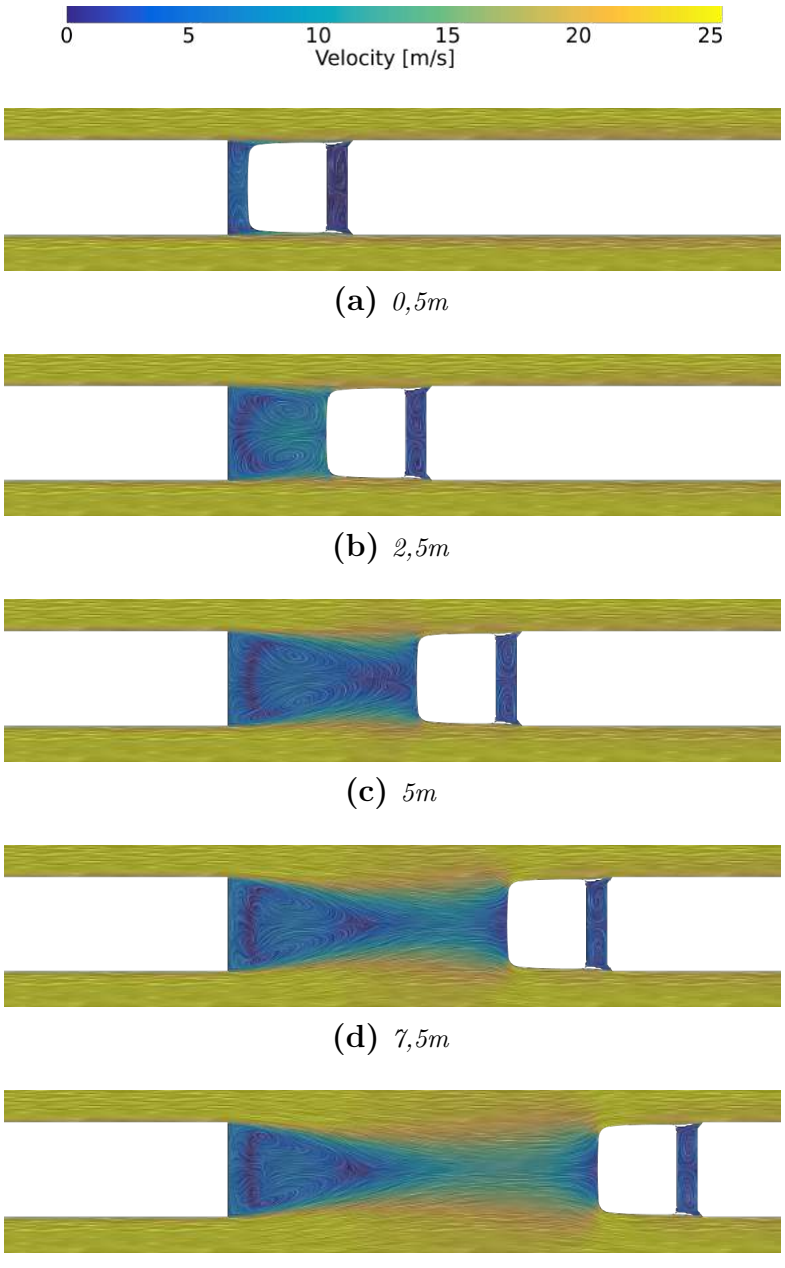

(a) *0,5m*

(b) *2,5m*

(c) *5m*

(d) *7,5m*

(e) *10m*

Figure 4.10: *Averaged velocity with Line integral convolution (similar to in plane streamlines), xy plane at z=2m,two trucks*

redirecting the flow and forcing more of the air to pass on the leeward side, thus increasing the yaw angle locally.

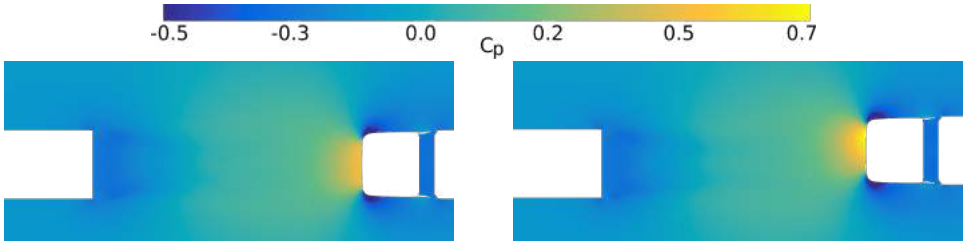

(a) *0m offset* (b) *0.5m offset*

Figure 4.11: *C_P for a plane at z=2m, 10m IVD, zero yaw.*

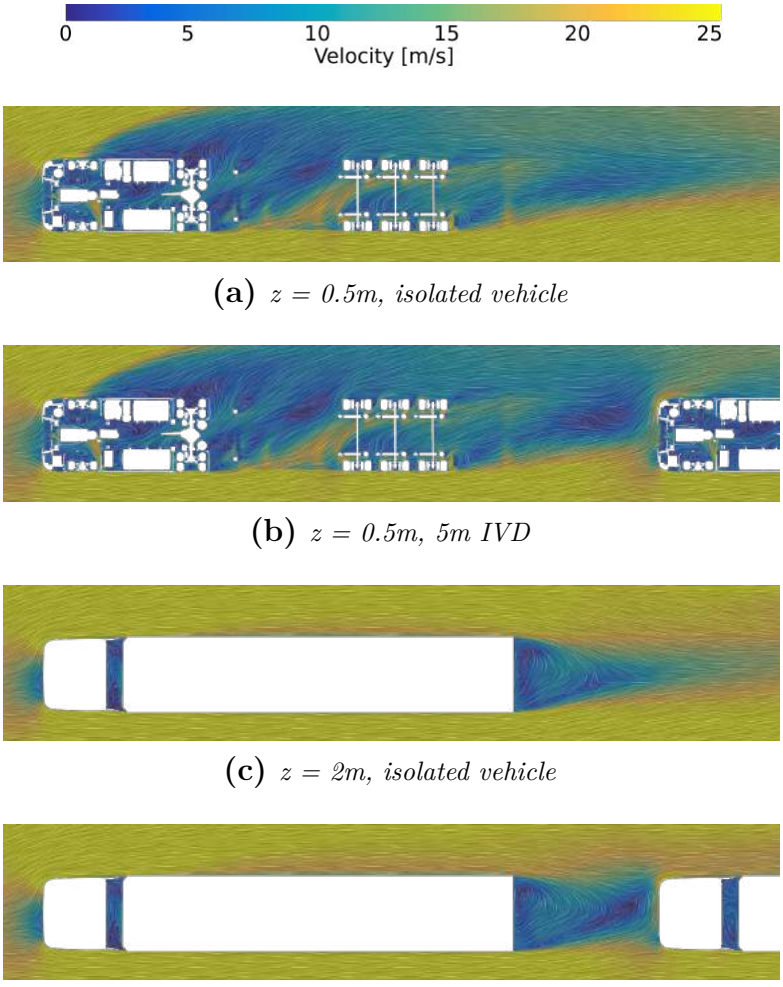

(a) *z = 0.5m, isolated vehicle*

(b) *z = 0.5m, 5m IVD*

(c) *z = 2m, isolated vehicle*

(d) *z = 2m, 5m IVD*

Figure 4.12: *Averaged velocity with line integral convolution, xy plane, 10° yaw, zero offset, two trucks*

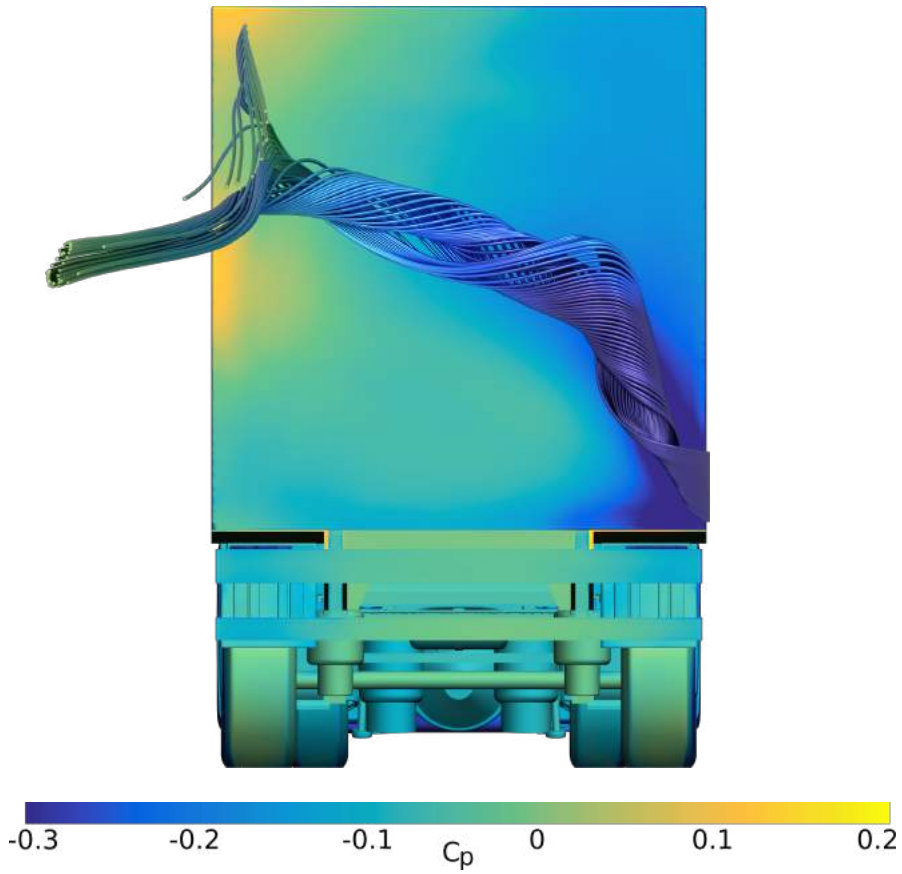

Figure 4.13: *Streamlines colored by Cp seeded along the bottom side edge of the leading truck showing a large vortex formation. Zero yaw, 0.5 m separation distance, and 0.5 m lateral offset.*

A lateral offset at very short distances produces a strong vortex along the diagonal of the base. This vortex is formed due to the increased lateral and vertical flow between the vehicles, Figure 4.13. The lateral flow is caused by a stagnation region formed at the front of the trailing vehicle on the exposed side. The vertical flow is induced by the high ground clearance of the leading trailer in combination with the low ground clearance and rake of the trailing tractor, forcing the air upward. This vortex generates a very low pressure locally on the base, increasing drag.

When a truck is leading a car at a very short separation distance, a slight increase in drag is observed in Figure 4.5a. This seems to be due to the wake of the truck being shortened and the vortex in the center of the wake being compressed and pushed upwards, Figure 4.14a. The shortening of the wake is known to increase drag, and the other changes to the wake seem to push the low-pressure area closer to the surface, reducing the base pressure and thus increasing drag, Figure 4.14b. This effect occurs as the top of the car is much lower than the top of the trailer, blocking the lower part of the wake and shifting the wake balance of the truck.

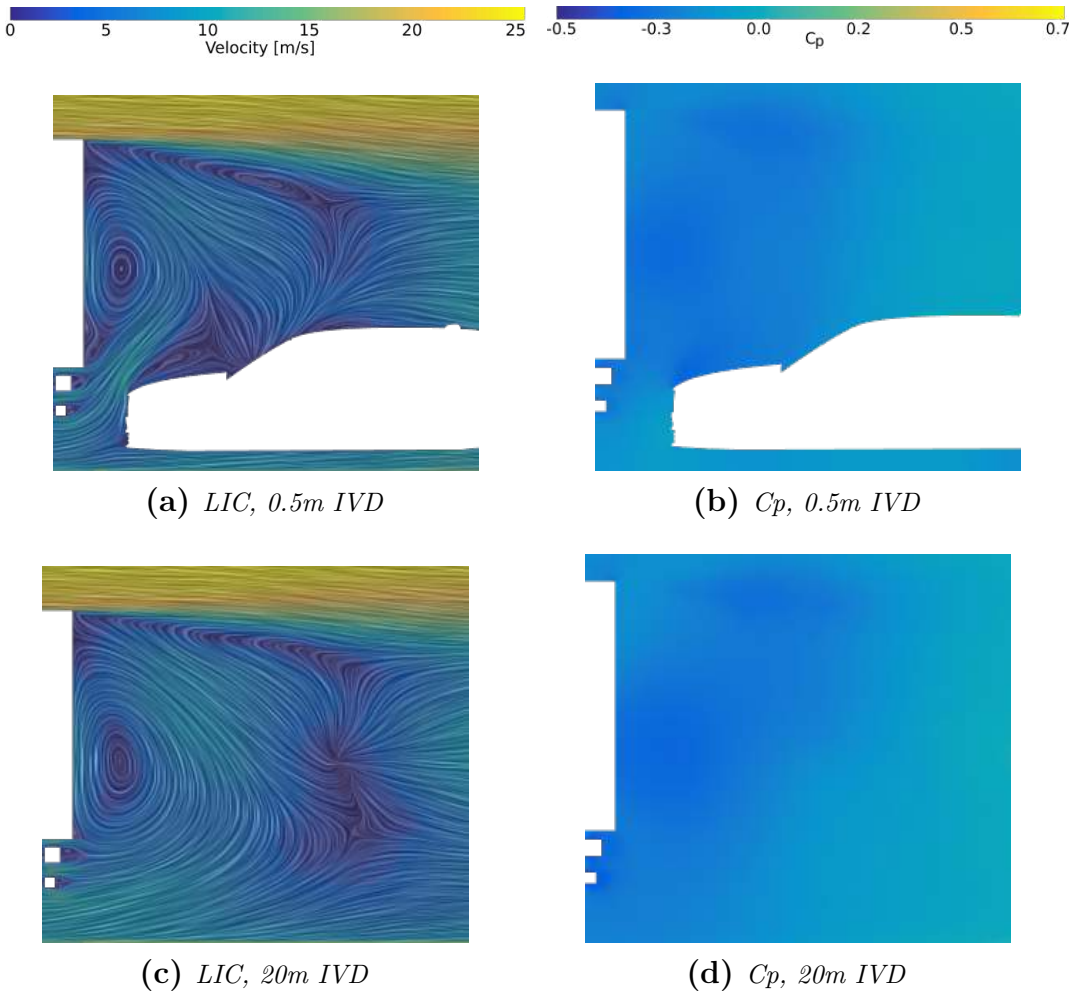

(a) *LIC, 0.5m IVD* **(b)** *Cp, 0.5m IVD*

(c) *LIC, 20m IVD* **(d)** *Cp, 20m IVD*

Figure 4.14: *Wake of the truck in front of car, xz plane on centerline. Left is line integral convolution colored by velocity magnitude, right is* C_p

When a car is in front of a truck at 0.5m IVD, an increased acceleration is seen on the lower part of the truck's front corners, a downwards direction of the flow behind the base as well as two small vortices on the side, lowering the pressure on the sides of the base of the car, Figure 4.15.

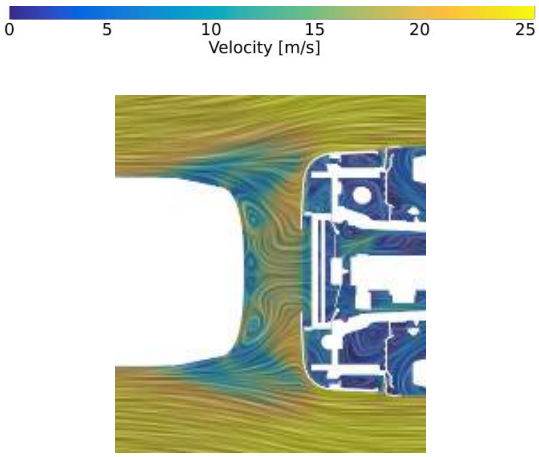

Figure 4.15: *Car leading truck at 0.5m IVD, zero yaw, zero offset. z=0.9m, xy plane, averaged velocity with Lic*

4.3.2 Trailing vehicle

Although the aerodynamic changes experienced by the trailing vehicle are much more complex than those of the leading vehicle, fewer special cases exist where specific flow changes only occur with certain vehicle combinations and distances. This makes the effects on the following vehicle more generic, with the major differentiating factors being the vehicle size (large frontal area—truck or bus, and small frontal area—SUV) and tractor-trailer gap of the truck. The vehicle size mainly causes changes in the magnitude of drag reduction, except for the shortest distance of a car leading a truck. The general changes are caused by differences in the flow velocity and angle, where the leading truck experiences changes mostly connected to pressure variations on the base created by the stagnation pressure of the vehicle behind. Many of these effects balance each other, where some yield an increase in drag and some a decrease in drag.

The main effects for the trailing vehicle are caused by a reduction of oncoming flow velocity, Figure 4.16, and a decrease in effective yaw angle, Figure 4.17. These cause a reduction in stagnation pressure (decrease in drag) on all investigated vehicle types at all distances and yaw angles. Another effect that is intrinsically linked with this is the reduction of acceleration on surfaces that have an acceleration when the vehicle is isolated, which causes an increase in drag. These two effects differ in how strong they are at different separation distances, resulting in a non-consistent drag behavior from the front of the vehicle.

An effect that is present for two trucks in platooning formation is the increase in tractor-trailer gap pressure, leading to higher drag, Figure 4.16. This increase in pressure is believed to be due to the changes in flow at the upper half of the gap between the vehicles resulting in poor performance of the roof air deflector, causing the flow to impinge on the top of the trailer front. Figure 4.16b shows that a vortex is formed at the top of the gap, which can be an indicator of an incorrectly

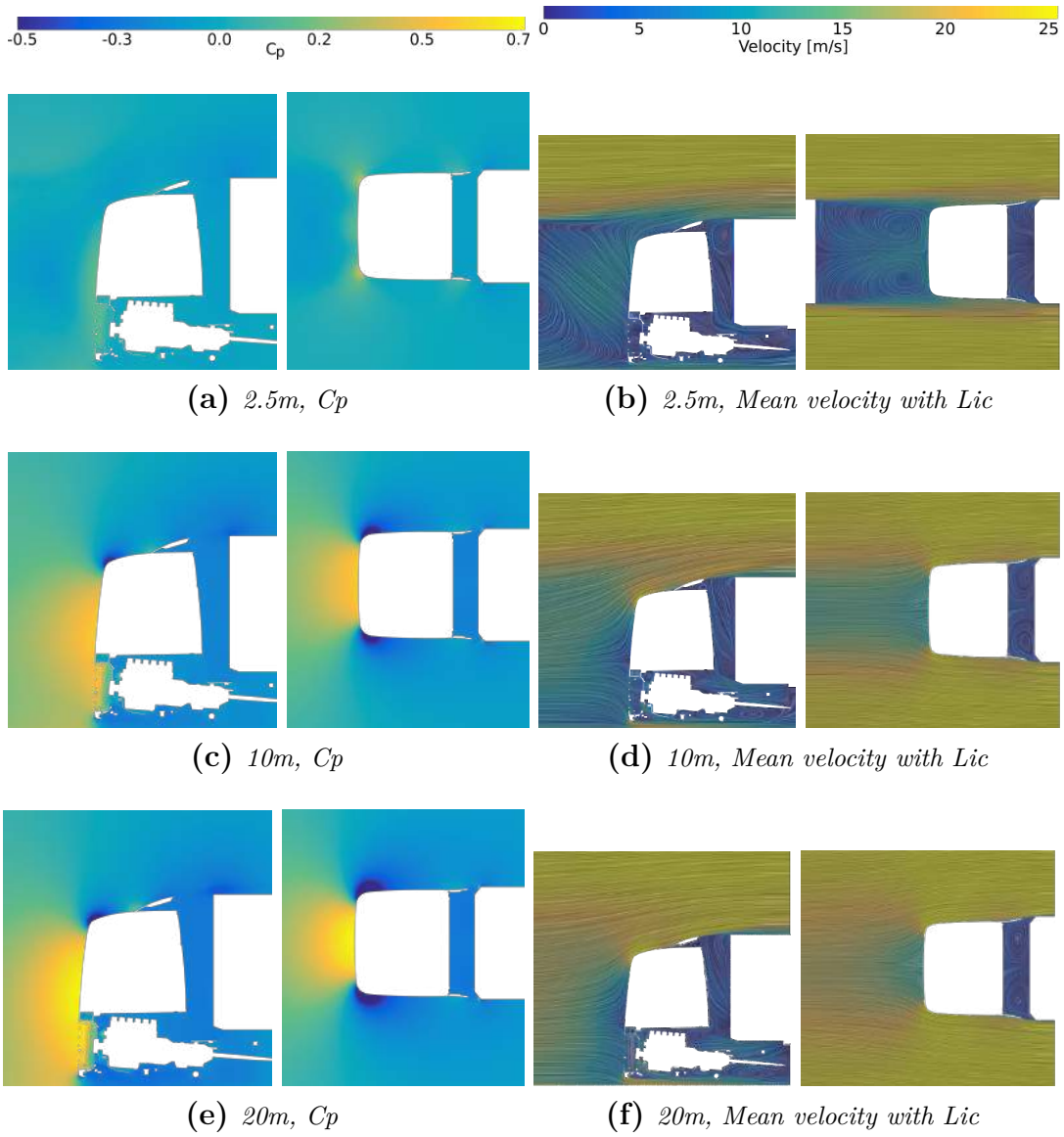

(a) *2.5m, Cp* **(b)** *2.5m, Mean velocity with Lic*

(c) *10m, Cp* **(d)** *10m, Mean velocity with Lic*

(e) *20m, Cp* **(f)** *20m, Mean velocity with Lic*

Figure 4.16: *Coefficient of pressure and line integral convolution at Y=0 plane (left) and Z=2m plane (right). Trailing truck, numerical results.*

set roof air deflector. The flow changes that are believed to cause the reduction in performance are that a general reduction in flow velocity, and reduced cooling flow, will not allow the air stream to clear the gap between the two bodies as well as the many changes near the top of the tractor leading to a different flow angle in front of the deflector, further reducing its efficiency. As the distance becomes lower than 5m, roughly the length of the recirculating wake of the leading truck, the structure of the two vortices inside the wake change, and as the distance decreases further to 2.5m, Figure 4.16b, they attach to the front of the trailing vehicle. This attachment of the vortices causes three separate stagnation areas to form on the

front of the trailing truck, increasing drag somewhat.

As was the case for the zero yaw conditions, the flow seen for the trailing vehicle under yaw is complex. There are two main effects: the first is a shifted wake of the leading vehicle causing a misalignment between the low-velocity wake and trailing vehicle, increasing the stagnation pressure and thus drag. The second is a decreased effective yaw angle as the leading vehicle works as a local flow straightener, and as was seen in the drag curves, Figure 4.2, this effect is strongest at shorter distances and large yaw angles. These two effects can be seen in Figure 4.17b-g, where the flow underneath the trailer has a smaller lateral component than that in Figure 4.17a.

It can also be noted that this is strengthened with shorter distances and larger angles. A reduction of the effective yaw angle slightly changes the direction of the wake. As expected, the wake from the leading vehicle travels toward the leeward direction. This causes the trailing vehicle to no longer be in the center of the wake, increasing the stagnation pressure on the now exposed side. The misalignment further reduces the acceleration on the leeward corner, compared to an isolated vehicle under the same conditions (not on the 20m and 10° yaw case as the wake essentially misses the trailing vehicle). To counteract this, a lateral offset is introduced, figures 4.17f and 4.17g, which further reduces the effective yaw angle (visible in the flow underneath the trailer and a slightly less asymmetric wake), as well as realigning the trailing vehicle with the central area of the wake. This is here presented for the 10m IVD, but is also present at other separation distances. The improved efficiency observed when a truck trails another truck at large yaw angles can be attributed to the reduction in effective yaw angle caused by the leading vehicle straightening the flow, Figure 4.17g. Added lateral offset in zero yaw conditions does cause an effect on the front similar to that of a larger yaw angle, thus increasing drag.

The effects on a truck behind a car are generally quite small as the car is much smaller than the truck, and thus the wake only covers part of its front face. The increase in drag for the truck at an IVD of 0.5m (Figure 4.1) is partially due to a larger stagnation area caused by the stagnation area being shifted to the front face above the grille, Figure 4.18. The car also causes a restriction for the air flowing downwards toward the underside of the truck, further increasing the stagnation area and drag.

The lower rate of change for the car trailing a truck at separation distances greater than 5m, i.e. there is only a small difference between the drag at 5m and at 20m, Figure 4.2 This small difference in drag stems from that the car is significantly smaller than the wake of the truck and thus remains completely inside the far wake up to longer distances than a truck would, Figure 4.19a. Thus the velocity field that the car experiences remains similar over a greater range of distances than a truck would. A decrease in velocity over the entire car (as compared to an isolated vehicle) is observed due to the large size of the vehicle in front. A

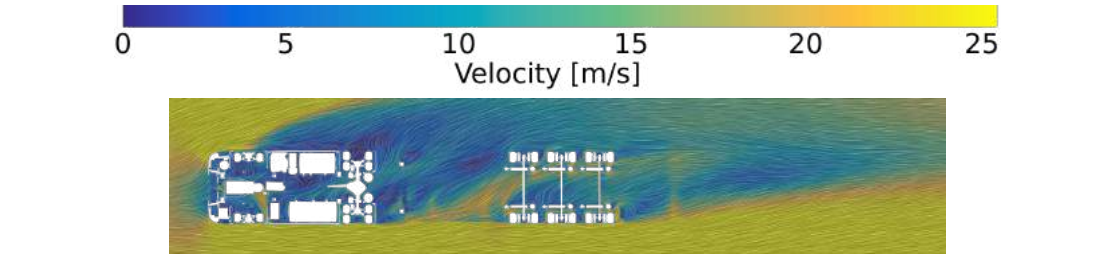

(a) *Isolated vehicle, 10° yaw*

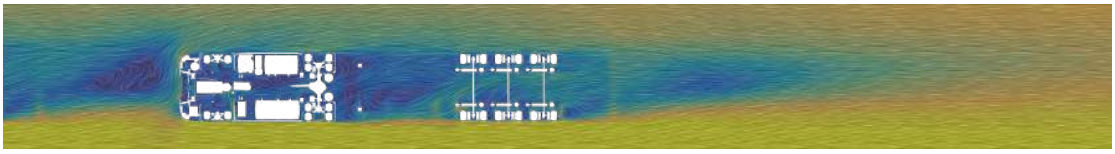

(b) *5m IVD, 5° yaw, zero offset*

(c) *5m IVD, 10° yaw, zero offset*

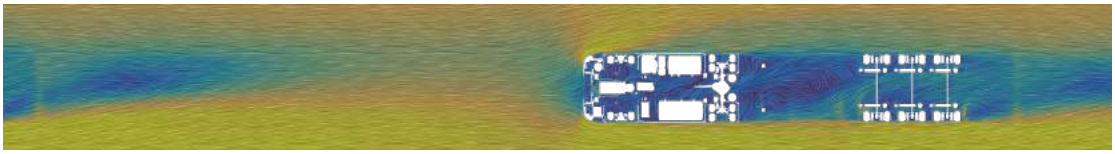

(d) *20m IVD, 5° yaw, zero offset*

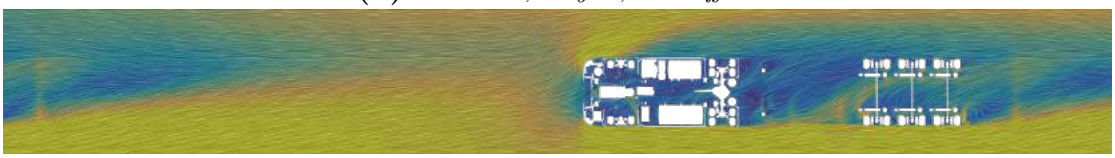

(e) *20m IVD, 10° yaw, zero offset*

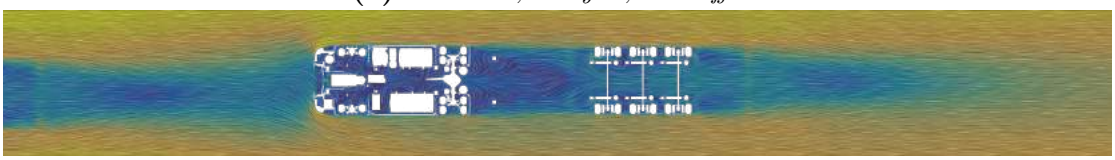

(f) *10m IVD, 0° yaw, 0.5m lateral offset*

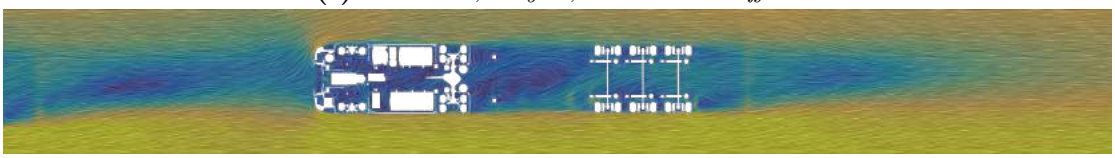

(g) *10m IVD, 5° yaw, 0.5m lateral offset*

Figure 4.17: *Line integral convolution plane colored by velocity at z=0.5m. Trailing truck, numerical results.*

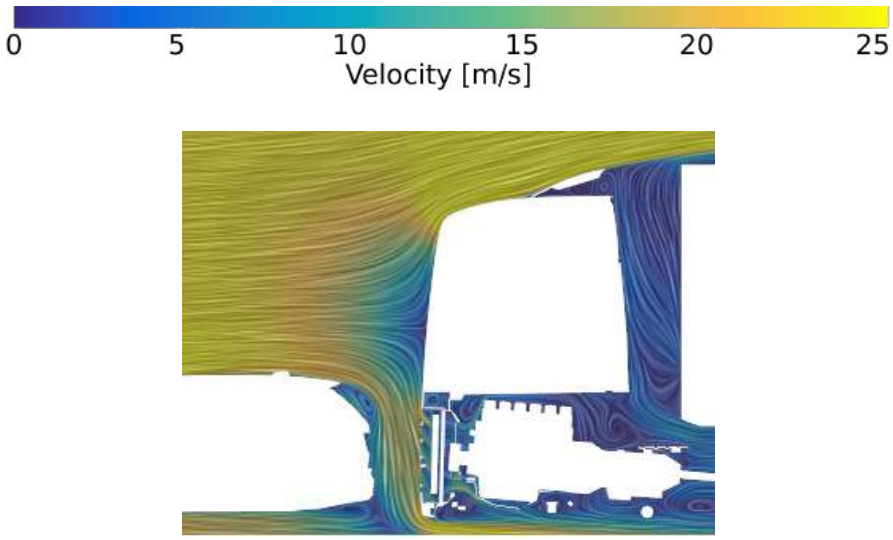

Figure 4.18: *Line integral convolution plane at y=0, 0.5m IVD, SUV in front of truck*

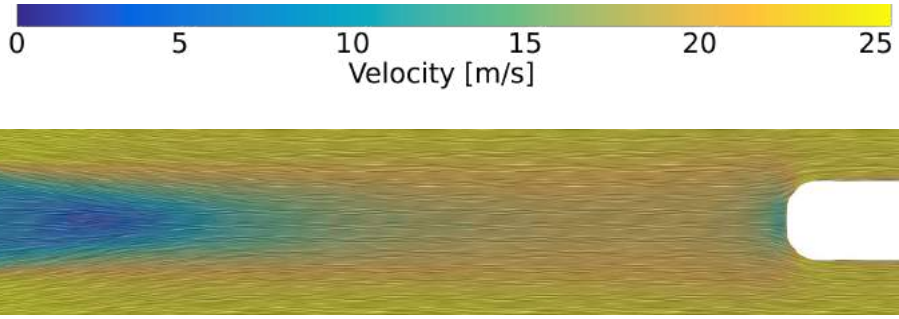

(a) *20m IVD.*

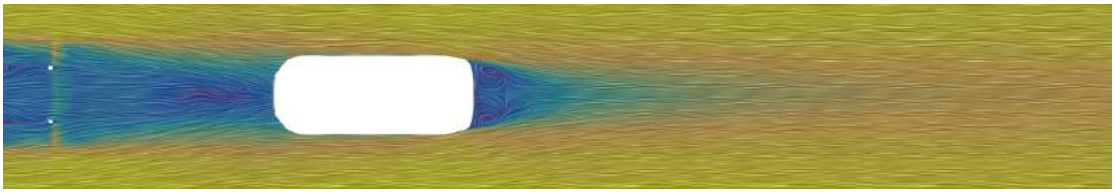

(b) *5m IVD.*

Figure 4.19: *Line integral convolution colored by velocity magnitude on plane at z=0.9m, zero yaw and offset, truck in front of SUV.*

significant drag reduction is observed as the trailing car approaches the leading truck as it is completely enveloped by the near wake, Figure 4.19b.

4.4 Variation of aerodynamic effects with IVD and combined drag

This section further describes the different aerodynamic effects present in a platoon of two vehicles and how they dominate the drag development, followed by the combined drag of the two vehicles.

4.4.1 Leading vehicle

The leading vehicle is mainly affected by the base pressure, as previously mentioned. This effect is very weak at longer IVDs as the pressure decreases quite rapidly with an increased distance from the stagnation area of the trailing vehicle. From Figure 4.20a, it can be seen that the base pressure changes very little between 30m and 25m IVD, consistent with drag trends observed in other studies for the leading vehicle [23, 29, 33, 40]. Below roughly 20m, the rate of change for the base pressure accelerates and then stagnates at an IVD of 5m and lower. The difference in base pressure between the 0° and 5° yaw cases remains consistent throughout the range of separation distances greater than 5m, further indicating that the change in drag for the leading vehicle is due to the increase in pressure caused by the trailing vehicle and not due to flow changes.

The only other effect that is present at distances above 0.5m for the leading vehicle is the increased effective yaw angle, present with large yaw angles and distances of 10m and less. This can be observed in Figure 4.20b, where the difference in C_P between the right side and left side of the base is divided by average base pressure. This effect, in combination with the constant offset in base pressure between yaw angles, causes the increase in normalized drag observed at yaw, Figure 4.1.

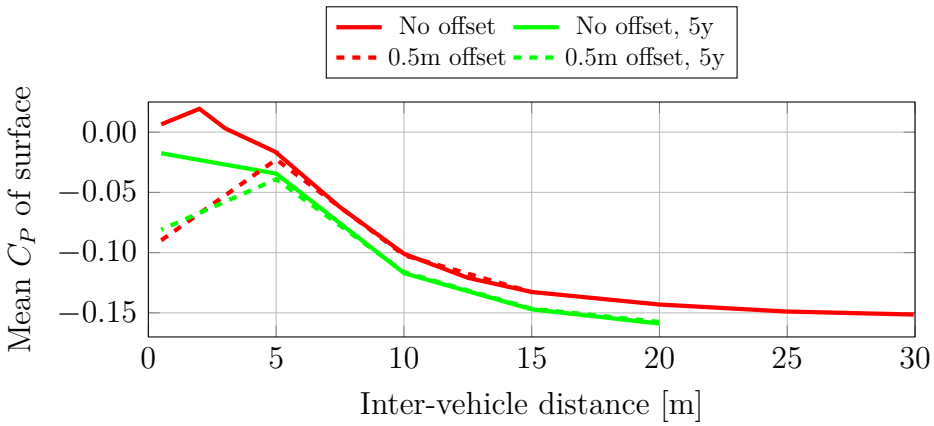

(a) *Base C_P, experimental data.*

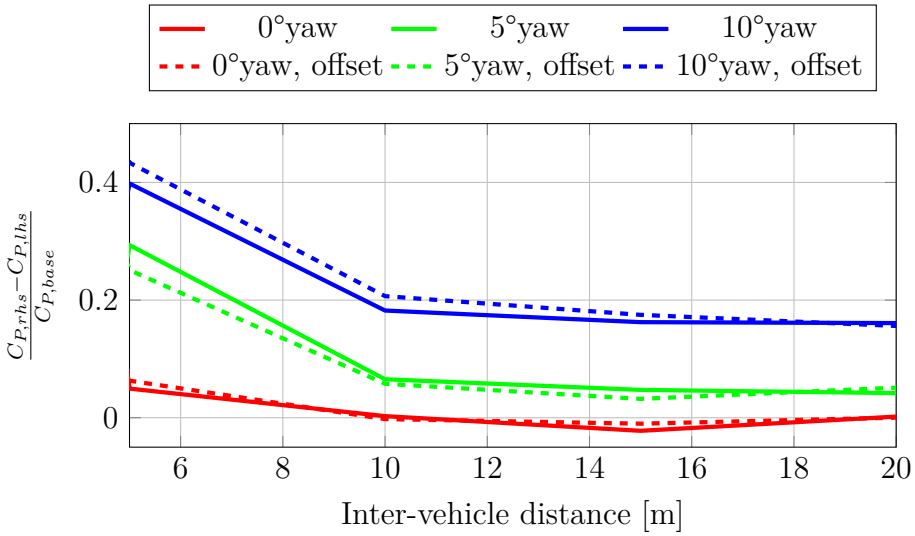

(b) *Difference in C_P between the right side and left side divided by average base pressure, numerical data.*

Figure 4.20: *Leading vehicle. Two truck platoon.*

4.4.2 Trailing vehicle

In order to separate the various effects occurring on the trailing truck, pressures are averaged over surfaces and plotted versus IVD, Figure 4.21. The figure shows that C_P at the front of the vehicle decreases continuously and the rate of change increases as the IVD becomes shorter (Figure 4.21a). The pressure at the top and sides of the cab is rapidly reduced between 5 and 15m (Figures 4.21b, 4.21c, and 4.21d). The tractor-trailer gap has a similar trend, although with a relatively constant pressure above 15m (4.21e). The primary effect at longer IVDs is thus the reduction in stagnation pressure caused by the far-wake of the leading vehicle. As the IVD shortens, the acceleration around the corners is reduced, increasing drag, and as the distance decreases further, the efficiency of the roof air deflector

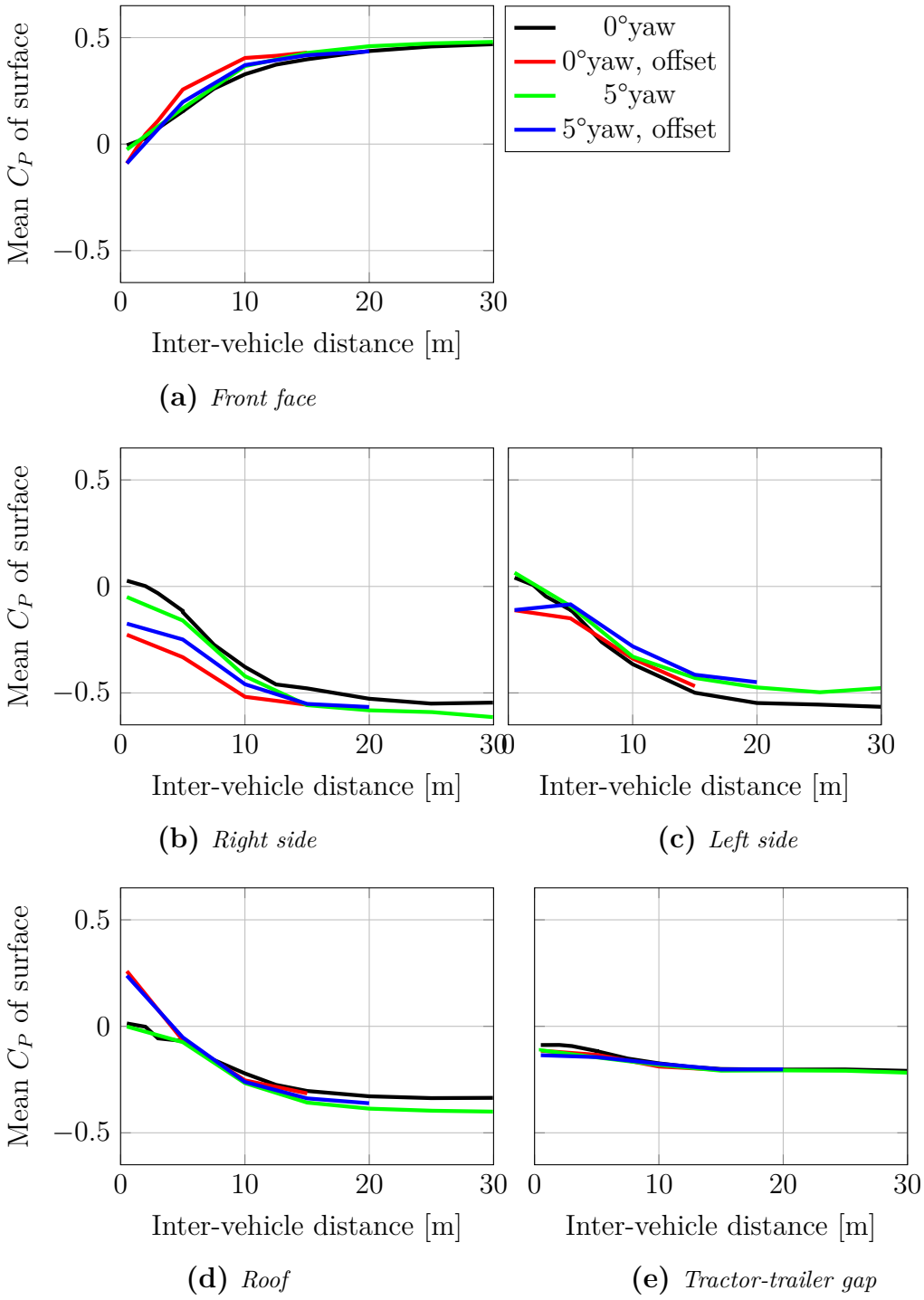

(a) *Front face*

(b) *Right side*

(c) *Left side*

(d) *Roof*

(e) *Tractor-trailer gap*

Figure 4.21: *Average C_P on the different surfaces on the front of the trailing truck versus IVD, experimental data (Dummy model).*

lessens, yielding greater drag. The drag then rises to 5m as the pressure in the tractor-trailer gap rises, followed by a large reduction in drag as the distance reaches 0.5m since the rate of change on the corners and in the gap decrease while it increases for the front face.

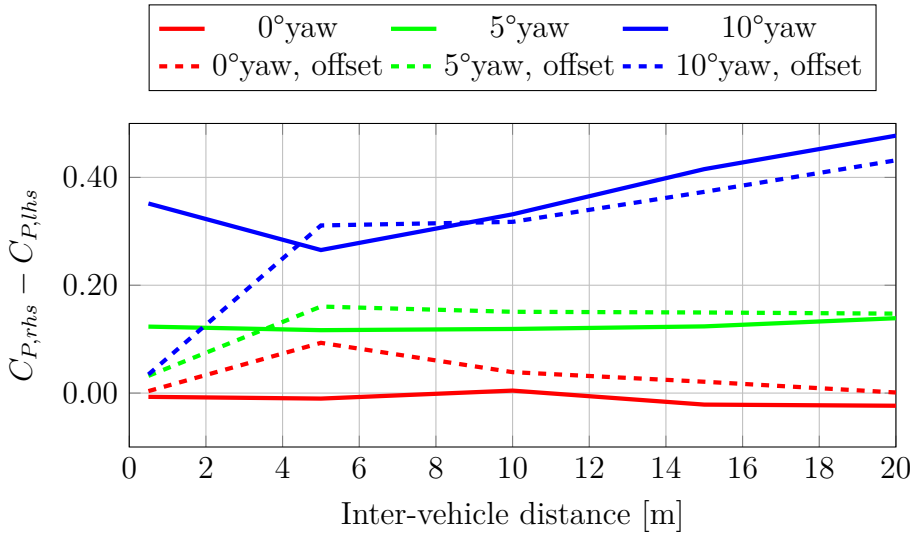

Figure 4.22: *Difference in C_P between right side and left side of cab for the trailing vehicle versus separation distance, numerical data.*

As was seen under yaw conditions, Section 4.1, there is a reduction of effective yaw angle as the IVD decreased, with this effect being stronger at larger yaw angles. So as to illustrate this, the difference in pressure between the two sides of the cab are plotted in Figure 4.22. The figure shows that the pressure difference remains fairly stable for the 0° and 5° yaw cases while the 10° yaw case shows a decrease in difference between the two sides with a reduced IVD, indicating a smaller effective yaw angle.

4.4.3 Combined system

The drag of the combined system remains quite constant as the distance decreases from 20m to 10m, and the effects of yaw remain fairly negligible, Figure 4.23. As the distance decreases, the drag of the system is rapidly reduced, and the negative effects of yaw increase but can be partially compensated for with a lateral offset. It can also be seen that for two trucks, it is most beneficial to drive at the shortest distance (0.5m). The effect of lateral offset at this shortest distance is, however, only beneficial at 10° yaw, which is a quite infrequent occurrence on the road.

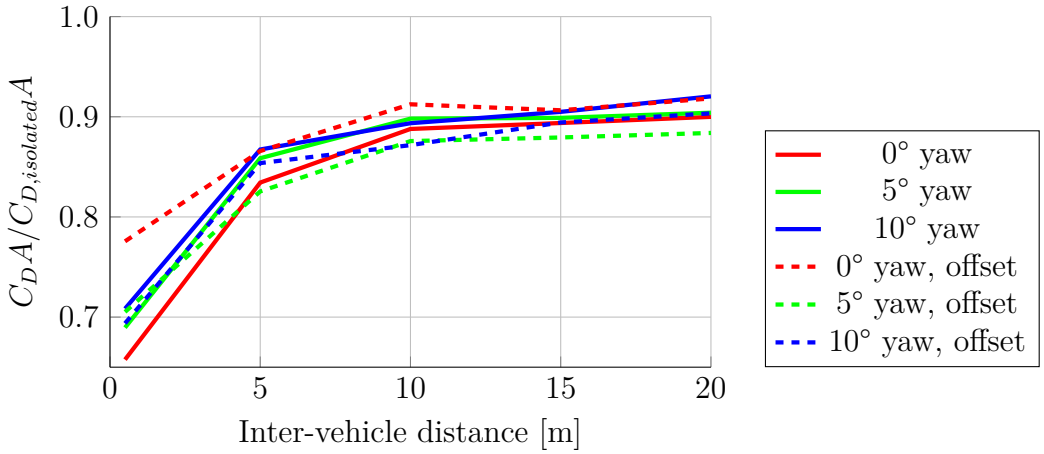

(a) *Normalized drag is computed as* $(C_{D,leading}A + C_{D,trailing}A)/(2 * C_{D,i}A)$

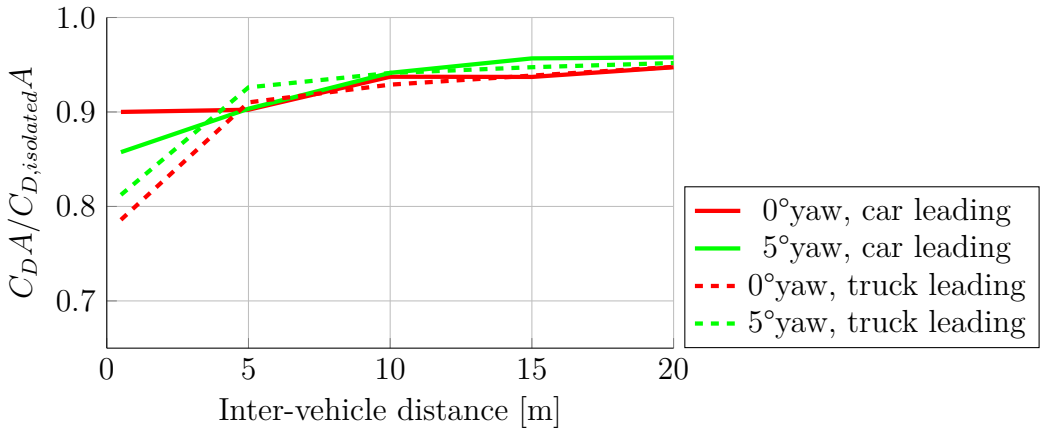

(b) *Normalized drag is calculated as* $(C_{D,t}A + C_{D,c}A)_{config}/(C_{D,t,i}A + C_{D,c,i}A)$ *where config is the corresponding configuration of the graph, separation distance, vehicle order, and yaw angle.*

Figure 4.23: *Combined drag of two vehicle combinations. The subscript t denotes truck, c car, and i isolated vehicle. Numerical data.*

For the combination of car and truck, there is a relatively constant decrease of the system drag as the separation distance decreases to 5m, whereafter the combination with the truck leading sees a rapid decrease, Figure 4.23b. This means that for very short distances, it is more beneficial for the truck to be the leading vehicle. This difference in performance at 0.5m stems from higher drag from the truck while trailing a car compared to it leading a car. It can also be observed that the combined drag decreases for a car leading a truck at 0.5m for greater yaw angles; this is the case as the drag of the truck increases less at this distance under yaw conditions.

Chapter 5

Concluding remarks

This thesis has had several goals, the first being to develop a robust, affordable, and sufficiently accurate numerical method for the simulation of vehicles in a platoon. The second goal was to design an experimental setup to allow vehicles in close proximity to be investigated while using a moving ground system. The two methods gave similar trends and further agreed well with the results of several other studies available in the literature. The third goal was to investigate the aerodynamic behavior of two vehicles (COE truck, SUV, and bus) in close proximity while varying inter-vehicle distance (IVD), lateral offset, and yaw.

The results have shown that the leading truck has a fairly straightforward drag reduction mechanism and that it is mainly pressure-based. The drag is determined largely by the increase in base pressure originating from the stagnation area of the trailing truck. Since this effect is mainly dependent on the distance from the trailing vehicle and is a fairly constant change, independent of yaw angle, it becomes a smaller fraction of the drag under yaw conditions, reducing the efficiency of the platoon. However, this is only the case at separation distances greater than roughly 5m. Below this distance, the space between the two trucks can be described as an open-sided cavity typically found in the tractor-trailer gap. Furthermore, the effective yaw angle of the leading truck increases at these short distances, further decreasing the efficiency of the platoon. A lateral offset at 0.5m IVD causes the formation of a very strong vortex, increasing drag for the leading vehicle.

As for the trailing truck, the general mechanisms are far more complex and produce both an increase and decrease in drag. The main effects at zero yaw and no lateral offset are, according to their importance, from the longest to the shortest IVD:

- A reduced oncoming velocity yielding lower stagnation pressures, decreasing drag, and decreasing accelerations around the front edge roundings, increasing drag;
- Flow impingement on the front radii at short IVDs, increasing drag:
- Reduced efficiency of the roof air deflector due to lower energy in the oncoming flow as well as changed flow angle on top of the vehicle, giving higher pressures in the tractor-trailer gap, increasing drag.

When varying the conditions of the platoon to account for yaw and lateral offset, the drag changes become more complex. The aerodynamic effects that influence the drag behavior under yaw conditions are, according to their importance, from the longest to the shortest IVD:

- A shifted wake that increases stagnation pressure and flow acceleration around the exposed corner of the trailing vehicle, increasing drag. (This is similar to the effect of a lateral offset under zero yaw conditions);
- Lateral offset positioning the trailing vehicle in the shifted wake under yaw conditions and reduction of the effective yaw angle, decreasing drag;
- Reduced effective yaw angle for the trailing vehicle, decreasing drag.

These effects result in a general increase in drag for small yaw angles and a decrease for larger yaw angles for the trailing vehicle, as seen in Figure 4.2.

The effects of platooning with different vehicle types are similar to those seen for two trucks but become weaker for the truck when it is paired with a smaller vehicle. A deviation from the drag behavior seen with two trucks is only observed at very short distances of less than 5m, where the truck generally sees an increase in drag compared to slightly longer distances. This is due to the vehicle size difference and causes changes in either the wake of the truck when the smaller vehicle is behind, or a moved and increased stagnation area on the front, when the smaller vehicle is leading the platoon. A car behind or in front of a truck generally sees larger reductions in drag than a truck would in a similar configuration; this is especially evident at 0.5m, where the drag of the car can even reach a negative value.

The drag of the combined system decreases with a reduced separation distance for almost all cases, although the decrease is slow above 10m. Yaw conditions almost always result in a net loss of performance for the system; however, some of the loss can be recovered by the addition of lateral offset. Up to 8% reduction of drag for the trailing vehicle in some cases. This means that a shorter distance will, most likely, be beneficial for the system as a whole. However, if distances below 5 to 10m cannot be achieved safely, a distance of 20m is potentially preferable as the loss of performance between 10 and 20m is small.

The combined drag of a platoon with a car and truck shows that the dominant factor in the total drag of the system is the truck, meaning that although very large decreases are seen for the car, it results in a modest decrease for the system as a whole. It is beneficial to position a truck in front of a car as otherwise, a large drag penalty occurs for the truck.

The behavior of a truck–bus platoon is very similar to that of a truck–truck platoon. Positioning a bus in front of a truck is most beneficial as the drag decrease is larger for the truck in this formation.

Finally, based on all the observations in this work, the best positioning for a long platoon of vehicles is likely to have buses at the front, trucks in the middle and cars at the very end.

Chapter 6

Future work

Although many of the effects between two vehicles have been investigated in this work, much work still remains to fully understand the effects under platooning scenarios. Other studies have shown that the effectiveness of add on devices can vary under platooning scenarios and in traffic. Thus, the effect of add-on drag reduction devices for heavy vehicles on the performance of platooning, some of this has been tested during the course of this work, although the results of this are yet to be thoroughly analyzed. The variability of performance with different vehicle shapes has been shown to heavily influence the performance of a platoon. The effects of other vehicle types is therefore also of importance, as there is great variety in the shape and size of vehicles on the road. Furthermore, the effect of longer platoons with more vehicles has been investigated in some studies, although the number of vehicles is still quite low. Significantly longer platoons should therefore also be investigated, although this is generally difficult and expensive.

The potential, although quite small, of a lateral offset could also be investigated further and its influence for longer platoons could also vary as the lateral space is quite limited in a single lane.

This work has focused solely on the aerodynamic drag changes, and the effect of reduced cooling flow has not been analyzed. Usage of the cooling fan to ensure acceptable engine and underhood temperatures can potentially reduce the fuel savings achieved by reducing the drag and should thus be investigated. The effect of drag reduction on fuel saving or reduced energy consumption is also vital for understanding the real impact of platooning. To enable this, the potential of forming platoons as well as the cost of forming platoons should likely be included.

To realize the potential savings, work has to be done on the assembling of platoons in real life as well as improvement to vehicle automation to ensure that short enough distances can be used. Finally, some method of sharing fuel or energy consumption reductions should probably be developed to increase adoption and reduce the disparity in cost savings between different positions in the platoon.

Chapter 7

Summary of papers

7.1 Paper I

The focus of this first paper was to develop and establish a numerical method as well as creating an initial understanding of the different flow phenomena in platooning. A numerical study was performed for two trucks in line with IVDs from 0.5 to 20m without yaw. This first study found that the drag of the leading truck decreases continuously as the distance decreases, with an increasing rate of decrease. This reduction was predominately caused by the increase in base pressure caused by proximity to the stagnation area on the trailing truck. The trailing truck sees a continuous increase in drag as the distance decreases down to 5m, whereafter a decrease is observed. These changes in drag are caused by several different factors, affected by the change in flow direction and decrease in velocity caused by the leading vehicles wake. The areas affected are the front face, experiencing lower stagnation pressure, front end roundings, seeing an increase in pressure due to decreased acceleration, and the tractor-trailer gap experiencing an increase in pressure due to worse performance of the roof air deflector.

7.2 Paper II

The second paper consists of development of an experimental method and evaluating many more configurations of platooning experimentally. Two of the truck models were used in the Volvo Cars Aerodynamic wind tunnel with moving ground and rotating wheels to evaluate the performance of platooning in various configurations. The parameters investigated were yaw angle (0° and 5°), IVD (0.5m to 30m), and lateral offset(0m, 0.5m, and 1m) as well as different reynolds numbers. The investigation showed that sufficiently high Reynolds numbers are essential for accurate prediction of platooning effects under yaw conditions. The leading vehicle saw the same effects as in the first paper and was relatively insensitive to changes in lateral offset and yaw, except at 0.5m IVD where a lateral offset yielded a significant increase in drag. The trailing vehicle saw a decrease in efficiency with yaw, which could partially be compensated for with the addition of lateral offset to the leeward direction.

7.3 Paper III

This third paper is a further analysis of the results obtained in the second paper and expanding with larger yaw angles using numerical simulations. Lateral offset, yaw and varying IVDs were investigated numerically and compared to the results of the second paper, yielding good correlation. The effects for the leading vehicle were shown to be dominated by base pressure, except at large yaw angles and short distances where a slight increase in effective yaw angle was observed. The effect of yaw on the trailing vehicle were caused by two main changes, being a misalignment of the wake from the leading vehicle and a reduced effective yaw angle as the leading vehicle works as a flow straightener. These effects cause opposite effects of drag and vary in strength with IVD and yaw angle. At longer distances the misalignment is large, causing an increase in drag and at short distances and large yaw angles the reduced effective yaw angle decreases drag. The effect of lateral offset was shown to realign the wake of the leading vehicle and the front of the trailing one under yaw conditions, thus reducing drag, while the opposite was true under zero yaw conditions.

7.4 Paper IV

The fourth paper is on the effects of platooning with an SUV and a truck, using both numerical and experimental data. The investigated parameters are Lateral offset, yaw, and IVD. The results show that platooning at very short distances is not especially beneficial for the truck, whereas it does see some reductions at longer IVDs. The effects on the car are significantly larger and the car can see negative drag values at extremely short distances. Many of the same effects that were observed for a truck-truck platoon also exist in an SUV-truck platoon. The negative effects observed at very short distances occur as the height of the car is much lower than the truck, changing the wake of the leading truck and shifting the stagnation point to the upper part of the front of the trailing truck.

Bibliography

[1] European Environment Agency. *Greenhouse gas emissions from transport*. 2019. URL: https://www.eea.europa.eu/data-and-maps/indicators/transport-emissions-of-greenhouse-gases/transport-emissions-of-greenhouse-gases-12 (visited on 10/19/2020).

[2] H. Ritchie and M. Roser. *Emissions by sector*. URL: https://ourworldindata.org/emissions-by-sector (visited on 04/19/2021).

[3] A. Davila, E. Aramburu, and A. Freixas. "Making the Best Out of Aerodynamics: Platoons". In: *SAE 2013 World Congress & Exhibition*. SAE International, 2013. DOI: https://doi.org/10.4271/2013-01-0767.

[4] F. Browand, J. Mcarthur, and C. Radovich. "Fuel Saving Achieved in the Field Test of Two Tandem Trucks". In: *Institute of Transportation Studies, UC Berkeley, Institute of Transportation Studies, Research Reports, Working Papers, Proceedings* (2004).

[5] C. Bonnet and H. Fritz. "Fuel Consumption Reduction in a Platoon: Experimental Results with two Electronically Coupled Trucks at Close Spacing". In: *Future Transportation Technology Conference & Exposition*. SAE International, 2000. DOI: https://doi.org/10.4271/2000-01-3056.

[6] M. P. Lammert, K. J. Kelly, and J. Yanowitz. "Correlations of Platooning Track Test and Wind Tunnel Data". In: (2018). DOI: 10.2172/1422885.

[7] A. A. Alam, A. Gattami, and K. H. Johansson. "An experimental study on the fuel reduction potential of heavy duty vehicle platooning". In: *13th International IEEE Conference on Intelligent Transportation Systems*. 2010, pp. 306–311. DOI: 10.1109/ITSC.2010.5625054.

[8] M. Michaelian and F. Browand. "Quantifying Platoon Fuel Savings: 1999 Field Experiments". en. In: Mar. 2001, pp. 2001–01–1268. DOI: 10.4271/2001-01-1268.

[9] C. KR. "A wind tunnel investigation into the fuel savings available from the aerodynamic drag reduction of trucks." English. In: *Quart. Bull. Div. Mech. Engng Nation. Aeronaut. Establ.; Canada; DA. 1976; NO 3; PP. 31-86* (1976).

[10] K. R. Cooper. "The Effect of Front-Edge Rounding and Rear-Edge Shaping on the Aerodynamic Drag of Bluff Vehicles in Ground Proximity". In: *SAE International Congress and Exposition*. SAE International, 1985. DOI: https://doi.org/10.4271/850288.

[11] K. R. Cooper. "Wind Tunnel and Track Tests of Class 8 Tractors Pulling Single and Tandem Trailers Fitted with Side Skirts and Boat-tails". In: *SAE International Journal of Commercial Vehicles* 5.1 (2012), pp. 1–17. ISSN: 1946-391X. DOI: https://doi.org/10.4271/2012-01-0104.

[12] J. Leuschen and K. R. Cooper. "Full-Scale Wind Tunnel Tests of Production and Prototype, Second-Generation Aerodynamic Drag-Reducing Devices for Tractor-Trailers". In: *SAE 2006 Commercial Vehicle Engineering Congress & Exhibition*. SAE International, 2006. DOI: https://doi.org/10.4271/2006-01-3456.

[13] K. R. Cooper and J. Leuschen. "Model and Full-Scale Wind Tunnel Tests of Second-Generation Aerodynamic Fuel Saving Devices for Tractor-Trailers". In: *2005 SAE Commercial Vehicle Engineering Conference*. SAE International, 2005. DOI: https://doi.org/10.4271/2005-01-3512.

[14] K. R. Cooper. "Truck Aerodynamics Reborn - Lessons from the Past". In: *International Truck & Bus Meeting & Exhibition*. SAE International, 2003. DOI: https://doi.org/10.4271/2003-01-3376.

[15] J. Leuschen. "Considerations for the Wind Tunnel Simulation of Tractor-Trailer Combinations: Correlation of Full- and Half-Scale Measurements". In: *SAE International Journal of Commercial Vehicles* 6.2 (2013), pp. 529–538. ISSN: 1946-391X. DOI: https://doi.org/10.4271/2013-01-2456.

[16] R. Wood. "Reynolds Number Impact on Commercial Vehicle Aerodynamics and Performance". In: *SAE International Journal of Commercial Vehicles* 8.2 (2015), pp. 590–667. ISSN: 1946-391X. DOI: https://doi.org/10.4271/2015-01-2859.

[17] J. Leuschen. "The Effects of Ground Simulation on Tractor-Trailer Combinations". In: *SAE International Journal of Commercial Vehicles* 6.2 (2013), pp. 510–521. ISSN: 1946-391X. DOI: https://doi.org/10.4271/2013-01-2454.

[18] J. Leuschen and Y. Mébarki. "Examination of the Maskell III Blockage Correction Technique for Full Scale Testing in the NRC 9-Meter Wind Tunnel". In: *SAE International Journal of Commercial Vehicles* 5.2 (2012), pp. 640–649. ISSN: 1946-391X. DOI: https://doi.org/10.4271/2012-01-2047.

[19] H. Martini, P. Gullberg, and L. Lofdahl. "Comparative Studies between CFD and Wind Tunnel Measurements of Cooling Performance and External Aerodynamics for a Heavy Truck". In: *SAE International Journal of Commercial Vehicles* 7.2 (2014), pp. 640–652. ISSN: 1946-391X. DOI: https://doi.org/10.4271/2014-01-2443.

[20] R. Sengupta, J. Beedy, and K. Horrigan. "Combined Analysis of Cooling Airflow and Aerodynamic Drag for a Class 8 Tractor Trailer Combination". In: *SAE International Journal of Commercial Vehicles* 4.1 (2011), pp. 263–274. ISSN: 1946-391X. DOI: https://doi.org/10.4271/2011-01-2288.

[21] D. Norrby. "A CFD Study Of The Aerodynamic Effects Of Platooning Trucks". en. In: (), p. 135.

[22] W. Hucho. *Aerodynamics of Road Vehicles*. Butterworth Limited, London England, 1987. ISBN: 9780750612678.

[23] B. McAuliffe et al. "Influences on Energy Savings of Heavy Trucks Using Cooperative Adaptive Cruise Control". In: *WCX World Congress Experience*. SAE International, 2018. DOI: https://doi.org/10.4271/2018-01-1181.

[24] R. Mihelic, J. Smith, and M. Ellis. "Aerodynamic Comparison of Tractor-Trailer Platooning and A-Train Configuration". In: *SAE International Journal of Commercial Vehicles* 8.2 (2015), pp. 740–746. ISSN: 1946-391X. DOI: https://doi.org/10.4271/2015-01-2897.

[25] K.-Y. Liang, J. Mårtensson, and K. H. Johansson. "Fuel-saving potentials of platooning evaluated through sparse heavy-duty vehicle position data". In: *2014 IEEE Intelligent Vehicles Symposium Proceedings*. 2014, pp. 1061–1068. DOI: 10.1109/IVS.2014.6856540.

[26] D. Bevly et al. "Heavy Truck Cooperative Adaptive Cruise Control: Evaluation, Testing, and Stakeholder Engagement for Near Term Deployment: Phase One Final Report". In: 2015.

[27] S. Tsugawa, S. Kato, and K. Aoki. "An automated truck platoon for energy saving". In: *2011 IEEE/RSJ International Conference on Intelligent Robots and Systems*. 2011, pp. 4109–4114. DOI: 10.1109/IROS.2011.6094549.

[28] A. Dávila and M. Nombela. "Sartre - Safe Road Trains for the Environment Reducing Fuel Consumption through Lower Aerodynamic Drag Coefficient". In: *SAE Brasil 2011 Congress and Exhibit*. SAE International, 2011. DOI: https://doi.org/10.4271/2011-36-0060.

[29] M. P. Lammert et al. "Effect of Platooning on Fuel Consumption of Class 8 Vehicles Over a Range of Speeds, Following Distances, and Mass". In: *SAE International Journal of Commercial Vehicles* 7.2 (2014), pp. 626–639. ISSN: 1946-391X. DOI: https://doi.org/10.4271/2014-01-2438.

[30] M. P. Lammert et al. "Impact of Lateral Alignment on the Energy Savings of a Truck Platoon". In: *WCX SAE World Congress Experience*. SAE International, 2020. DOI: https://doi.org/10.4271/2020-01-0594.

[31] Y. Zhang et al. "A methodology for measuring the environmental effect of autonomous bus considering platooning". en. In: *Transportation Research Part D: Transport and Environment* 107 (June 2022), p. 103300. ISSN: 13619209. DOI: 10.1016/j.trd.2022.103300.

[32] B. McAuliffe et al. “Impact of Mixed Traffic on the Energy Savings of a Truck Platoon”. In: *SAE International Journal of Advances and Current Practices in Mobility* 2.3 (2020), pp. 1472–1496. ISSN: 2641-9637. DOI: https://doi.org/10.4271/2020-01-0679.

[33] B. McAuliffe et al. “Fuel-economy testing of a three-vehicle truck platooning system”. In: LTR-AL-2017-0008. Laboratory Technical Report (National Research Council of Canada. Aerospace. Aerodynamics Laboratory), 2017. DOI: https://doi.org/10.4224/23001922.

[34] E. Stegner et al. “New Metrics for Quantifying the Energy Efficiency of Platoons in the Presence of Disturbances”. en. In: Mar. 2022, pp. 2022–01–0526. DOI: 10.4271/2022-01-0526.

[35] J. Nuszkowski et al. “Increasing the on-road fuel economy by trailing at a safe distance.” In: *Proceedings of the Institution of Mechanical Engineers, Part D: Journal of Automobile Engineering* 231.9 (2017), pp. 1303 –1311. ISSN: 09544070.

[36] R. Veldhuizen, G. Van Raemdonck, and J. van der Krieke. “Fuel economy improvement by means of two European tractor semi-trailer combinations in a platooning formation”. In: *Journal of Wind Engineering and Industrial Aerodynamics* 188 (2019), pp. 217–234. ISSN: 0167-6105. DOI: https://doi.org/10.1016/j.jweia.2019.03.002.

[37] S. Tsugawa. “Results and issues of an automated truck platoon within the energy ITS project”. In: *2014 IEEE Intelligent Vehicles Symposium Proceedings*. 2014, pp. 642–647. DOI: 10.1109/IVS.2014.6856400.

[38] P. Hong et al. “Drag Forces Experienced by Two, Full-Scale Vehicles at Close Spacing”. In: *International Congress & Exposition*. SAE International, 1998. DOI: https://doi.org/10.4271/980396.

[39] B. McAuliffe et al. “Track-Based Aerodynamic Testing of a Two-Truck Platoon”. In: *SAE International Journal of Advances and Current Practices in Mobility* 3.3 (2021), pp. 1450–1472. ISSN: 2641-9637. DOI: https://doi.org/10.4271/2021-01-0941.

[40] B. R. McAuliffe and M. Ahmadi-Baloutaki. “A Wind-Tunnel Investigation of the Influence of Separation Distance, Lateral Stagger, and Trailer Configuration on the Drag-Reduction Potential of a Two-Truck Platoon”. In: *SAE International Journal of Commercial Vehicles* 11.2 (2018), pp. 125–150. ISSN: 1946-391X. DOI: https://doi.org/10.4271/02-11-02-0011.

[41] M. Zabat, S. Frascaroli, and F. K. Browand. “Drag Measurements on 2, 3 and 4 Car Platoons”. In: *International Congress & Exposition*. SAE International, 1994. DOI: https://doi.org/10.4271/940421.

[42] A. Altinisik, O. Yemenici, and H. Umur. “Aerodynamic Analysis of a Passenger Car at Yaw Angle and Two-Vehicle Platoon”. In: *Journal of Fluids Engineering* 137.12 (2015). 121107. ISSN: 0098-2202. DOI: 10.1115/1.4030869. eprint: https://asmedigitalcollection.asme.org/fluidsengineering/article-pdf/137/12/121107/6195310/fe_137_12_121107.pdf.

[43] K. Salari and J. Ortega. “Experimental Investigation of the Aerodynamic Benefits of Truck Platooning”. In: *WCX World Congress Experience*. SAE International, 2018. DOI: https://doi.org/10.4271/2018-01-0732.

[44] D. Telionis, C. Fahrner, and G. Jones. “An experimental study of highway aerodynamic interferences.” In: *Journal of Wind Engineering & Industrial Aerodynamics* 17.3 (1984), pp. 267 –293. ISSN: 0167-6105.

[45] S. Watkins and G. Vino. “The effect of vehicle spacing on the aerodynamics of a representative car shape”. In: *Journal of Wind Engineering and Industrial Aerodynamics* 96.6 (2008). 5th International Colloquium on Bluff Body Aerodynamics and Applications, pp. 1232–1239. ISSN: 0167-6105. DOI: https://doi.org/10.1016/j.jweia.2007.06.042.

[46] K. Salari and J. Ortega. “Experimental Investigation of the Aerodynamic Benefits of Truck Platooning”. In: *WCX World Congress Experience*. SAE International, 2018. DOI: https://doi.org/10.4271/2018-01-0732.

[47] B. McAuliffe and M. Ahmadi-Baloutaki. "An Investigation of the Influence of Close-Proximity Traffic on the Aerodynamic Drag Experienced by Tractor-Trailer Combinations". In: *SAE International Journal of Advances and Current Practices in Mobility* 1.3 (2019), pp. 1251–1264. ISSN: 2641-9637. DOI: https://doi.org/10.4271/2019-01-0648.

[48] P. Schito and F. Braghin. "Numerical and Experimental Investigation on Vehicles in Platoon". In: *SAE International Journal of Commercial Vehicles* 5.1 (2012), pp. 63–71. ISSN: 1946-391X. DOI: https://doi.org/10.4271/2012-01-0175.

[49] D. Mitra and A. Mazumdar. "Pollution control by reduction of drag on cars and buses through platooning". In: *International Journal of Environment and Pollution - INT J ENVIRON POLLUTION* 30 (2007). DOI: 10.1504/IJEP.2007.014504.

[50] G. Le Good et al. "Effects on the Aerodynamic Characteristics of Vehicles in Longitudinal Proximity Due to Changes in Style". In: *CO2 Reduction for Transportation Systems Conference*. SAE International, 2018. DOI: https://doi.org/10.4271/2018-37-0018.

[51] G. Le Good et al. "An Investigation of Aerodynamic Characteristics of Three Bluff Bodies in Close Longitudinal Proximity". In: *WCX SAE World Congress Experience*. SAE International, 2019. DOI: https://doi.org/10.4271/2019-01-0659.

[52] C. A. Fletcher and G. Stewart. "Bus drag reduction by the trapped vortex concept for a single bus and two buses in tandem". In: *Journal of Wind Engineering and Industrial Aerodynamics* 24.2 (1986), pp. 143–168. ISSN: 0167-6105. DOI: https://doi.org/10.1016/0167-6105(86)90004-8.

[53] M. Hammache, M. Michaelian, and F. Browand. "Aerodynamic Forces on Truck Models, Including Two Trucks in Tandem". In: *SAE 2002 World Congress & Exhibition*. SAE International, 2002. DOI: https://doi.org/10.4271/2002-01-0530.

[54] P. Schito and F. braghin. "Numerical and Experimental Investigation on Vehicles in Platoon". In: *SAE International Journal of Commercial Vehicles* 5.1 (2012), pp. 63–71. ISSN: 1946-391X. DOI: https://doi.org/10.4271/2012-01-0175.

[55] L. Tsuei and Ö. Savaş. "Transient aerodynamics of vehicle platoons during in-line oscillations". In: *Journal of Wind Engineering and Industrial Aerodynamics* 89.13 (2001), pp. 1085–1111. ISSN: 0167-6105. DOI: https://doi.org/10.1016/S0167-6105(01)00073-3.

[56] J. Huang, T. Chan, and Y. Zhou. "Three-dimensional flow structure measurements behind a queue of studied model vehicles". In: *International Journal of Heat and Fluid Flow* 30.4 (2009), pp. 647–657. ISSN: 0142-727X. DOI: https://doi.org/10.1016/j.ijheatfluidflow.2009.03.010.

[57] B. Marcu and F. Browand. "Aerodynamic Forces Experienced by a 3-Vehicle Platoon in a Crosswind". In: *International Congress & Exposition*. SAE International, 1999. DOI: https://doi.org/10.4271/1999-01-1324.

[58] F. H. Robertson et al. "An experimental investigation of the aerodynamic flows created by lorries travelling in a long platoon". In: *Journal of Wind Engineering and Industrial Aerodynamics* 193 (2019), p. 103966. ISSN: 0167-6105. DOI: https://doi.org/10.1016/j.jweia.2019.103966.

[59] F. van Tilborg et al. "Flow Analysis between Two Bluff Bodies in a Close Distance Platooning Configuration". en. In: *SAE International Journal of Commercial Vehicles* 12.3 (July 2019), pp. 02–12–03–0015. ISSN: 1946-3928. DOI: 10.4271/02-12-03-0015.

[60] K. Tadakuma et al. "Prediction formula of Aerodynamic Drag Reduction in Multiple-Vehicle Platooning Based on Wake Analysis and On-Road Experiments". In: *SAE International Journal of Passenger Cars - Mechanical Systems* 9.2 (2016), pp. 645–656. ISSN: 1946-3995. DOI: https://doi.org/10.4271/2016-01-1596.

[61] H. Humphreys and D. Bevly. "Computational Fluid Dynamic Analysis of a Generic 2 Truck Platoon". In: *SAE 2016 Commercial Vehicle Engineering Congress*. SAE International, 2016. DOI: https://doi.org/10.4271/2016-01-8008.

[62] J. Smith et al. “Aerodynamic Impact of Tractor-Trailer in Drafting Configuration”. In: *SAE International Journal of Commercial Vehicles* 7.2 (2014), pp. 619–625. ISSN: 1946-391X. DOI: https://doi.org/10.4271/2014-01-2436.

[63] P. Vegendla et al. “Investigation of Aerodynamic Influence on Truck Platooning”. In: *SAE 2015 Commercial Vehicle Engineering Congress*. SAE International, 2015. DOI: https://doi.org/10.4271/2015-01-2895.

[64] H. L. Humphreys et al. “An Evaluation of the Fuel Economy Benefits of a Driver Assistive Truck Platooning Prototype Using Simulation”. In: *SAE 2016 World Congress and Exhibition*. SAE International, 2016. DOI: https://doi.org/10.4271/2016-01-0167.

[65] H. L. Humphreys et al. “An Evaluation of the Fuel Economy Benefits of a Driver Assistive Truck Platooning Prototype Using Simulation”. In: *SAE 2016 World Congress and Exhibition*. SAE International, 2016. DOI: https://doi.org/10.4271/2016-01-0167.

[66] R. Laxhammar and A. Gascón-Vallbona. “COMPANION D4.3. Vehicle models for fuel consumption”. In: *European Commission* Ref. Ares(2015)4007967 (2015).

[67] M. He et al. “Detached eddy simulation of a closely running lorry platoon”. In: *Journal of Wind Engineering and Industrial Aerodynamics* 193 (2019), p. 103956. ISSN: 0167-6105. DOI: https://doi.org/10.1016/j.jweia.2019.103956.

[68] M. Segata, A. Stedile, and R. L. Cigno. “Modeling Slipstreaming Effects in Vehicle Platoons”. en. In: *2020 IEEE Vehicular Networking Conference (VNC)*. New York, NY, USA: IEEE, Dec. 2020, pp. 1–8. ISBN: 978-1-72819-221-5. DOI: 10.1109/VNC51378.2020.9318331.

[69] A. Davila et al. “Environmental Benefits of Vehicle Platooning”. en. In: Jan. 2013, pp. 2013–26–0142. DOI: 10.4271/2013-26-0142.

[70] C.-H. Bruneau, K. Khadra, and I. Mortazavi. “Flow analysis of square-back simplified vehicles in platoon”. In: *International Journal of Heat and Fluid Flow* 66 (2017), pp. 43–59. ISSN: 0142-727X. DOI: https://doi.org/10.1016/j.ijheatfluidflow.2017.05.008.

[71] H. Ebrahim and R. Dominy. “Wake and surface pressure analysis of vehicles in platoon”. In: *Journal of Wind Engineering and Industrial Aerodynamics* 201 (2020), p. 104144. ISSN: 0167-6105. DOI: https://doi.org/10.1016/j.jweia.2020.104144.

[72] M. Ellis, J. I. Gargoloff, and R. Sengupta. “Aerodynamic Drag and Engine Cooling Effects on Class 8 Trucks in Platooning Configurations”. In: *SAE International Journal of Commercial Vehicles* 8.2 (2015), pp. 732–739. ISSN: 1946-391X. DOI: https://doi.org/10.4271/2015-01-2896.

[73] T. Gheyssens and G. Van Raemdonck. “Effect of the Frontal Edge Radius in a Platoon of Bluff Bodies”. In: *SAE International Journal of Commercial Vehicles* 9.2 (2016), pp. 371–380. ISSN: 1946-391X. DOI: https://doi.org/10.4271/2016-01-8149.

[74] S. N. P. Vegendla et al. “Investigation on Underhood Thermal Analysis of Truck Platooning”. In: *SAE International Journal of Commercial Vehicles* 11.1 (2018), pp. 5–16. ISSN: 1946-391X. DOI: https://doi.org/10.4271/02-11-01-0001.

[75] B. Block et al. “Analysis of the Effect of Vehicle Platooning on the Optimal Control of a Heavy Duty Engine Thermal System”. In: *SAE International Journal of Advances and Current Practices in Mobility* 1.4 (2019), pp. 1661–1671. ISSN: 2641-9637. DOI: https://doi.org/10.4271/2019-01-1259.

[76] H. Ebrahim, R. Dominy, and K. Leung. “Evaluation of vehicle platooning aerodynamics using bluff body wake generators and CFD.” In: (2017). ISSN: 1-4673-9028-3.

[77] D. Uystepruyst and S. Krajnović. “LES of the flow around several cuboids in a row”. In: *International Journal of Heat and Fluid Flow* 44 (2013), pp. 414–424. ISSN: 0142-727X. DOI: https://doi.org/10.1016/j.ijheatfluidflow.2013.07.011.

[78] S. Price and M. Paidoussis. "The aerodynamic forces acting on groups of two and three circular cylinders when subject to a cross-flow". In: *Journal of Wind Engineering and Industrial Aerodynamics* 17.3 (1984), pp. 329–347. ISSN: 0167-6105. DOI: https://doi.org/10.1016/0167-6105(84)90024-2.

[79] M. Zdravkovich and D. Pridden. "Interference between two circular cylinders; Series of unexpected discontinuities". In: *Journal of Wind Engineering and Industrial Aerodynamics* 2.3 (1977), pp. 255–270. ISSN: 0167-6105. DOI: https://doi.org/10.1016/0167-6105(77)90026-5.

[80] B. Blocken et al. "Aerodynamic drag in cycling team time trials". In: *Journal of Wind Engineering and Industrial Aerodynamics* 182 (2018), pp. 128–145. ISSN: 0167-6105. DOI: https://doi.org/10.1016/j.jweia.2018.09.015.

[81] B. Blocken et al. "Aerodynamic drag in cycling pelotons: New insights by CFD simulation and wind tunnel testing". In: *Journal of Wind Engineering and Industrial Aerodynamics* 179 (2018), pp. 319–337. ISSN: 0167-6105. DOI: https://doi.org/10.1016/j.jweia.2018.06.011.

[82] C. Li et al. "Flow topology of a container train wagon subjected to varying local loading configurations". In: *Journal of Wind Engineering and Industrial Aerodynamics* 169 (2017), pp. 12–29. ISSN: 0167-6105. DOI: https://doi.org/10.1016/j.jweia.2017.06.011.

[83] D. Flynn, H. Hemida, and C. Baker. "On the effect of crosswinds on the slipstream of a freight train and associated effects". In: *Journal of Wind Engineering and Industrial Aerodynamics* 156 (2016), pp. 14–28. ISSN: 0167-6105. DOI: https://doi.org/10.1016/j.jweia.2016.07.001.

[84] D. Soper, C. Baker, and M. Sterling. "Experimental investigation of the slipstream development around a container freight train using a moving model facility". In: *Journal of Wind Engineering and Industrial Aerodynamics* 135 (2014), pp. 105–117. ISSN: 0167-6105. DOI: https://doi.org/10.1016/j.jweia.2014.10.001.

[85] S. Maleki, D. Burton, and M. C. Thompson. "Flow structure between freight train containers with implications for aerodynamic drag". In: *Journal of Wind Engineering and Industrial Aerodynamics* 188 (2019), pp. 194–206. ISSN: 0167-6105. DOI: https://doi.org/10.1016/j.jweia.2019.02.007.

[86] S. Maleki, D. Burton, and M. C. Thompson. "Assessment of various turbulence models (ELES, SAS, URANS and RANS) for predicting the aerodynamics of freight train container wagons". In: *Journal of Wind Engineering and Industrial Aerodynamics* 170 (2017), pp. 68–80. ISSN: 0167-6105. DOI: https://doi.org/10.1016/j.jweia.2017.07.008.

[87] J. Allan. "Aerodynamic drag and pressure measurements on a simplified tractor-trailer model". In: *Journal of Wind Engineering and Industrial Aerodynamics* 9.1 (1981), pp. 125–136. ISSN: 0167-6105. DOI: https://doi.org/10.1016/0167-6105(81)90083-0.

[88] J. Östh and S. Krajnović. "The flow around a simplified tractor-trailer model studied by large eddy simulation". In: *Journal of Wind Engineering and Industrial Aerodynamics* 102 (2012), pp. 36–47. ISSN: 0167-6105. DOI: https://doi.org/10.1016/j.jweia.2011.12.007.

[89] K. P. Garry. "Some effects of ground clearance and ground plane boundary layer thickness on the mean base pressure of a bluff vehicle type body". In: *Journal of Wind Engineering and Industrial Aerodynamics* 62.1 (1996), pp. 1–10. ISSN: 0167-6105. DOI: https://doi.org/10.1016/S0167-6105(96)00054-2.

[90] T. Avadiar et al. "The influence of reduced Reynolds number on the wake of the DrivAer estate vehicle". In: *Journal of Wind Engineering and Industrial Aerodynamics* 188 (2019), pp. 207–216. ISSN: 0167-6105. DOI: https://doi.org/10.1016/j.jweia.2019.02.024.

[91] T. Lajos, L. Preszler, and L. Finta. "Effect of moving ground simulation on the flow past bus models". In: *Journal of Wind Engineering and Industrial Aerodynamics* 22.2 (1986). Special Issue 6th Colloquium on Industrial Aerodynamics Vehicle Aerodynamics, pp. 271–277. ISSN: 0167-6105. DOI: https://doi.org/10.1016/0167-6105(86)90090-5.

[92] M. Sardou. ""Reynolds effect" and "moving ground effect" tested in a quarter scale wind tunnel over a high speed moving belt". In: *Journal of Wind Engineering and Industrial Aerodynamics* 22.2 (1986). Special Issue 6th Colloquium on Industrial Aerodynamics Vehicle Aerodynamics, pp. 245–270. ISSN: 0167-6105. DOI: https://doi.org/10.1016/0167-6105(86)90089-9.

[93] J. E. Hackett et al. "On the Influence of Ground Movement and Wheel Rotation in Tests on Modern Car Shapes". In: *SAE International Congress and Exposition*. SAE International, 1987. DOI: https://doi.org/10.4271/870245.

[94] J. Howell and K. Everitt. "The underbody flow of an EDS-type advanced ground transport vehicle". In: *Journal of Wind Engineering and Industrial Aerodynamics* 8.3 (1981), pp. 275–294. ISSN: 0167-6105. DOI: https://doi.org/10.1016/0167-6105(81)90026-X.

[95] M. Kim and D. Geropp. "Experimental investigation of the ground effect on the flow around some two-dimensional bluff bodies with moving-belt technique". In: *Journal of Wind Engineering and Industrial Aerodynamics* 74-76 (1998), pp. 511–519. ISSN: 0167-6105. DOI: https://doi.org/10.1016/S0167-6105(98)00046-4.

[96] S. Wang et al. "Effect of moving ground on the aerodynamics of a generic automotive model: The DrivAer-Estate". In: *Journal of Wind Engineering and Industrial Aerodynamics* 195 (2019), p. 104000. ISSN: 0167-6105. DOI: https://doi.org/10.1016/j.jweia.2019.104000.

[97] B. Fago, H. Lindner, and O. Mahrenholtz. "The effect of ground simulation on the flow around vehicles in wind tunnel testing". In: *Journal of Wind Engineering and Industrial Aerodynamics* 38.1 (1991), pp. 47–57. ISSN: 0167-6105. DOI: https://doi.org/10.1016/0167-6105(91)90026-S.

[98] K. Burgin, P. Adey, and J. Beatham. "Wind tunnel tests on road vehicle models using a moving belt simulation of ground effect". In: *Journal of Wind Engineering and Industrial Aerodynamics* 22.2 (1986). Special Issue 6th Colloquium on Industrial Aerodynamics Vehicle Aerodynamics, pp. 227–236. ISSN: 0167-6105. DOI: https://doi.org/10.1016/0167-6105(86)90087-5.

[99] C. Baker and N. Brockie. "Wind tunnel tests to obtain train aerodynamic drag coefficients: Reynolds number and ground simulation effects". In: *Journal of Wind Engineering and Industrial Aerodynamics* 38.1 (1991), pp. 23–28. ISSN: 0167-6105. DOI: https://doi.org/10.1016/0167-6105(91)90024-Q.

[100] E. Jacuzzi and K. Granlund. "Passive flow control for drag reduction in vehicle platoons". In: *Journal of Wind Engineering and Industrial Aerodynamics* 189 (2019), pp. 104–117. ISSN: 0167-6105. DOI: https://doi.org/10.1016/j.jweia.2019.03.001.

[101] E. Ljungskog, S. Sebben, and A. Broniewicz. "Inclusion of the physical wind tunnel in vehicle CFD simulations for improved prediction quality". In: *Journal of Wind Engineering and Industrial Aerodynamics* 197 (2020), p. 104055. ISSN: 0167-6105. DOI: https://doi.org/10.1016/j.jweia.2019.104055.

[102] P. Ekman et al. "Accuracy and Speed for Scale-Resolving Simulations of the DrivAer Reference Model". In: *WCX SAE World Congress Experience*. SAE International, 2019. DOI: https://doi.org/10.4271/2019-01-0639.

[103] S. B. Pope. "Ten questions concerning the large-eddy simulation of turbulent flows". In: *New Journal of Physics* 6 (2004), pp. 35–35. DOI: 10.1088/1367-2630/6/1/035.

[104] E. Ljungskog, C. tekniska högskola. Division of Division of Vehicle Engineering, and A. Systems. *Evaluation and Modeling of the Flow in a Slotted Wall Wind Tunnel*. Doktorsavhandlingar vid Chalmers tekniska högskola. Department of Mechanics, Maritime Sciences, Division of Vehicle Engineering, and Autonomous Systems, Chalmers University of Technology, 2019. ISBN: 9789179052195.

[105] M. Urquhart, S. Sebben, and L. Sterken. "Numerical analysis of a vehicle wake with tapered rear extensions under yaw conditions". In: *Journal of Wind Engineering and Industrial Aerodynamics* 179 (2018), pp. 308–318. ISSN: 0167-6105. DOI: https://doi.org/10.1016/j.jweia.2018.06.001.

[106] L. Davidson. "Large Eddy Simulations: How to evaluate resolution". In: *International Journal of Heat and Fluid Flow* 30.5 (2009). The 3rd International Conference on Heat Transfer and Fluid Flow in Microscale, pp. 1016–1025. ISSN: 0142-727X. DOI: https://doi.org/10.1016/j.ijheatfluidflow.2009.06.006.

[107] J. Sternéus, T. Walker, and T. Bender. "Upgrade of the Volvo Cars Aerodynamic Wind Tunnel". In: *SAE World Congress & Exhibition*. SAE International, 2007. DOI: https://doi.org/10.4271/2007-01-1043.

Appendix A

Non-normalized drag deltas

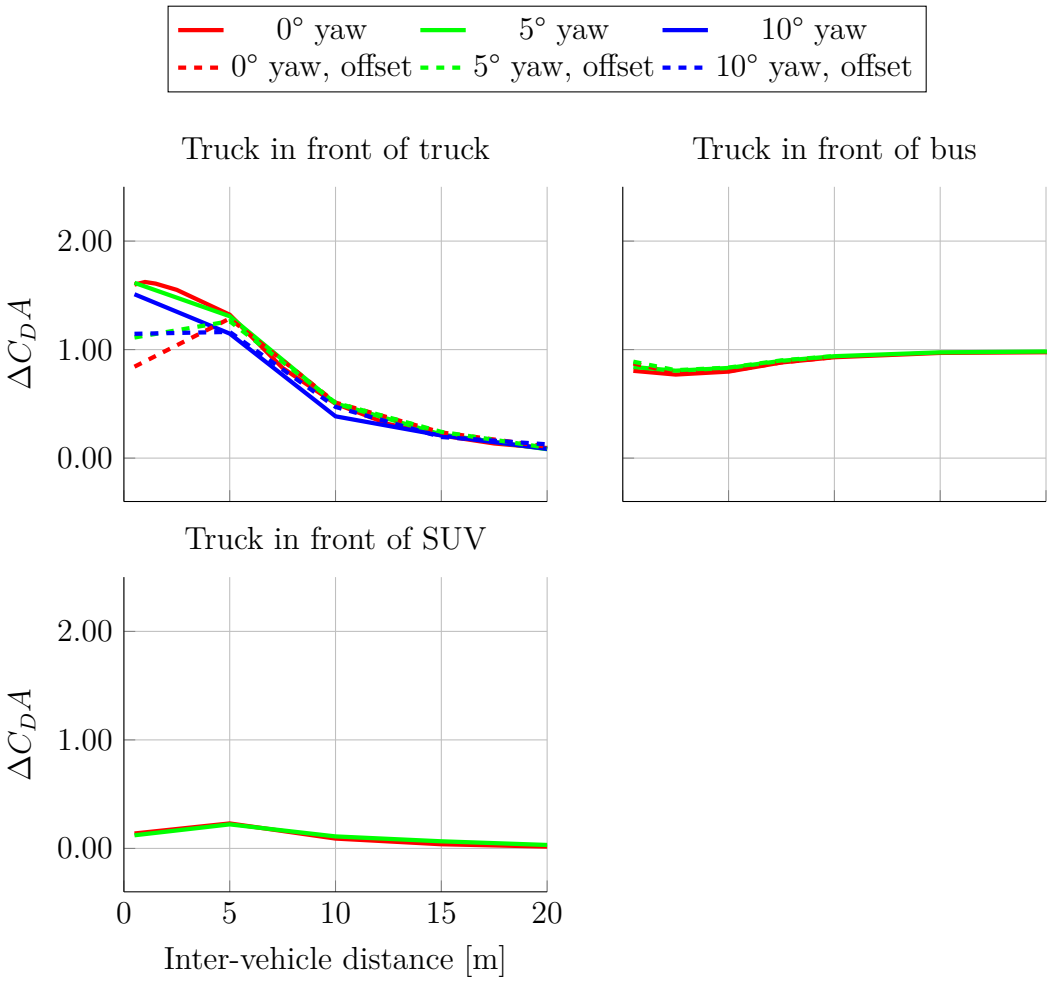

Figure A.1: *Delta $C_D A$ versus separation distance for the leading vehicle with and without lateral offset (0.5m) and yaw. Results from CFD computations, except for truck in front of bus results which are experimental.*

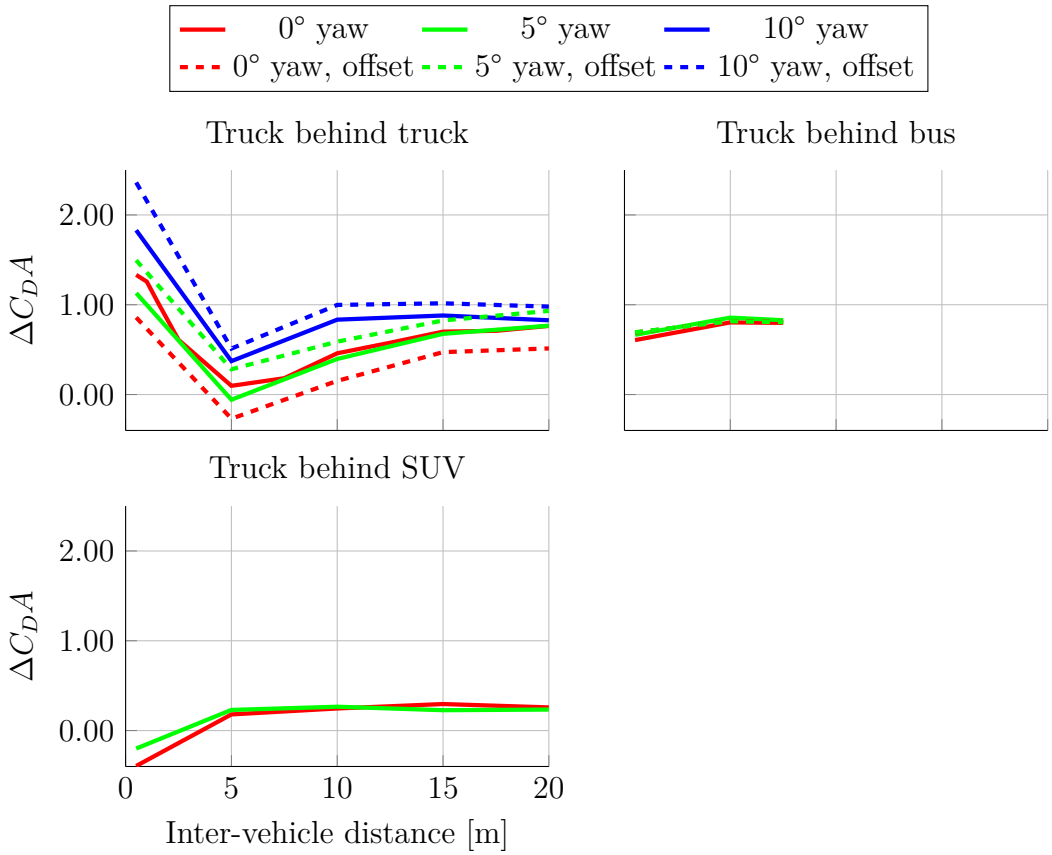

Figure A.2: *Delta $C_D A$ versus separation distance for the leading vehicle with and without lateral offset (0.5m) and yaw. Results from CFD computations, except for truck behind bus results which are experimental.*

Appendix B

Configurations investigated

The appendicies here show most of the configurations simulated in CFD and in the wind tunnel, roughly 250 configurations have been investigated.

B.1 Two–truck platoon

Yaw	0°	0°	0°	5°	5°	5°	10°	10°
Lateral offset	0m	0.5m	1m	0m	0.5m	1m	0m	0.5m
Distance								
0.5	CLTP	CLTP	TP	CLTP	CLTP	LTP	C	C
1.0	CTP	TP		TP	TP			
1.5	C							
2.0	LTP	LTP	TP	LTP	LTP	LTP		
2.5	C							
3.0	LTP	LTP	LP	LTP	LTP	LP		
4.0	TP	TP	TP	TP	TP	TP		
5.0	CTLP	CTLP		CLTP	CLTP		C	C
7.5	CLP	LP		LP	LP			
10.0	CLP	CLP		CLP	CLP		C	C
12.5	CLP	LP		LP	LP			
15.0	CLP	CLP		CLP	CLP		C	C
17.5	C							
20.0	CLP	C		CLP	CLP		C	C
25.0	LP			LP				
30.0	LP			LP				

Table B.1: *Configurations tested for a two – truck platoon. C signifies simulation, L is leading vehicle experimental drag, T is trailing vehicle experimental drag, and P is experimental pressure measurements on both vehicles.*

B.2 Truck–car platoon

Yaw	0°	0°	0°	5°	5°	5°	10°	10°
Lateral offset	0m	0.5m	1m	0m	0.5m	1m	0m	0.5m
Distance								
0.5	CTPSP	TP	TPSP	CTP	TP	TP	C	
1.0	TP	TP	TP	TP	TP	TP		
2.0	TP	TP	TP	TP	TP	TP		
3.0	TPSP	TP		TP	TP			
5.0	CTPSP	TP	SP	CTP	TP		C	
7.5	TP	TP	TP	TP		TP		
10.0	CTPSP	TP	TP	CTP	TP		C	
12.5	TP	TP		TP	TP			
15.0	CTP	TP		CTP	TP		C	
20.0	C			C			C	

Table B.2: *Configurations tested for a truck in front of an SUV. C signifies simulation, TP is truck experimental drag and pressure, SP is experimental drag on the SUV and pressure on both vehicles.*

Yaw	0°	0°	0°	5°	5°	5°	10°	10°
Lateral offset	0m	0.5m	1m	0m	0.5m	1m	0m	0.5m
Distance								
0.5	CTPSP	TP		CTP	TP		C	
2.5	TP	TP	TP	TP	TP	TP		
3.0	SP		SP					
5.0	CTPSP	TPSP	SP	CTP			C	
7.5	TP			TP				
10.0	CTPSP	TP		CTP	TP		C	
15.0	C			C			C	
20.0	CSP			C			C	
30.0	SP							

Table B.3: *Configurations tested for a SUV in front of an truck. C signifies simulation, TP is truck experimental drag and pressure, SP is experimental drag on the SUV and pressure on both vehicles.*

B.3 Truck–bus platoon

Yaw Lateral offset	0° 0m	0° 0.5m	0° 1m	5° 0m	5° 0.5m	5° 1m	10° 0m	10° 0.5m
Distance								
0.5	TP	TP		TP	TP			
5.0	TP	TP		TP	TP			
7.5	TP	TP		TP	TP			

Table B.4: *Configurations tested for a bus in front of a truck. C signifies simulation, T is truck experimental drag, and P is experimental pressure measurements on both vehicles.*

Yaw Lateral offset	0° 0m	0° 0.5m	0° 1m	5° 0m	5° 0.5m	5° 1m	10° 0m	10° 0.5m
Distance								
0.5	TP	TP		TP	TP			
2.5	TP	TP		TP	TP			
5.0	TP	TP		TP	TP			
7.5	TP			TP	TP			
10.0	TP			TP	TP			
15.0	TP			TP				
30.0	TP			TP				

Table B.5: *Configurations tested for a truck in front of a bus. C signifies simulation, T is truck experimental drag, and P is experimental pressure measurements on both vehicles.*